The Dissertation Committee for Samraat Shashikant Pawar certifies that this is the approved version of the following dissertation:

Community assembly, stability and food web structure

Committee:

Sahotra Sarkar, Supervisor

Daniel Bolnick

Timothy Keitt

Matthew Leibold

Lauren Meyers

John Scalo

Community assembly, stability and food web structure

by

Samraat Shashikant Pawar, B.S.; M.S.

Dissertation

Presented to the Faculty of the Graduate School of

The University of Texas at Austin

in Partial Fulfillment

of the Requirements

for the Degree of

Doctor of Philosophy

The University of Texas at Austin

May 2009

Acknowledgments

What a journey it has been. In august 2002, I flew from the old world to the new, landing directly in the lone star state. As a popular bumper sticker says, "*I wasn't born in Texas, but I got here as fast as I could*". Well, I did get here, not necessarily as fast as I could, but more or less intentionally. For this, I must thank Ayşegül Birand, who pestered me into applying to Graduate school, and Eric Pianka, who undertook to mentor me, apparently overlooking my many inadequacies and a rather impracticable (but enthusiastic) statement of purpose. Anyway, upon being set free in the wonderfully unfettered milieu of the "Section of Integrative Biology" at UT, I promptly performed a sailor's midnight walk over the next few years; through coursework, ideas, prelims, more ideas, PhD proposals, still more ideas, and finally a dissertation that was originally a byproduct of what started off as the main topic of my PhD research. But that is a story for another time and place.

At the early stages of my graduate "career", Eric helped me strengthen my interest in field ecology and prevented me from becoming a "rabid experimentalist" (aka succumbing to the dark side). Larry Gilbert must also share the blame for keeping my interest in community ecology, tropical biology and field ecology alive and kicking. The trip to Sirena (Costa Rica) with Larry was a stimulating one, and strongly influenced the orientation of my PhD research. The need to make sense of observed biological patterns in nature inexorably led me to pursue mathematical modeling. This change of direction resulted in my shift from Eric's lab to Sahotra Sarkar's. Here again I must thank Eric for accepting my decision with equanimity. I also thank Sahotra for taking me on, showing great patience and faith in my various schemes, and deftly guiding my training in theoretical biology. To a large extent I also attribute my subsequent progress in grad school to John Scalo. John granted me a series of research assistantships in the department of astronomy that afforded me the luxury to immerse myself in my research. We also sought extraterrestrial life. Well not quite, though that is fun too, as any good astrobiologist will tell you. John and I pursued some exciting themes in population genetics, during which I learnt heaps. I am in awe of the range of issues across physics, astronomy and biology that John is interested in, and understands deeply. I also owe a big thanks to my prelim and dissertation committees. The latter in particular- Lauren Meyers, Tim Keitt, Dan Bolnick, Matthew Leibold and John Scalo, showed great patience and tolerance in the face of a rather mutable PhD research project. For the successful completion of my dissertation, I also thank Jordan Scaff who despite his million hours of classes, volunteered to assist me in data compilation and analysis. On top of this, he had to listen to me blabber endlessly about networks, food webs, and such.

A large portion of my financial support also came in the form of teaching assistantships. Here I thank K. Sathasivan, who taught me to teach efficiently, creatively, patiently, and effectively. Sata's influence will always be evident in my future pedagogical undertakings.

To the choppy seas of grad school and life, which at times I felt I was navigating with leaky boat, a measure of placidity was brought by Mike Singer and Camille Parmesan. They were and endless source of advice and support throughout. So were my my fellow graduate students, especially the extended cohort: Rob, Barrett, Ron, Naiara, Natalia, Sasha, Krushnamegh, Jelena, Juan, Deepa, Evan, Christian, Simone, Juanita, and Trevon. They provided or shared to various degrees, stimulating drinks, stimulating conversation, support, optimism, pessimism, multi-cultural food, bbq evenings, humor, buck-u-uppos and advice; I cannot visualize how I would have gotten through without them.

I am also grateful to the cheerful and efficient staff of the section of Integrative Biology. In particular, Sandy Monahan, who was always there to smooth the bureaucracy for we graduate students.

I am indebted to a number of people outside UT too. Ever since we were acquainted and bought counterfeit paintings in Beijing during the Santa Fe Institute's 2005 summer school in China, Oskar Burger invested a lot of time thinking with me about species interaction networks and metabolic allometric scaling, helping me resolve many issues that arose at the early stages of my research. Let's finish that paper man! I must also thank him for making me realize that a couple of bottles of fine cognac is all a tropical person needs to roll around in the snow wearing bare essentials. I also thank Jennifer Dunne, Van Savage, and Nicolas Loeuille for discussions that facilitated my progress and greatly improved my research.

Finally, I would like to thank my family – Aai, Daddy, Soni and Sheffi. It is partly due to their endless support and belief that led me to embark on the pursuit of a PhD degree. And of course, my wife, friend, philosopher and guide Catalina. She made my quest beautiful, all the more fulfilling and filled it with (sometimes bilingual) puns. Finally finally, Maya. Her I thank for arriving at an opportune time. She made my dissertation writing infinitely more enjoyable, and dutifully entertained me day and night (as any good daughter should).

This PhD dissertation research was funded by the Section of Integrative Biology, the Private Lands Research Grants-Environmental Science Institute, and the Department of Astronomy (through a grant from NASA's exobiology program), University of Texas at Austin.

Community assembly, stability and food web structure

Samraat Shashikant Pawar, Ph.D.
The University of Texas at Austin, 2009
Supervisor: Sahotra Sarkar

Natural communities of species embody complex interrelationships between the structure of the interspecific interaction network, dynamics of species' populations, and the stability of the system as a whole. Studying these interrelationships is crucial for understanding the survival of species in nature. In this context, studying the food web (the network of who-eats-whom) embedded in each interaction network is particularly important because trophic interactions are the main channels of energy flow in all ecosystems. Using a combination of mathematical modeling and empirical data analyses, this study explores the interrelationship between food web structure and multi-species coexistence in local communities.

Chapter 1 of this thesis places the overall dissertation study in context of the history of research on species interaction networks and food webs.

In Chapter 2, I use a population dynamical model to show how the requirements of stable multi-species coexistence results in the emergence of specific, nonrandom configurations of food web structure during community assembly. These structural "signatures" can be used to empirically gauge the importance of interaction-driven dynamical stability constraints in natural communities.

In Chapter 3, I extend the model analyzed in Chapter 2 by imposing biologically feasible constraints on its parameters. This is made possible by the allometric scaling between individual metabolism and body size, and the constraints on interspecific trophic interactions due to body size differences between pairs of interacting species. I show that, using this approach, it is possible to interlink three aspects of local communities that have typically been studied in isolation: the species' body mass distribution, the distribution of ratios of body sizes of consumer and resource species (e.g., predator and prey), and certain food web structural features. Some of these features have previously lacked explanatory models.

Finally in Chapter 4, using empirical data from nine communities across a range of habitats, I test some theoretical predictions of the previous chapter. The results provide strong evidence that the food web structure of natural communities do indeed exhibit signatures of dynamical stability constraints, and that the model developed in Chapters 2 and 3 is successfully able to predict a number of empirically observed food web structural features.

Table of Contents

Acknowledgments ..... **iii**

Abstract ..... **v**

Chapter 1: Introduction **1**

1.1 Population interaction networks and Darwin's *Gedankenexperiment* 1

1.1.1 Food webs as population interaction networks **4**

1.2 Interrelating population dynamics and food web structure 4

1.2.1 The importance of body size **7**

Figures **9**

Chapter 2: Community assembly, stability and signatures of stability constraints on food web structure **10**

2.1 Introduction 10

2.2 A dynamical model 12

2.2.1 Community assembly, stability and changes in food web structure **13**

2.2.2 Interlinking food web structural features and community stability **14**

2.2.3 Predicted signatures of stability constraints on food web structure **18**

2.3 Signatures of stability constraints in simulated model communities 20

2.3.1 Methods **20**

2.3.2 Results **21**

2.4 Discussion 23

2.4.1 Caveats **25**

Tables **29**

Figures **31**

Chapter 3: The effect of species body size variation on community assembly, stability and food web structure **35**

3.1 Introduction **35**

3.2 Body size based parameterization of the dynamical food web model **37**

3.3 Model analysis 40

3.3.1 Null expectations under relaxed assembly **40**

3.3.2 PHS and the scaling of interaction strengths **43**

3.3.3 Signatures of stability constraints on body size based food web structural features **46**

3.3.4 Signatures of stability constraints on SBM and CRBR distributions **49**

3.4 Community assembly simulations 50

3.4.1 Methods 50
3.4.2 Results 52
3.5 Discussion 54
3.5.1 Caveats 57
Tables 60
Figures 62
Chapter 4: Signatures of stability constraints on food web structure in natural communities 67
4.1 Introduction 67
4.2 Methods 70
4.2.1 Food web data 70
4.2.2 Food web structural measures and theoretical predictions 71
4.2.3 Data analyses 73
4.3 Results 78
4.3.1 Stability of observed vs. size-randomized communities 78
4.3.2 Signatures of dynamical stability constraints 78
4.3.3 Species' optimal foraging vs. community dynamical stability constraints 80
4.3.4 A tale of missing links? 80
4.4 Discussion 82
4.4.1 Signatures of dynamical stability constraints in natural community food webs 82
4.4.2 Optimal foraging vs. population stability constraints 85
4.5 Conclusions 86
Tables 87
Figures 92
Appendices 98
Glossary 111
Bibliography 112
Vita 119

Chapter 1: Introduction

"…it is quite credible that the presence of a feline animal in large numbers in a district might determine, through the intervention first of mice and then of bees, the frequency of certain flowers in that district!"

"When we look at the plants and bushes clothing an entangled bank, we are tempted to attribute their proportional numbers and kinds to what we call chance. But how false a view is this!"

"…what war between insect and insect–between insects, snails, and other animals with birds and beasts of prey–all striving to increase, all feeding on each other, or on the trees…" (Darwin, 1859, p. 88)

1.1 Population interaction networks and Darwin's *Gedankenexperiment*

Interactions between species' populations are ubiquitous and fascinating. For at least a century and a half now, biologists have been interested in the effects of direct and indirect interspecific interactions on the survival of individual species, and the persistence of species-rich communities. Indeed, Darwin's observations on the "entangled bank", and his *Gedankenexperiment* about the indirect effect of cats on flowering plants through a network of interspecific interactions is an early investigation into one of the foremost challenges still facing contemporary biologists: understanding the feedback between persistence of single species' populations and the stability of the community as a whole (Pascual and Dunne, 2006). This challenge is of course itself embedded within the wider one of understanding the feedbacks between levels of biological organization ranging molecules and genes to the biosphere. Obviously, studying how organisms survive within the context of a network of interspecific interactions requires both ecological and evolutionary approaches. However, for practical reasons, this dissertation is largely restricted to the study of population interaction networks with respect to ecological processes such as numerical population dynamics, immigration, and extinction. Indeed, most of the historical development of the study of population interaction networks occurred in ecology, which I will attempt to outline here briefly.

Soon after the publication of Darwin's seminal book (Darwin, 1859), Herbert Spencer (1864) published his ideas about the emergence of order in nature, which helped embed the notion of community stability (the "balance of nature") and its relationship to species interactions in the

ecologist's psyche. By the beginning of the 20th century, as population and community ecology we developing into distinct disciplines, a belief in the equilibrium state of communities and stability of interspecific interactions had become widespread. In particular, Elton's (1927) views that species interactions formed a scaffolding that rendered communities inherently stable found considerable support for many decades (Hutchinson, 1959; MacArthur, 1955; Odum, 1953). As MacArthur says in his seminal mathematical analysis of community stability and food web structure (MacArthur, 1955),

"...a large number of paths through each species is necessary to reduce the effect of overpopulation of one species."

and therefore,

"...stability increases as the number of links increases."

This was also the period when the concept of food webs as organized systems gathered firm footing (Elton, 1927; Lindeman, 1942). In particular, Elton pointed out certain regularities that appeared to exist in the structure of food webs, such as the distribution and abundance of species across trophic levels.

During the "golden age of theoretical ecology" from 1920 to 1940 (Scudo and Ziegler, 1978) the foundations for the mathematical study of species interaction networks were laid. A particularly important development was rediscovery of Verhulst's logistic equation by Pearl in the 1920s and its extension to interacting populations (e.g., Gause, 1934; also see Kingsland, 1985). In particular, the stability of predator-prey interactions received considerable attention, partly because of the potential applications of studying them. In this context of trophic interactions, another important development, which will be discussed in Chapter 2, was the introduction of the concept of consumer functional response (prey-density dependent changes in predator consumption rate) (Holling, 1959), and its mathematical analysis by Rosenzweig & MacArthur (1963). Eventually, larger systems with arbitrary numbers of interacting species began to be studied mathematically (e.g., Gardner and Ashby, 1970), including the landmark works by May (1973; 1974) and Levins (1974; 1975)[1]. Using different mathematical techniques,

[1] Here it is important to note that a substantial body of work in this area was also concurrently published in the erstwhile USSR Logofet, D.O., 1993. Matrices and graphs: stability problems in mathematical ecology. CRC Press, Boca Raton..

both May and Levins showed that stability of the community as a whole was strongly *limited* by the number and strengths of interspecific interactions. In other words, the more complex a community, the harder it is to find a configuration of interactions that guarantees the persistence of all species. This result contradicted the Eltonian view because it meant that increasing the number of species and the interactions between them *decreased* community stability. This mathematical fact was difficult to reconcile with biological intuition, resulting in the "diversity-stability debate" that continues today (McCann, 2000). But this debate apart, the studies by May and Levins were also the beginning of an important phase in not just in ecology but in biology in general: the use of dynamical systems models combined with network (graph) theory to study the interrelationships between interaction network structure and system stability (Hofbauer and Sigmund, 1988; Logofet, 1993). Darwin's *Gedankenexperiment* was finally beginning to be analyzed mathematically. In this respect, Levins' (1974; 1975) work is particularly important. Unlike May, Levins focused directly on subcommunities that were network structural "modules" or "motifs" (sub-networks representing well connected subcommunities of at least two species; see Milo et al., 2002) and showed how "loop analysis" could be used to examine their effect on community stability. Loop analysis still remains an important technique, and will be revisited in more detail below.

Interestingly, around the same period that these advances were being made in the study of population interaction networks, MacArthur and Wilson's (MacArthur and Wilson, 1967) theory of island biogeography began to attract considerable attention. This is noteworthy because this theory (later extended by Hubbell (2001)) was "neutral" in the sense that it attempted to explain local community structure using a model of stochastic immigration and extinction processes, in which species interactions played no part. Partly motivated by this neutral biogeographic theory, a series of papers by Connor, Simberloff and others sparked a controversy by questioning the importance of species interactions in structuring local communities (Connor and Simberloff, 1983; Connor et al., 1984; Gilpin et al., 1984). These studies, which focused mainly on interspecific competition, developed purely statistical models that made no assumptions about interactions among species, and showed that they often provided an adequate explanation of co-occurrence data. These subsequently became "null models" from which the deviation of observed patterns could be measured to gain insights into the importance of species interactions in local communities (Harvey et al., 1983). Such an approach will be used repeatedly in this dissertation as well, mainly to differentiate between randomly assembled and dynamically constrained configurations of food web structure.

1.1.1 Food webs as population interaction networks

An important aspect of May (1974) and Levins' (1974; 1975) studies is that they included the entire spectrum of interspecific interactions: competition (– /–) , mutualism (+/+), trophic (consumer-resource interactions, +/–), amensalism (–/0), and commensalism (+/0). This led to interesting conclusions about the relative importance of different interactions types to community stability. Indeed, the simultaneous consideration of all types of interactions is important for a comprehensive understanding of natural communities. However, a majority of subsequent studies tended to concentrate on networks of trophic interactions (food webs) (Logofet, 1993; Pimm, 1982). I identify three distinct reasons for this.

First, as mentioned above, there are obvious practical applications of studying predator-prey dynamics. Second, trophic interactions are undoubtedly the strongest channels of energy flow through ecosystems (relative to more subtle interactions such as mutualism and competition) (Odum, 1953). Third, trophic interactions are relatively easy to detect and quantify in the field. This is clearly evinced by the fact that among the different types of interspecific interactions, relatively more empirical data are available on trophic ones (e.g., Brose et al., 2005). It also means that there is a much better empirical basis for model development with respect to trophic interactions. Thus, although the food web is only a subset of the complete population interaction network of any local community, its study offers certain advantages. In this study too, I will concentrate on the food web and not the whole population interaction network. However, as will be seen in Chapter 2, the main theoretical results of this study pertain to the strengths of interspecific interactions, and not their sign. Hence, many of the results should hold even upon the inclusion of other interaction types such as mutualism and competition.

1.2 Interrelating population dynamics and food web structure

The relationship between interaction network structure, species' population dynamics, and stability of the community as a whole is essentially a feedback between different levels of organization (Levins, 1975; May, 2006; Proulx et al., 2005). As mentioned above, May (1973; 1974) and Levins (1974; 1975) were the first to show such a feedback mathematically. Their results carried the largely implicit assumption that real communities undergo a selection process that eliminates destabilizing interaction network (henceforth, food web) configurations. In May's words,

"*In nature we deal not with arbitrary complex systems, but rather with ones selected by a long and intricate process. The emergent moral is that theoretical work should not try to prove any general theorem that "complexity implies stability", but instead should focus on elucidating the very special sorts of complexity, the singular strategies, which may promote such mathematically atypical stability.*" (May, 1974, pp. 3-4).

Levins was more explicit about the implications of such a "selection" process, and sought to relate it to natural selection and evolutionary dynamics:

"*…mendelian selection in a single species may stabilize or destabilize the community as a whole, may introduce oscillations, and may affect community stability in ways that are not intuitively obvious.*" (Levins, 1975, p. 17).

In fact a clear message emerges from Levins' work: strategies that are good for a single species (a node of the network) may not be good for the system (network) as a whole.

In principle, the overall process that leads to emergence of stabilizing (to the community) single species' characteristics and food web structures is simple: during community assembly, less stable structural configurations of the food web are weeded out through a combination of adaptive changes, extinctions, and recolonizations of species' populations, until a stable state is achieved. By definition this state either does not change anymore, or as fast. The food web structure of this stable system is therefore a nonrandom subset of all possible ones for given biotic constraints and an abiotic setting. However, a quantification of this process is far from simple, and must simultaneously address three issues:

(i) *Assembly*: How does food web structure change during community assembly, how important is the pattern of species' immigration?

(ii) *Relationships between network structure and stability*: What features of food web structure have relatively strong effects on stability?

(iii) *Mechanisms of structural change*: What mechanisms result in the selection of specific food web structural configurations, and at what level do they act (e.g., individuals, populations, or groups of populations (sub-communities))?

Over the three decades or so following May and Levins' works these three issues were addressed to different degrees, but rarely in a single theoretical framework. Community assembly dynamics and food web structure became the focus of a set of studies that began with theoretical and empirical work in the 1980s (e.g., Law and Morton, 1996; Post and Pimm, 1983; Robinson

and Dickerson, 1987; Virgo et al., 2006). However, other than the traditional measure of complexity (as defined by May) (i.e., its components: n, c and C_T), these studies typically did not attempt to relate more detailed food web structural features (such as species' trophic generality, or chain lengths) to stability in assembling communities, until recently (Bastolla et al., 2005; Kristensen, 2008; Neutel et al., 2007; Virgo et al., 2006).

The contribution of May (1974) and subsequent authors who concentrated on the relationship between complexity and stability (Cohen and Newman, 1985; Geman, 1986; Hastings, 1982) mainly addressed the second of the above three issues, i.e., the relationship between food web structure and stability. May showed that for a given species richness n, the mean of the absolute magnitudes of interaction strengths c and connectance C_T (fraction of potential links that are realized), community "complexity", $c\sqrt{nC_T}$, is a measure of interaction network structure that undermines the probability of stable species coexistence[2]. In contrast to May's study, Levins' (1974; Levins, 1975) showed interaction structure of subcommunities of two or more species (network motifs or modules) could be linked to community stability using a method called loop analysis. Levins' approach was to consider the stability properties of communities at equilibrium: a state wherein all species populations remain consistent, or fluctuate only weakly (this state will be given a mathematically exact definition in Chapter 2). Fig. 1.1 shows an example of such a community. Given some function $f_i(\bullet)$ representing the rate of change of the i^{th} species' population (or biomass) size x_i, the "community matrix" consists of the coefficients $c_{ij} = \partial\left(f_i(\bullet)\right)/\partial x_j$, evaluated when all populations are at equilibrium. The i^{th} species' function $f_i(\bullet)$ consists of terms representing the strengths and signs of inter- and intraspecific interactions, as well as sizes of the three populations. One explicit form for $f_i(\bullet)$ is defined in Chapter 2 of this dissertation. Levins showed that it is possible to infer configurations of magnitudes of the c_{ij}'s (strengths) and their signs (qualitative, who-eats-whom relationships) in the interaction network that impart community stability. This is achieved by breaking up the food web into its component loops and examining their contribution to the stability of the system. A loop is a series of trophic links that begin and end at the same species node without visiting any other node more than once. For example, the coefficient c_{11} in Fig. 1.1 represents a length-1 loop of species 1's effect on itself, coefficients $c_{12}c_{21}$ a length-2 loop of the interaction between species' 1 & 2, and coefficients s$c_{21}c_{32}c_{13}$ & $c_{12}c_{31}c_{23}$ the two length-3 loops of the indirect interaction across all three species. Clearly, increasing loop lengths correspond to increasing levels of network structural

[2] Measured as the probability of a random interaction network with particular values for n, c and C_T and fixed intraspecific density dependence having a negative leading Jacobian eigenvalue; see Chapter 2.

organization; hence loop analysis also allows different levels of community organization to be linked to its stability. Subsequent studies sought to further elucidate the effects of particular food web structural modules on community stability, such as trophic chains, a prey and two shared predators, omnivory, etc. (McCann et al., 1998; Neutel et al., 2007; Neutel et al., 2002; Pimm and Lawton, 1977; Yodzis, 1981), but typically without the context of community assembly (the study by Neutel et al., 2007 is a notable exception).

The third issue, i.e., the mechanisms of structural change, has received the least attention of the three. However, a series of theoretical studies have recently started to consider the role of behavioral and evolutionary processes in community stabilization and the emergence of specific network structural attributes (Drossel et al., 2004; Loeuille and Loreau, 2005; Uchida et al., 2007).

Chapter 2 of this thesis seeks to take a step towards simultaneously addressing the above issues (i-iii) using a relatively simple mathematical model (a Lotka-Volterra type model) of species linked by trophic interactions. Using a combination of analytic and computational tools, I show how food web structure changes dynamically during community assembly, during which certain stabilizing structural configurations are favored. This results in certain measurable network structural "signatures" that can be used to gauge the importance of interaction-driven stability constraints on communities during and after assembly in natural communities. This work has been accepted for publication in the *Journal of Theoretical Biology* (Pawar, 2009).

1.2.1 The importance of body size

Natural communities can consist of species with average body sizes spanning up to 20 or so orders of magnitude (Brown et al., 2004; Peters, 1983). This is an important consideration while studying food web structure because body size strongly constrains interspecific interactions in two distinct ways. First, whole organism metabolic rate increases allometrically with body mass according to a remarkably consistent power law relationship (Brown et al., 2004; Kleiber, 1961; Peters, 1983). This in turn determines species life history characteristics such as biomass production, birth, and mortality rates. Second, depending upon the environmental context, the average size difference between individuals of consumer and resource species sets physical limits on the frequency with which the two encounter each other, as well as the rate at which the former can exploit the latter following encounter (Dial et al., 2008).

Thus altogether, body size provides a means to map individual-level biological constraints onto population- and community-level dynamics. Moreover, because body size is relatively easy

to measure in nature, it has the potential to render the otherwise difficult task of confronting food web theory with empirical data somewhat easier. The importance of body size as a driver of foraging preferences and niche differentiation in communities was first considered in the 1950's (Brown and Wilson, 1969; Hutchinson, 1959; Hutchinson and MacArthur, 1959). However, the actual incorporation of the size-metabolism allometry in models of community dynamics appears to have been pioneered by Peters (1983), who used it to parameterize trophic interactions in a simulation model of community assembly. Subsequently, Yodzis & Innes (1992) used allometric scaling to parameterize the Rosenzweig-MacArthur predator-prey model (Rosenzweig and MacArthur, 1963). A different approach was taken by Cohen et al (1993), who drew inferences about the importance of species' body sizes on food web organization by examining their distribution across trophic levels and the ratios of consumer-resource body size differences in real communities. Another important study in this context was by Law & Morton (1996), who were the first to incorporate body sizes into a community assembly model based upon a Lotka-Volterra type model. Since then, the use of body size in empirical descriptions as well as theoretical models of trophic interactions and food webs community ecology has rapidly increased, especially in the last five years or so (Berlow et al., 2009; Brose et al., 2006a; Brose et al., 2008; Jonsson and Ebenman, 1998; Lewis et al., 2008; Loeuille and Loreau, 2005; Otto et al., 2007; Petchey et al., 2008; Vasseur and McCann, 2005; Virgo et al., 2006; Weitz and Levin, 2006; Woodward et al., 2005a; Woodward et al., 2005b). This has been partly driven by recent advances in the theory of size-metabolism allometric scaling (Brown and Gillooly, 2003; Brown et al., 2004), and the increasing availability of data on body size structure in food webs (Brose et al., 2005).

In Chapter 3 of this thesis, I literally put meat on the bare bones of the LV-type model of Chapter 2 by developing a set of body size based parameterizations. I show that using this approach, it is possible to interlink three aspects of local communities that have typically been studied in isolation: the species' body mass distribution (Allen et al., 2006b), the distribution of ratios of body sizes of consumer and resource species (e.g., predator and prey) (Brose et al., 2006b), and food web structure. As I have mentioned above, there is a growing pool of studies in the literature that have quantified the body sizes of species involved in trophic interactions. Using nine relatively good quality datasets from these, in Chapter 4 I examine some of the predictions from Chapters 2 and 3 about the relationship between food web structure and stability of natural communities.

Figures

Figure 1.1. The community matrix and food web (interaction network) of a hypothetical three-species community. The interaction sign structure is represented using Levins' (1974; Levins, 1975) scheme: lines (network edges) ending in arrows represent positive effects (and direction of biomass flow) and those ending in circles, negative ones. Species 1 is basal (primary producer), 2 a consumer of 1, and 3 a consumer of both 1 & 2.

$$\begin{bmatrix} c_{11} & c_{12} & c_{13} \\ c_{21} & c_{22} & c_{23} \\ c_{31} & c_{32} & c_{33} \end{bmatrix}$$

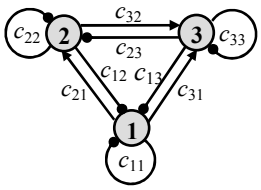

Chapter 2: Community assembly, stability and signatures of stability constraints on food web structure

Abstract. To understand the dynamics of natural species communities, a major challenge is to quantify the relationship between their assembly, stability, and underlying food web structure. To this end, two complementary aspects of food web structure can be related to community stability: sign structure, which refers to the distributions of trophic links irrespective of interaction strengths, and interaction strength structure, which refers to the distributions of interaction strengths with or without consideration of sign structure. In this paper, using data from a set of relatively well documented community food webs, I show that natural communities generally exhibit a sign structure that renders their stability sensitive to interaction strengths. Using a Lotka-Volterra type population dynamical model, I then show that in such communities, individual consumer species with high values of a measure of their total biomass acquisition rate, which I term "weighted generality", tend to undermine community stability. Thus consumer species' trophic modules (a species and all its resource links) should be "selected" through repeated immigrations and extinctions during assembly into configurations that increase the probability of stable coexistence within the constraints of the community's trophic sign structure. The presence of such constraints can be detected by the incidence and strength of certain nonrandom structural characteristics. These structural signatures of stability constraints are readily measurable, and can be used to gauge the importance of interaction-driven dynamical stability constraints on communities during and after assembly in natural communities.

2.1 Introduction

The relationship between food web structure and dynamical stability of the component species' populations is essentially a feedback between different levels of community organization (May, 2006; Proulx et al., 2005). In order to understand this feedback, an explicit mapping between structure and dynamics is needed (Dunne et al., 2005; Pascual et al., 2006). Such a mapping was first established by May (1974), who showed that for a given species richness n, the mean of the absolute magnitudes of interaction strengths c and connectance C_T (fraction of potential links that are realized), community "complexity", $c\sqrt{nC_T}$, is a measure of interaction network structure that undermines the probability of stable species coexistence. This result

carried the largely implicit assumption that communities undergo a "selection" process that favors network structural configurations that enhance multi-species coexistence stability.

In principle, the overall process that leads to the emergence of stabilizing food web structures due to stability constraints is simple: during community assembly, less stable structural configurations of the food web are weeded out through a combination of adaptive changes, extinctions, and recolonizations of species' populations, until a stable state is achieved. By definition this state either does not change anymore, or as fast. The network structure of this stable system is therefore a nonrandom subset of all possible ones for a given biotic and abiotic setting. However, a quantification of this process is far from simple, and must simultaneously address the dynamics of three aspects: (i) community assembly, (ii) the relationship between food web structure and stability, and (iii) the mechanisms by which food web structure changes (how certain food web structural configurations are actually favored).

Past studies have addressed these issues to various degrees, but very few have included all in a single theoretical framework. Food web assembly dynamics have been the focus of a set of studies that began with theoretical and empirical work in the 1980s (e.g., Law and Morton, 1996; Post and Pimm, 1983; Robinson and Dickerson, 1987; Virgo et al., 2006). However, other than the traditional measures of connectance and species richness, these studies have not related food web structure and stability to assembly until recently (Bastolla et al., 2005; Kristensen, 2008; Neutel et al., 2007).

May (1974)'s seminal contribution mainly addressed the second issue, i.e., of the relationship between food web structure and stability. Subsequent studies sought to elucidate effects of food web structural measures more meaningful than complexity on community stability, such as structural modules consisting of trophic chains, a prey and two shared predators, omnivory, etc. (McCann et al., 1998; Neutel et al., 2007; Neutel et al., 2002; Pimm and Lawton, 1977; Yodzis, 1981), but typically without the context of community assembly (the study by Neutel et al., 2007 is a notable exception). However, there is still very little consensus about which food web structural features (modules) play an important part in determining dynamical community stability.

The third issue, i.e., of the mechanisms of structural change, has received very little attention in the past. However, a series of theoretical studies have recently started to consider the role of behavioral and evolutionary processes in stabilization of communities (Drossel et al., 2004; Loeuille and Loreau, 2005; Uchida et al., 2007). Thus on the whole, major gaps currently remain in our understanding of relationship between community assembly, stability, and food web structure. This study seeks to make a contribution by simultaneously studying the issues of

community assembly, food web structure and stability using a mathematical model. In particular, I will study what food web structural modules are particularly important to community stability, and how they change during assembly.

2.2 A dynamical model

Let $\mathfrak{N}$ denote the set of unique species indices 1, 2,…, n in an n-species community. I will use a Lotka-Volterra (LV) type model of community population dynamics:

$$\frac{dx_i}{dt} = x_i\left(b_i - d_i + \sum_{j=1}^{n}\alpha_{ij}x_j\right), \forall i \in \mathfrak{N} \quad (2.1a)$$

Here, x_i is the total biomass of the i^{th} species' population, b_i its autonomous biomass production (including reproduction) rate (0 for all consumers) and d_i its intrinsic density-independent biomass loss (including mortality) rate. The constant coefficient α_{ii} represents biomass loss rate due to direct intraspecific interference of the i^{th} species, while α_{ij} represents its rate of per-unit biomass loss or gain from interaction with the j^{th} species. If the j^{th} species is a consumer of the i^{th} one, biomass gain rate of the former (α_{ji}) and loss of the latter (α_{ij}) are related such that,

$$\alpha_{ji} = -e_j\alpha_{ij}, \text{ (when } j \text{ consumes } i) \quad (2.1b)$$

e_j is the fraction of biomass lost due to assimilation and production inefficiency of the j^{th} consumer. I assume that all interactions result in a net flow of biomass from one species to another. Thus in the case where two species are capable of consuming each other (e.g., at different life history stages), it is assumed that the interaction, when integrated across all life stages, results in a net flow from one species to another. This also implies that the indices in expression 2.1b cannot be reversed for a given species pair. For analytical tractability, I follow previous studies (Hofbauer and Sigmund, 1998; Logofet, 1993; May, 1974) in assuming that α_{ij} is a linear, simplified representation of encounter and consumption rates. Below (section 2.4.1) I show that that under some reasonable assumptions, inclusion of a functional response of consumers to increasing availability of resource species' will not affect the main results of the analyses that follow.

2.2.1 Community assembly, stability and changes in food web structure

Consider community assembly starting with the establishment of at least one basal species (indexed by 1), which we will assume was able to grow in the absence of consumers to a positive equilibrium biomass density, $\hat{x}_1 = -(b_1 - d_1)/\alpha_{11}$. During assembly, the i^{th} immigrant arriving at a community already consisting of m residents ($m \geq 1$) will grow in biomass density when rare (invade) if the condition

$$\sum_{j \in \mathcal{G}_i} |\alpha_{ij}| \, e_i \hat{x}_j > \sum_{k \in \mathcal{V}_i} |\alpha_{ik}| \, \hat{x}_k + d_i \,, \; j,k = 1,2,...,m \tag{2.2}$$

is satisfied (Roughgarden, 1996 ; Strobeck, 1973), where $\mathcal{G}_i$ and $\mathcal{V}_i$ denote the index sets of the immigrant's resource and consumer species, respectively. Equation 2.2 states that the biomass gain rate must be greater than loss rate, measured when all resident species are at equilibrium. If the immigrant can invade, and if subsequently all m+1 (= n) populations converge on a vector of equilibrium sizes $\hat{\boldsymbol{x}}$ that is a point within the positive orthant $\mathbb{R}_+^n$ of the n-dimensional Euclidean state space (i.e., no population goes extinct), the system is (at least) Hurwitz stable (or locally asymptotically stable) if the n x n Jacobian $\boldsymbol{C}$ (the familiar "community matrix"; May, 1974) with elements (e.g., see Logofet, 1993),

$$c_{ij} = \left. \frac{\partial \left(dx_i / dt \right)}{\partial x_j} \right|_{\boldsymbol{x} = \hat{\boldsymbol{x}}} = \alpha_{ij} \hat{x}_i \,, \forall i, j \in \mathcal{N} \tag{2.3}$$

has all its eigenvalues $\lambda_i(\boldsymbol{C})$, $i \in \mathcal{N}$ lying in the negative half of the complex plane i.e., given that

$\lambda_{\max}(\boldsymbol{C}) \equiv \max\left\{ \mathrm{Re}\left(\lambda_i(\boldsymbol{C}) \right) \right\} \forall \; i \in \mathcal{N}$, the inequality

$$\lambda_{\max}(\boldsymbol{C}) < 0 \,, \tag{2.4}$$

must hold. The element c_{ij} ($i \neq j$) of $\boldsymbol{C}$ represents the population-level effect of a change in sthe j^{th} species' biomass density on the i^{th} one, or the dependence of the i^{th} species on its own density (if $i = j$), at biomass equilibrium. Note that it is possible for one or more populations under in the LV model to actually settle into periodic or chaotic trajectories. In this case, the system actually

converges to the vicinity of a periodic or chaotic attractor (e.g., see Gilpin, 1979), and criterion 2.4 does not hold. However, as will be seen below, the assumption of a point equilibrium allows the use of the Jacobian matrix and Hurwitz stability criterion, which in turn allows food web structure to be explicitly linked to community stability. Whether predictions about the relationships between food web structure and community stability based upon this assumption are valid will be tested with numerical simulations (section 2.3 below). Note also that an additional condition to satisfy $\lambda_{max}(\boldsymbol{C}) < 0$ is that there be no disconnected subcommunities in the "community" (the community's graph should be irreducible; Logofet, 1993). But this need not concern us here because the above criteria and all the subsequent results of this paper can be applied to subcommunities separately.

Now, using criteria 2.2 and 2.4 together, changes in food web structure during assembly can be understood from the following alternative scenarios after an immigrant's arrival (again, ignoring periodic or chaotic dynamics):

- *Inequality 2.2 is not satisfied*. The immigrant cannot invade and there is no impact on food web structure.
- *Inequalities 2.2* and *2.4 are both satisfied*. The community grows and food web structure changes by addition of a species and its trophic links. I will call this a "stable invasion".
- *Inequality 2.2 is satisfied, but 2.4 is not*. The immigrant invades but one or more populations eventually go extinct, which may or may not include the immigrant. Hence community size either shrinks or remains the same and food web structure changes by the loss of at least one species and its trophic links. I will call this a "species sorting" event.

Stable invasions result in gradual changes in food web structure during assembly, whereas species sorting events can cause greater structural upheavals. Thus the probability of an invaded community satisfying inequality 2.4 and being Hurwitz stable (PHS) is crucial for understanding changes in food web structure. PHS is the probability of a randomly chosen community matrix from the space of all possible matrices with the same n, sign structure (the distribution of trophic links across species), and statistical properties of the intra- and interspecific interaction strengths. Before considering assembly dynamics in greater detail, I will show how particular food web structural features can be explicitly linked to community stability.

2.2.2 Interlinking food web structural features and community stability

In order to relate food web structure to PHS, we need to consider food web structural measures that directly determine the sign of the real part of the leading eigenvalue (inequality 2.4

). To this end, two approaches have been used in the past: the consideration of sign structure irrespective of interaction strengths, and the consideration of interaction strength structure, (distributions of interaction strengths across trophic links), with or without consideration of the strength structure (Logofet, 1993; May, 1974). The first approach requires the concept of sign stability. Sign stable communities have a pattern of trophic linking between species that guarantees Hurwitz stability irrespective of the magnitudes of the interaction strengths α_{ij} (or c_{ij}) (Logofet, 1993; May, 1974). Thus food web structural configurations that lead to sign stability can be determined. The problem with this approach is that one of the necessary conditions for sign stability precludes the presence of omnivory (because no cycles of length greater than three should be present; Logofet, 1993; May, 1974), even though it is prevalent in empirical food webs (Williams and Martinez, 2004). Here I will focus on the second approach for relating food web structure to stability: consideration of interaction strength structure. May's (1974) complexity measure is an example of this approach because it links PHS to average interaction strength for a given level of connectance (C_T), community size (n), and negative intraspecific density dependence. However, this measure and its refinements (Cohen and Newman, 1985; Geman, 1986; Hastings, 1982) do not show how species-level strategies and small-world food web structural features (involving the interactions between a few species) are related to stability. A solution to this was proposed by Neutel et al. (2007; 2002), who suggested that given the matrix $\underline{\boldsymbol{C}}$ with elements defined as,

$$\forall i, j \in \mathfrak{N},\ \underline{c}_{ij} = \begin{cases} \left|c_{ij}\right| & \text{if } i \neq j, \\ 0 & \text{if } i = j, \end{cases} \tag{2.5}$$

a community with a given level of intraspecific density dependence across species (the c_{ii}'s) was guaranteed to be globally stable (and hence Hurwitz stability) if the spectral radius,

$$\rho(\underline{\boldsymbol{C}}) \equiv \max\left\{\left|\mathrm{Re}\left(\lambda_i\left(\underline{\boldsymbol{C}}\right)\right)\right|\right\},\ \forall\ i \in \mathfrak{N} \tag{2.6}$$

is sufficiently small. Biologically, $\rho(\underline{\boldsymbol{C}})$ can be interpreted as a single measure of the overall interaction strength structure of the community. Thus food web structural properties that mitigate $\rho(\underline{\boldsymbol{C}})$ should be favored during community assembly (Neutel et al., 2007). In Appendix A I show that Neutel et al.'s conjecture is flawed ($\rho(\underline{\boldsymbol{C}})$ does *not* provide conditions for global stability),

but also that $\rho(\underline{\boldsymbol{C}})$ can still be related to Hurwitz stability because $\lambda_{max}(\boldsymbol{C})$ monotonically increases with it (crossing the critical boundary beyond some value of $\rho(\underline{\boldsymbol{C}})$) for certain sign structures. In such communities, PHS is inversely related to $\rho(\underline{\boldsymbol{C}})$, and any interaction strength configuration (within that sign structure) that determines $\rho(\underline{\boldsymbol{C}})$ can thus be related to stability. I call this property "interaction-strength sensitivity" (ISS), and can be estimated from the correlation coefficient between $\lambda_{max}(\boldsymbol{C})$ and $\rho(\underline{\boldsymbol{C}})$ (r_{ISS}) over a sufficiently large number of interaction strength randomizations (IS-randomizations; the simulation methodology is described in Appendix A). To gauge the prevalence of ISS in the real world, I examined sixteen relatively well documented community food webs from a variety of terrestrial and aquatic habitats (see Appendix C for data description). Table 2.1 indicates that all of them show some degree of ISS (r_{ISS} ranging from 0.08 to 0.83). Fig. 2.1 shows the actual relationship between $\lambda_{max}(\boldsymbol{C})$ and $\rho(\underline{\boldsymbol{C}})$ for two contrasting examples from these communities.

Given this wide variation in ISS of the sixteen communities, can a general conclusion be drawn about the prevalence and strength of ISS in nature? Table 2.1 also shows the correlation of r_{ISS} with a suite of commonly measured features of food web sign structure (Pascual and Dunne, 2005). Except mean vulnerability, r_{ISS} is significantly correlated with all of them, suggesting that multiple sign structural features tend to influence ISS. Note that these correlations need to be interpreted with the knowledge that these structural features are not mutually independent (for example, connectance and link density tend to be positively correlated). However, because all these sign structural measures are known to be sensitive to inadequate sampling of interactions (Goldwasser and Roughgarden, 1997) , these correlations also suggest that ISS may be underestimated across the communities. In this context, that r_{ISS} is most strongly correlated with mean trophic chain length and omnivory degree is particularly noteworthy because recent studies indicate that these features have been underestimated in the past due to the omission of host-parasite links (Lafferty et al., 2008). In fact, of the sixteen empirical food webs, all five that include parasites and parasitoids (Carpinteria Salt Marsh, Company Bay Mudflat, Scotch Broom, Grand Caricaie Marsh, and Ythan Estuary) show relatively high ISS.

Below I will show that model communities resulting from fairly general assembly algorithms also show consistently high ISS. Hence I concentrate on ISS in this paper, and consider food web structural properties that determine $\rho(\underline{\boldsymbol{C}})$ (and hence PHS) during assembly. To this end, in Appendix B I establish the following relationship between food web structure and $\rho(\underline{\boldsymbol{C}})$. First define the quantity,

$$\bar{\underline{c}}_{ij} = \sqrt{\underline{c}_{ij}\underline{c}_{ji}}\ ,\ \forall i, j \in \mathfrak{N} \tag{2.7}$$

i.e., geometric mean of the absolute magnitudes of each pair of interaction coefficients constituting a trophic link. The $\bar{\underline{c}}_{ij}$'s will henceforth be called "trophic link strengths" to differentiate them from the interaction strengths α_{ij}'s as well as the elements of $\boldsymbol{C}$. Now consider each species' "weighted generality", which is defined for the i^{th} species to be,

$$G_i^w = \sum\nolimits_{j\in\mathfrak{G}_i} \bar{\underline{c}}_{ij}, \forall\ i \in \mathfrak{N}\ ,` \tag{2.8}$$

where $\mathfrak{G}_i$ is the set of its resource species. Then, the following relationship holds (Appendix B):

$$\frac{2G_{tot}^w}{n} \le \rho(\underline{\boldsymbol{C}}), \tag{2.9}$$

where

$$G_{tot}^w \equiv \sum\nolimits_n G_i^w = \sum\nolimits_n \sum\nolimits_{j\in\mathfrak{G}_i} \bar{\underline{c}}_{ij}$$

i.e., the total weighted generality of species in the community. Expression 2.9 says that $\rho(\underline{\boldsymbol{C}})$ (and hence PHS in ISS communities) is limited by species' weighted generalities. Fig. 2.2 gives a graphic overview of the analytical steps that allow species trophic generality modules to be thus related to PHS.

The advantage of converting the c_{ij}'s into $\bar{\underline{c}}_{ij}$'s is apparent; the pair of interaction coefficients associated with each trophic link (effect of consumer on resource and *vice versa*) are reduced to a measure of the overall interaction strength. Moreover, from expressions 2.1b and 2.3, $\bar{\underline{c}}_{ij} = |\alpha_{ij}|\sqrt{e_i\hat{x}_i\hat{x}_j}$ (when i consumes j) and hence

$$G_i^w = \sqrt{e_i\hat{x}_i}\sum_{j\in\mathfrak{G}_i}\left(|\alpha_{ij}|\sqrt{\hat{x}_j}\right), \forall\ i \in \mathfrak{N}\ , \tag{2.10}$$

which shows that G_i^w is essentially a measure of the total biomass acquisition rate of the i^{th} species population at equilibrium. Thus expression 2.9 further implies that species with relatively high biomass acquisition rates tend to undermine community stability (decrease PHS) (assuming the species' negative intraspecific density dependence, i.e., self-regulation, is not too strong). I will now show that due to the dynamical stability constraints indicated by expression 2.9, the emergence of certain stabilizing

2.2.3 Predicted signatures of stability constraints on food web structure

I will now show that species' weighted generality modules are a fundamental feature that should result in a suite of food web structural "signatures" (specific non-random structural features) indicative of stability constraints during community assembly. During assembly, because the number of trophic links per species (link density, or L_D) typically increases with n (Martinez, 1992; because at least some residents acquire additional links at every immigration event; e.g., Piechnik et al., 2008), G_{tot}^w tends to increase, and hence PHS decreases. As assembly proceeds, PHS eventually decreases to the extent that stable invasions are approximately balanced by species sorting events (as defined in section 2.2.1 above), resulting in invasion-extinction quasi-equilibrium (IEE). At this stage, intermittent immigrations prevent the community from reaching a fixed equilibrium in the sense of expression 2.4, but on average, n remains constant over time (with variance proportional to immigration rate; see Bastolla et al., 2005). Thus as indicated by expression 2.9, during assembly, food web structural configurations that mitigate species' weighted generalities (relative to increasing L_D) will be favored by successive stable invasions and species sorting events. Furthermore, because G^w is a measure of the i^{th} species' total biomass acquisition rate (see expression 2.10), a reexamination of inequality 2.2 indicates a tradeoff between the invasibility of an immigrant and PHS of the augmented community; the immigrant's G^w should be sufficient to satisfy 2.2, but not so much as to destabilize the augmented community by increasing $\rho(\underline{\boldsymbol{C}})$ too much.

Thus the modulation of species' trophic generality characteristics such that G_{tot}^w is mitigated, will allow stable invasions and community growth during assembly, and maintenance of species richness at IEE. This means that species' generality-averaged weighted generality,

$$\bar{G}_i^w \equiv \frac{G_i^w}{G_i} = \frac{\sqrt{\hat{x}_i}\sum_{j\in\mathcal{C}_i}\left(|\alpha_{ij}|\sqrt{e_i\hat{x}_j}\right)}{G_i}, \forall i \in \mathfrak{N} \qquad (2.11)$$

should be mitigated (or constrained). Thus a species' $\bar{G}^w$ is the average of the strengths of trophic links it has with its resource species (or alternatively, a measure of its generality-averaged biomass acquisition rate). From expression 2.11, it is clear that assuming that efficiencies are similar across taxa, G_{tot}^w mitigation can happen by a modulation of either the interaction coefficients (α_{ij}'s), or equilibrium biomass sizes ($\hat{x}$'s). The contribution of changes in species' consumption strategies alone (without the effects of the $\hat{x}$'s) can be gauged by the degree to which generality-averaged interaction strengths,

$$\bar{\alpha}_{G,i} \equiv \frac{\sum_{j \in \mathcal{B}_i} |\alpha_{ij}|}{G_i}, \forall i \in \mathfrak{N} \tag{2.12}$$

are constrained. Apart from stable invasions and species sorting, this can also happen by behavioral or evolutionary changes in species' consumption characteristics (although not within the confines of LVM model, where the coefficients α_{ij} are assumed to be constant) (e.g., Drossel et al., 2004; Loeuille and Loreau, 2005; Uchida et al., 2007). On the other hand, changes in equilibrium biomasses ($\hat{x}$) can happen through trophic cascades (Pace et al., 1999; Polis et al., 2000). For example, some populations may equilibrate at lower biomass densities due to density effects propagated along trophic chains upon the successful invasion of a new species (Neutel et al., 2007; Neutel et al., 2002). Thus, by considering the dynamics of food web structural changes during community assembly, it can be inferred that repeated stable invasion and species sorting events (see section 2.2.1) should favor to the emergence of the following two signatures of stability constraints on food web structure at IEE:

(i) *A negative correlation between species' generality (G) and* $\bar{G}^w$. Because G^w's should be mitigated during assembly due to stability constraints, increasing generality of a species should be offset by a decrease in its $\bar{G}^w$ (expression 2.11). This relationship can be measured by a correlation coefficient (see below), and will henceforth be denoted by $r\left(G, \bar{G}^w\right)$.

(ii) *A negative correlation between species' trophic level and* $\bar{G}^w$. Later immigrants arrive at a community that is progressively being saturated (approaching IEE). Hence, if community assembly is such that later immigrants tend to occupy successively higher trophic levels (*TL*'s)(i.e., are more likely to occupy the role of consumers rather than resources), community

augmentation will be facilitated if species at higher trophic levels have relatively lower $\bar{G}^w$'s. This signature will henceforth be denoted by $r\left(TL, \bar{G}^w\right)$.

2.3 Signatures of stability constraints in simulated model communities

The emergence of the food web structural signatures predicted in the previous section (2.2.3) is tightly linked to the pattern of community assembly. Hence I now perform numerical simulations to evaluate the robustness of the above analyses by studying assembly dynamics and food web structural changes in model communities.

2.3.1 Methods

The community assembly algorithm consisted of three steps based upon the LV model (equation 2.1):

- *Immigration*. Beginning with the establishment at least one basal species, at 1000 time step intervals, a species population was introduced at an extinction threshold biomass abundance x_e. Each immigrant species was generated by randomly sampling death rate d_i, interspecific interaction coefficients α_{ij}, and intraspecific density-dependence coefficient α_{ii} from the half-normal probability distribution (distribution of the absolute value of a normally distributed random variable with mean 0 and variance σ^2) with fixed means (denoted by μ_d, $\mu_{\alpha,ij}$ and $\mu_{\alpha,ii}$, respectively). The mathematical specification of this distribution and the justification for using it is given in Appendix A. The consumption efficiency of all consumers was fixed at some value e.
- *Trophic linking*. Upon colonization, the j^{th} immigrant established a trophic link to the i^{th} pre-existing one with a connectance probability p_c. For each assembly simulation, conditional upon p_c, I also set a "vulnerability probability" p_v ranging between 0.5–1; $p_v = 0.5$ meant that the j^{th} immigrant was equally likely to be a resource or a consumer of the i^{th} resident species (provided it was not basal), while $p_v = 1$ meant that the j^{th} immigrant could only be a consumer. p_v replaces the more strict trophic linking rules of static food web structural models such as "cascade" (immigrants can only feed on resident species below them in a undimensional niche ranking; Cohen et al., 1990) and "niche" (immigrants can only feed on resident species that lie within some interval representing a undimensional niche; Williams and Martinez, 2000), because recent studies that include parasites suggest that all consumers

do not necessarily feed according to such rules (Lafferty et al., 2008). Instead, depending upon the choice of p_v, trophic structures lying on a continuum ranging from relatively non-hierarchical with cycles (such as that resulting from the niche model; Williams and Martinez, 2000) at $p_v = 0.5$, to hierarchical and acyclic (such as that imposed by the cascade model; Cohen et al., 1990) at $p_v = 1$, can be assembled.

- *Interaction driven extinction*. After immigration, the augmented system was integrated forward for 1000 time steps, during which most populations either reached a nonzero equilibrium size or went extinct. A species was considered extinct and deleted from the system if its density dropped below x_e, or decreased during this period.

This algorithm was iterated till the system reached IEE. Simulations were performed in MATLAB using the Runge-Kutta one-step solver ode45. During each assembly simulation run, changes in key community characteristics were measured at 1000 time-step intervals (coinciding with the interval for numerical integration).

Simulation parameters and their numerical ranges are listed in Table 2.2. 150 replicated assembly simulations were executed, with a total number of time steps sufficient to reach IEE given a particular combination of parameter values. In the LV model, the main factors determining species richness at IEE are the strength of intraspecific density dependence relative to interspecific interactions, and connectance. Hence, for a given p_C and $\mu_{\alpha,ij}$, $\mu_{\alpha,ii}$ was chosen according to a target mean species richness at IEE. For example, for $p_C = 0.3$ and $\mu_{\alpha,ij} = 1$, to obtain webs that reached 50 species on average at IEE, $\mu_{\alpha,ii}$ had to be set to 4. Across all simulations, μ_d was chosen to be orders of magnitude smaller than $\mu_{\alpha,ij}$ and b_i in keeping with the patterns observed in empirical data (cf. Peters, 1983). For all the results shown below, communities were assembled on a single basal species with autonomous biomass production rate of 1. The conversion efficiency for all species was chosen to be 0.5. Simulations with greater variation in number of basal species, connectance probability, intrinsic biomass loss rates, efficiency, or extinction threshold (parameter ranges given in Table 2.2) only affected the size of communities at IEE, and not the main results. The use of a uniform instead of the half-normal distribution also did not alter the main results. Furthermore, similar results were obtained using discrete time assembly simulations (using the recursive form of equation 2.1).

2.3.2 Results

ISS of model communities. Because we are interested in modeling the dynamics and structure of interaction strength sensitive communities, it is first necessary to gauge the ISS of sign

structures resulting from the above assembly algorithm. Fig. 2.3 compares the r_{ISS} for communities assembled from the trophic linking rules of the dynamical assembly algorithm with those of the cascade (Cohen et al., 1990) and niche (Williams and Martinez, 2000) models (for a detailed description of the assembly rule sets of the latter two models, see Stouffer et al., 2005). For each model, I generated sets of 50 communities across different values of n for the same expected value of connectance. Fig. 2.3 shows that in all community types, r_{ISS} increases asymptotically with n, reaching values comparable with those of empirical communities with high ISS (Table 2.1). Within communities assembled using the dynamical assembly rules, for a given n, r_{ISS} increases with p_v (i.e., non-hierarchical communities show more ISS). This is consistent with patterns of ISS in empirical communities, where relatively non-hierarchical communities with higher omnivory degrees tend to have higher r_{ISS} than the others (see Table 2.1 and section 2.2.2). Note that on the other hand, the association between n and r_{ISS} in model communities need not necessarily be seen in the empirical ones because the latter have variable connectance (Table 2.1), resulting at least partly from uneven sampling of interactions (see section 2.2.2). The r_{ISS} curves for the cascade and niche models are comparable to those of the dynamical model, especially for $p_v = 1$. Thus at least as far as ISS of the sign structure is concerned, the simpler trophic linking rules of the dynamical assembly algorithm are able to produce communities comparable to those assembled from static structure models.

Signatures of stability constraints on the structure of model food webs. Fig. 2.4 shows the three predicted signatures of stability constraints observed at IEE in a typical model community assembled with an intermediate p_v value (0.75). Because of the nonlinear change of $\bar{G}_i^w$ in all three signatures, their strengths were measured using the Spearman rank correlation coefficient. Table 2.3 compares the incidences and strengths of signatures for communities assembled at different levels of trophic hierarchy. All three signatures are seen across assembly types, but as expected, the decrease in weighted generality with trophic level ($r\left(TL, \bar{G}^w\right)$) was the weakest with lowest incidence in relatively non-hierarchical communities ($p_v < 1$) (see section 2.2.3). Surprisingly, the other two signatures also became less pronounced as $p_v \rightarrow 0.5$ even though ISS increases in the same direction (see "*ISS of model communities*" above), suggesting that relaxation of hierarchical assembly decreases stability limitations on communities. This conclusion is supported by the fact that average n at IEE increased as $p_v \rightarrow 0.5$ (Table 2.3).

Fig. 2.5 shows actual changes in community characteristics during assembly (for $p_v = 0.75$) that culminate in the structural signatures seen in Fig. 2.4 and Table 2.3. As link density (L_D)

increases with n during assembly (Fig. 2.5a&b), so do G_{tot}^{w} and $\rho(\underline{\boldsymbol{C}})$ (Fig. 2.5c&d). As expected, G_{tot}^{w} increases linearly with L_D (Fig. 2.5c inset), and $\rho(\underline{\boldsymbol{C}})$ with G_{tot}^{w}/n (Fig. 2.5d inset) (the latter as indicated by expression 2.9). The numbers of extinctions, which include both failed invasions and species sorting events (counted in epochs of 1000 time steps) also increase and then equilibrate, resulting in IEE. Again as expected, the numbers of extinctions increase linearly with G_{tot}^{w}/n (because it increases $\rho(\underline{\boldsymbol{C}})$). Finally, Fig. 2.5f shows changes in the most fundamental of the two signatures ($r\left(G,\bar{G}^{w}\right)$), and the contribution of changes in species' trophic generality characteristics ($\bar{\alpha}_i$) alone to it ($r(G,\bar{\alpha})$). For both, an increasingly negative correlation is seen as assembly proceeds, indicating the increasing level of stability constraints (decreasing PHS) with assembly. As Table 2.1 indicates, patterns similar to those in Fig. 2.4 were seen in communities assembled at p_v =1 and 0.5, but with a more gradual decline in $r\left(G,\bar{G}^{w}\right)$ and $r(G,\bar{\alpha})$ (result not shown).

Signatures of stability constraints on the structure of model food webs. In order to compare communities assembled under stability constraints with those assembled under relatively weaker constraints ("relaxed assembly"), I increased the value of $\mu_{\alpha,ii}$ while keeping all other parameter values the same. This imposed higher intraspecific density dependence across species, which increased the PHS, and hence decreased the number of extinctions due to species sorting events. Because increasing $\mu_{\alpha,ii}$ results in larger feasible communities, assembly was terminated when n reached the average IEE species richness value of dynamically constrained communities assembled using the same parameter values. Fig. 2.6a shows that during relaxed assembly, the number of epochal extinctions decreases as expected (reflecting a decrease in the number of species sorting events). Fig. 2.6b&c show that as a result, the decline in $r\left(G,\bar{G}^{w}\right)$ and $r(G,\bar{\alpha})$ becomes weaker (the structural signatures of stability constraints emerge more slowly).

2.4 Discussion

This study is a step towards bridging the gaps in our understanding of the interrelationship between community assembly, stability, and food web structure. I have shown that natural communities typically show a sign structure that renders their Hurwitz stability sensitive to the distribution of interaction strengths (ISS, estimated using r_{ISS}). In such communities, consumer species with a high weighted generality (a measure of their total biomass acquisition rate) tend to

undermine community stability. As a result, species associated with trophic modules carrying high weighted generality are eliminated through a process of repeated colonization and extinction (species sorting) events during community assembly. This ultimately results in the emergence of a non-random food web structure wherein weighted generality has been constrained across species. This can be detected using two distinct food web structural signatures (section 2.2.3 and Fig. 2.4), the incidences and strengths of which can allow a measurement of the importance of stability constraints during assembly. The overall picture that emerges is fascinating, wherein communities assemble and persist through dynamic feedbacks between food web structure and stability, resulting in certain non-random structural configurations. The predicted existence of signatures of stability constraints is an interesting and important result because it means that the influence of stability constraints imposed by the requirement of multi-species stable coexistence can be inferred from snapshots of community food web structure in nature.

To the best of my knowledge, this is the first study to explicitly show how interaction strength properties of food web structural modules consisting of consumer species and their trophic links affect community stability. Previous such studies have focused on the effects of trophic chains (Pimm and Lawton, 1977), loops (Neutel et al., 2002) and omnivory (Neutel et al., 2007). Further studies are needed to compare the importance of these different structural features to community stability. Insofar that trophic generality is a small world property of food webs, the results of this study are in agreement with those of Allesina and Pascual (2008), who used a different theoretical technique to show that small predator-prey modules (consisting of groups of a few connected species) have strong effects on community stability.

Because the above structural signatures involve a measure of foraging characteristics of consumers, they provide deeper insights into the feedback between community-level dynamics of multi-species coexistence and individual species' survival strategies. Thus the frequently observed pattern that interaction strength distributions are skewed towards weaker values, presumably due to stability constraints (Berlow et al., 2004; Drossel et al., 2004; McCann et al., 1998), can now be linked to changes in trophic properties of single species or small groups of species. This is important because treating each trophic link as an entity that can be somehow modulated independent of other links is inconsistent with the fact that biological mechanisms either affect aggregate properties of trophic modules consisting of multiple species (e.g., as seen in species sorting), or individual species' trophic characteristics as a whole (e.g., behavioral or adaptive changes in a species' foraging strategies simultaneously affect all its trophic links).

In terms of food web structural changes during assembly, the above results complement those of a recent study by Neutel *et al*. (2007; 2002), who find evidence for directional changes in

distributions of interactions along trophic loops and 3-species omnivorous trophic modules in soil community food webs, also driven by stability constraints. Apart from their focus on different structural features, there are two key differences between the results of this study and those of Neutel et al. First, they only consider stability constraints on species' equilibrium biomasses ($\hat{x}$'s; one of the two components of each interaction strength at equilibrium; see expression 2.3), and the stabilizing effects of trophic cascades (as defined in section 2.2.3 of this paper). However, here I have shown that stability constraints can also force interaction strengths (α_{ij}'s) to decrease through modification of species' trophic characteristics such that the $\overline{\alpha}$'s (expression 2.12) are constrained across species (see Fig. 2.5f). This also means that in contrast to the conclusions of some recent papers (Beckerman et al., 2006; Petchey et al., 2008), species' foraging strategies are expected to be determined not just by their energetic requirements, but also by their impact on community stability. Second, Neutel et al. (2007; 2002), stress upon the importance of asymmetry in top-down and bottom up effects (the pairs of coefficients c_{ij} and c_{ji} respectively, when j eats i) on stability, whereas I have shown here that a measure that combines these effects (the trophic link strengths $\overline{c}_{ij}$; expression 2.7) can provide simpler insights into the relationship between food web structure and stability.

Because ISS is essentially a measure of the lack of quasi-sign stability (QSS) (as defined by Allesina and Pascual, 2008), it is interesting to compare the results of this study with theirs. A problem that precludes a direct comparison is that only three communities are common between the two studies. This is because I imposed certain criteria for selecting datasets (see Supplementary Appendix 1) and used additional datasets apparently not considered by them. Nevertheless, the levels of r_{ISS} observed across the communities in this study clearly indicate that QSS may not be as prevalent as suggested by Allesina and Pascual (2008). Moreover, I also found some evidence that interaction strength sensitivity might be underestimated in natural communities because of inadequate sampling of trophic interactions (see section 2.2.2). In particular, community food web datasets that include host-parasite links tend to show stronger ISS, suggesting that the inclusion of such interactions has non-trivial effects on the elucidation of population dynamical properties of communities, and their effects on food web structure, as has been suggested by recent studies (Lafferty et al., 2008; Marcogliese, 2003; Marcogliese and Cone, 1997).

2.4.1 Caveats

The importance of instraspecific density dependence. In deriving the relationship between interaction strength structure and community stability (section 2.2.2), I have largely ignored the role of the diagonal elements of C by assuming them to be fixed (or lying within a fixed range). However, a community can also be stabilized by increasing the diagonal elements c_{ii} (i.e., the negative intraspecific density dependences). The importance of this issue depends upon how strong intraspecific density dependence is in nature (and how it is regulated). There is some direct evidence for such effects in real systems (e.g., Agrawal et al., 2004; Schmitt and Holbrook, 2007), and more empirical studies are needed on the feedback between intra-population interactions and community stability, or the relationship between inter- and intraspecific interactions (e.g., Bystrom and Garcia-Berthou, 1999; Kratina et al., 2009; Wahlstrom et al., 2000).

Other mechanisms of interaction strength modulation. Further studies are needed to understand the mechanisms by which G_{tot}^{w} mitigation actually occurs. This will lead to the development of more detailed hypotheses about the signatures of stability constraints of food web structural features. To this end, we need to look well beyond basic Lotka-Volterra type models for a comprehensive understanding of stabilizing mechanisms. These mechanisms include adaptive foraging behavior and physiological changes (e.g., consumer functional response) and coevolution. In particular, consumer functional responses (wherein the α_{ij}'s change in response to increasing availability of resource species' biomass abundance) are relevant at ecological time scales. Under certain assumptions, the inclusion of functional responses into the above model will not affect the main results of this study. To see this, let us assume a type II saturating functional response of the j^{th} consumer to increasing availability of i^{th} resource species' biomass abundance such that α_{ij} decreases with increasing x_i,

$$g_{ij}(t) = \frac{\alpha_{ij}}{1 + \frac{1}{x_{0,j}} \sum_{k \in G_j} \left(\alpha_{kj} x_k(t) \right)}$$

where given the set of resource species $\mathcal{G}_j$ of the j^{th} consumer, α_{ij} is the average per-unit biomass exploitation exerted by the j^{th} consumer on the i^{th} resource species, and $x_{0,j}$ the half-saturation constant of total resource species' biomass density (Drossel et al., 2001; Ramos-Jiliberto, 2005). As $x_{0,j} \to \infty$ of course, $g_{ij}(t) \to \alpha_{ij}$, and the linear (Type I) functional response assumed in the main analysis above is recovered. Now consider the case where $x_{0,j} \to 0$, i.e., (consumers show satiation

to increasing resource availability). As such, the stability definition in section 2.2.1 above only holds if the solution of the system (equation 2.1) is time independent, i.e., it is a unique point equilibrium in $\mathbb{R}_+^n$. On the contrary, it is known that non-linear functional responses can lead to stable coexistence without a point equilibrium (e.g., limit cycles)(Armstrong and McGehee, 1980; Oaten and Murdoch, 1975). Hence, using the above approach of interrelating food web structural measures and stability raises potentially intractable analytical problems. However, if consumers experience negative density dependence ($g_{ii}(t) < 0$) bounded solutions with minimal cycles can be guaranteed (Ikeda and Siljak, 1982). Hence, assuming some level of intraspecific density dependence across consumers, we expect that as populations settle into their equilibrium biomass densities, the Jacobian matrix ($\boldsymbol{C}$) evaluated at the approximate equilibrium $\hat{\boldsymbol{x}}$ (analogous to expression 2.3) will tend towards relative time independence. Hence, the above analysis should also hold with type II responses as long as a sufficient number of species experience negative density dependence.

Other definitions of stability. Only one of many different definitions of stability (Grimm and Wissel, 1997; Ives and Carpenter, 2007) has been used in this study. Some of these definitions are more general than Hurwitz stability, either because they guarantee global stability of the multi-species point equilibrium ($\hat{\boldsymbol{x}}$), or do not require a point equilibrium (e.g., permanence; see Hofbauer and Sigmund, 1998; Law and Morton, 1996). This is an important consideration because in Lotka-Volterra type models, populations may actually converge to the vicinity of a periodic or chaotic attractor instead of a point equilibrium (e.g., see Gilpin, 1979). I have ignored this in the above analysis by using the Jacobian matrix and the Hurwitz stability criterion, because it allows food web structure to be explicitly linked to community stability (also see May, 1974). The numerical simulations of section 2.3 show that the predictions about the relationships between food web structure and stability based upon this assumption are well supported, indicating either or both, that periodic or chaotic population trajectories are not dominant, and that they not substantially alter the predicted relationship between food web structure and stability. Another reason why others definitions of stability need to be explored is that some of them quantify the speed of return to equilibrium following external perturbations (e.g., resilience; Harrison, 1979). For example, in addition to Hurwitz stability, the distribution of interaction strengths in the community matrix $\boldsymbol{C}$ also determines short- and long-term population dynamics following external perturbations (Neubert et al., 2004). Further work will show how food web structure is related to such measures of stability.

Applicability to nontrophic interactions. Finally, though I have only considered trophic interactions in this study, population dynamics in real communities are also partly governed by interspecific competitive and mutualistic interactions. Hence it is worth noting that the fundamental results of this study do not change even upon the inclusion of these interaction types, because we will still only need to consider the nonnegative matrix $\underline{\boldsymbol{C}}$

Tables

Table 2.1. The interaction strength sensitivity of sixteen empirical communities (shown in order of decreasing r_{ISS}), estimated from 2000 IS randomizations. All correlation coefficients are highly significant (two-tailed p <0.0005). Various food web characteristics and their correlation with r_{ISS} (r^2 values in parentheses) (Spearman's rank correlation) are also shown: species richness (n), link density (L_D), connectance (C_T), average generality of consumers ($\overline{G}$), average vulnerability of resources ($\overline{V}$), average trophic chain length ($\overline{T}_c$), and omnivory degree (O_{deg}). Correlations with p <0 .05 and <0.005 are flagged with a single and double asterisk, respectively. $\overline{T}_c$ was estimated from a sample of all paths (to all consumers) arising from basal species (obtained using the path search algorithm described in Appendix D). O_{deg} is the mean of the standard deviations of each consumer species' trophic height (standard deviation of the lengths all the paths to the species from all its basal species (Goldwasser and Roughgarden, 1993)).

Name	r_{ISS}	n	L_D (0.26*)	C_T (0.30*)	$\overline{G}$ (0.32*)	$\overline{V}$ (0.15)	$\overline{T}_c$ (0.65**)	O_{deg} (0.54**)
Carpinteria Salt Marsh	0.83	125	14.4	0.23	16.6	14.8	7.4	2.7
Skipwith Pond	0.82	33	9.7	0.61	17.8	10.4	4.2	0.6
Broadstone Stream	0.78	28	4.9	0.37	15.3	5.1	4.6	0.8
Company Bay Mudflat	0.77	76	6.8	0.18	7.5	7.8	6.9	1.5
Scotch Broom	0.72	153	2.4	0.03	10.2	77.0	3.2	0.1
Grand Caricaie Marsh	0.71	163	12.8	0.16	24.0	12.9	4.8	1.1
Caribbean Sea	0.59	248	13.1	0.11	13.5	13.1	4.6	0.5
Bridge Brook Lake	0.57	73	7.3	0.20	15.8	7.5	3.4	0.2
Ythan Estuary	0.56	121	3.3	0.05	6.1	63.5	3.1	0.6
Eastern Weddell Sea	0.49	391	4.3	0.02	9.5	196.0	2.9	0.2
Tuesday Lake	0.48	72	5.4	0.15	12.3	5.7	3.8	0.2
Martins Stream	0.45	96	2.7	0.06	5.4	3.7	2.9	0.2
Little Rock Lake	0.32	117	4.3	0.07	5.6	7.2	3.9	0.3
Dempster's Tussock Stream	0.28	107	9.0	0.17	16.9	10.3	3.1	0.3
Mill Stream	0.17	74	5.0	0.14	8.2	10.5	1.2	0.0
North Carolina Pine Logs	0.08	90	1.7	0.04	1.7	4.0	1.7	0.0

Table 2.2. Simulation parameters and their values used for assembling model communities.

Parameter	Description	Values
p_c	Connectance probability	0.3
p_v	Vulnerability probability	0.5 – 1
$\mu_{\alpha,ij}$	Mean of half-normal probability distribution to sample interspecific interaction coefficients	1-10
$\mu_{\alpha,ii}$	Mean of half-normal probability distribution to sample intraspecific interaction coefficients	Dependent upon $\mu_{\alpha,ij}$ and target community size
x_e	Extinction threshold	$10^{-32} – 10^{-3}$
e_j	Conversion efficiency of j^{th} consumer	0.1 – 1
b_i	Intrinsic birth rate of i^{th} basal species	$1 – 10^{10}$
μ_d	Mean of half-normal probability distribution to sampe intrinsic death rates	$0 – 10^{-3}$

Table 2.3. Signatures of stability constraints in model food webs at IEE: correlation (Spearman's rank correlation coefficient) between species' generality and generality-averaged weighted generality ($r\left(G,\bar{G}^{w}\right)$), and trophic level ($r\left(TL,\bar{G}^{w}\right)$). Tabulated values give the percentage of 150 model food webs that showed the expected negative correlation (Spearman's rank correlation coefficient) with a *p*-value <0.01 (two-tailed), along with the mean value (±SD) of corresponding correlation coefficients in parentheses. Features in columns 2 & 3 correspond to those in Fig. 2.4a&b. The mean species richness (±SD) values at IEE for each assembly type are also shown.

Assembly type (p_v)	Species richness at IEE	Signatures of stability constraints	
		$r\left(G,\bar{G}^{w}\right)$	$r\left(TL,\bar{G}^{w}\right)$
1	39.7 (±5.5)	100 (-0.78±.07)	100 (-0.82±.08)
0.75	46.4 (±9.6)	100 (-0.65±.08)	52 (-0.67±.10)
0.5	50.1 (±10.8)	100 (-0.63±.08)	18 (-0.34±.12)

Figures

Figure 2.1. The relationship between $\lambda_{max}(\boldsymbol{C})$ and $\rho(\underline{\boldsymbol{C}})$ across 2000 IS-randomizations in two empirical community food webs: (A) Mill stream (r_{ISS} = 0.08) and (B) Skipwith pond (r_{ISS} = 0.83).

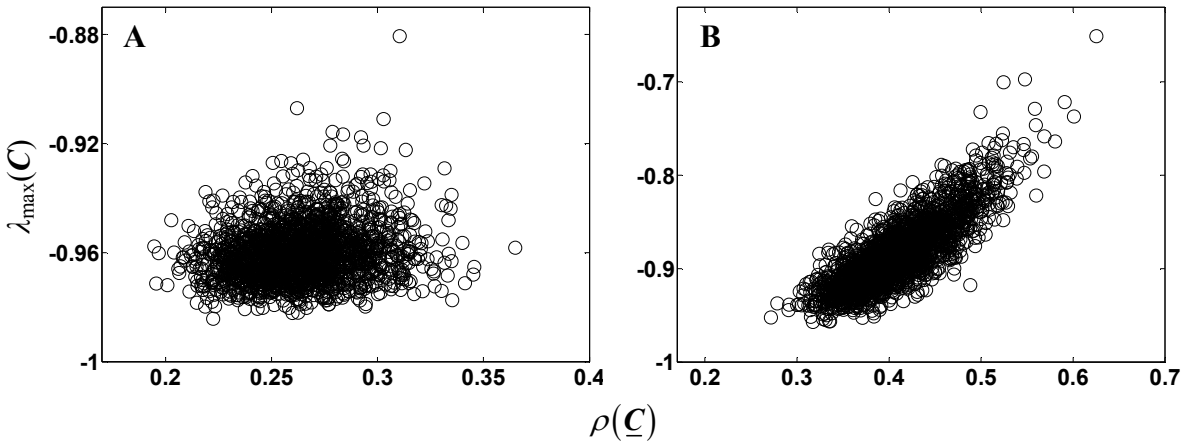

Figure 2.2. The analytical steps involved in interrelating food web structure and Hurwitz stability illustrated using a hypothetical four-species community. (a) The community matrix C (as defined in expression 2.3) and associated network representation. The interaction sign structure is represented using Levins (1974)'s scheme: edges ending in arrows represent positive effects (and direction of biomass flow) and those ending in circles, negative ones. (b) The simplified matrix $\underline{\boldsymbol{C}}$ (with elements defined in expression 2.5) and associated network representation. (c) The symmetrized matrix $S(\underline{\boldsymbol{C}})$ (with elements $\overline{\underline{c}}_{ji} = \overline{\underline{c}}_{ij} = \sqrt{\underline{c}_{ij}\underline{c}_{ji}}$; see Appendix B) and the associated network representation into species' trophic generality modules (these modules and their corresponding interaction coefficients are enclosed in dashed boxes).

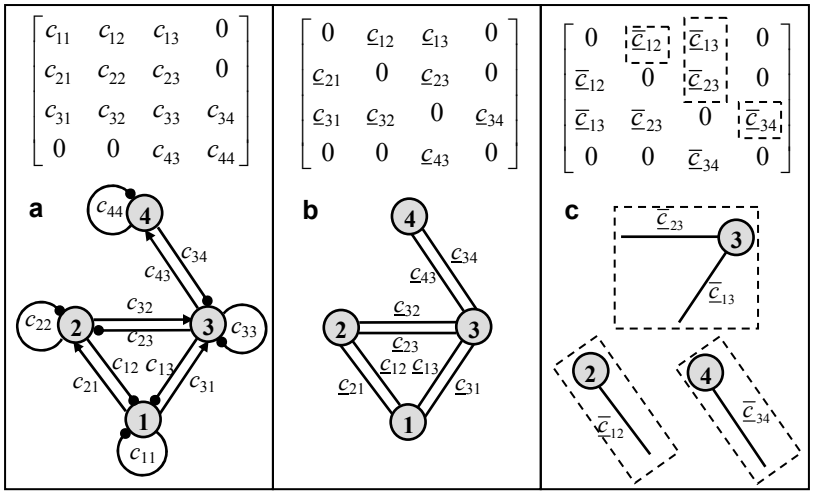

Figure 2.3. Change in ISS with increasing species richness in communities assembled using the trophic linking rules of the dynamical assembly algorithm (section 2.3.1), as well as two static food web structural models (niche and cascade). For each species richness value in each community type (a specific assembly algorithm), the mean ISS across 50 communities is shown with 99% confidence intervals. ISS was estimated from 2000 IS-randomizations. All assembly algorithm runs had the same connectance probability (p_c = 0.3).

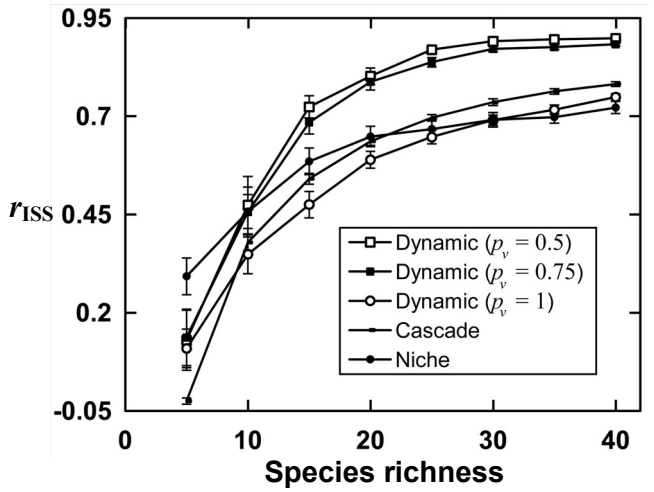

Figure 2.4. Signatures of stability constraints on food web structure in a 45-species community at IEE: The correlation of $\bar{G}^w$ with species' (a) generality (G), and (b) trophic level (TL). The same measures in a typical community assembled with weaker constraints ($\mu_{\alpha,ii}$ = 100; see Fig. 2.6) are shown in the inset figures. This community was assembled with p_v = 0.75; changes in the incidence and strengths of these signatures with variation in p_v are summarized in Table 2.2.

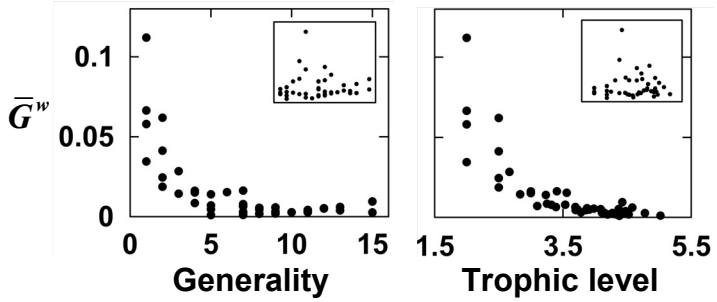

Figure 2.5. Changes in key food web properties of model communities during assembly. Mean values with 99% confidence intervals (grey lines) across 150 simulation runs over 350000 time steps are shown for, (a) species richness (n), (b) Link density ($L_D = L/n$), (c) total weighted generality (G_{tot}^{w}), (d) spectral radius of $\underline{\boldsymbol{C}}$ ($\rho(\underline{\boldsymbol{C}})$), (e) the total number of extinctions in 1000 time step epochs, and (f) Spearman rank correlation coefficient between generality and $\bar{G}^{w}$ ($r\left(G,\bar{G}^{w}\right)$) (lower lines) and $\bar{\alpha}$ ($r\left(G,\bar{\alpha}\right)$)(upper lines). The relationships of features b-f with those that directly determine them are shown in the inset figures. These assembly trends are for $p_v = 0.75$ communities; similar trends are seen across the range $0.5 \leq p_v < 1$. For a given p_v, these assembly patterns remain essentially the same across a wide range of parameter values (see Table 2.2).

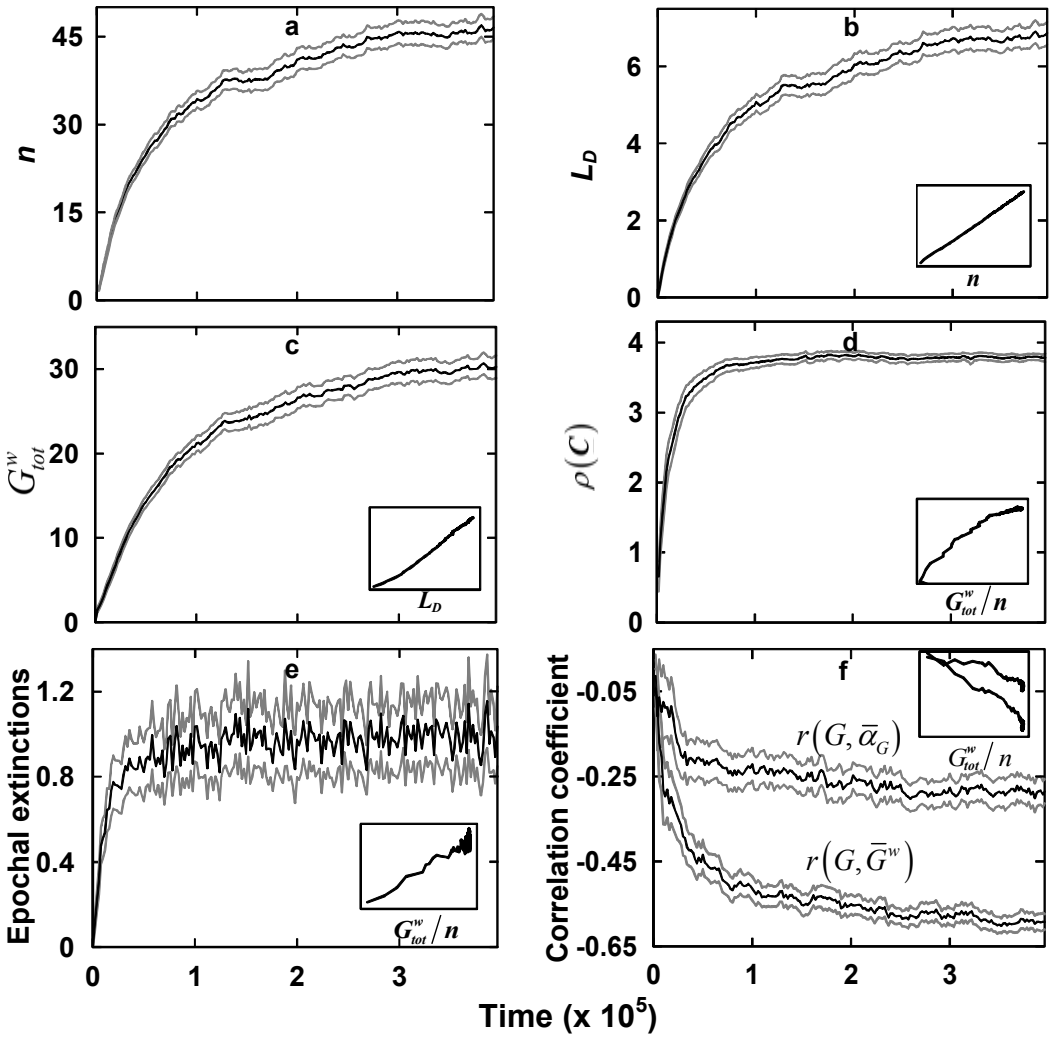

Figure 2.6. The effect of relaxation of stability constraints (increasing $\mu_{\alpha,ii}$) on changes in key structural signatures during assembly of model communities, for p_v = 0.75. Mean values with 99% confidence intervals (grey lines) of 150 assembly simulation runs over 350000 time steps for, (a) logarithm of the cumulative number of extinctions in 1000 time-step epochs (b) $r\left(G,\bar{G}^w\right)$ and (c) $r\left(G,\bar{\alpha}_G\right)$. Each variable is plotted against n to allow comparison between different types of assembly. In contrast to Fig. 2.5e, extinction trends are shown as a logarithm of cumulative numbers to allow visual comparison of the three different assembly types, which have large differences in extinction numbers. Also note that the assembly trends for $\mu_{\alpha,ii}$ = 4 are from the same simulations shown in Fig. 2.5. These differences between communities assembled under different $\mu_{\alpha,ii}$'s were similar across wide ranges of values of other model parameters (see Table 2.2). The greater fluctuations in all lines representing $\mu_{\alpha,ii}$ = 4 (dynamically constrained assembly) towards the later assembly stages is a result of the fact that the communities are at IEE on average.

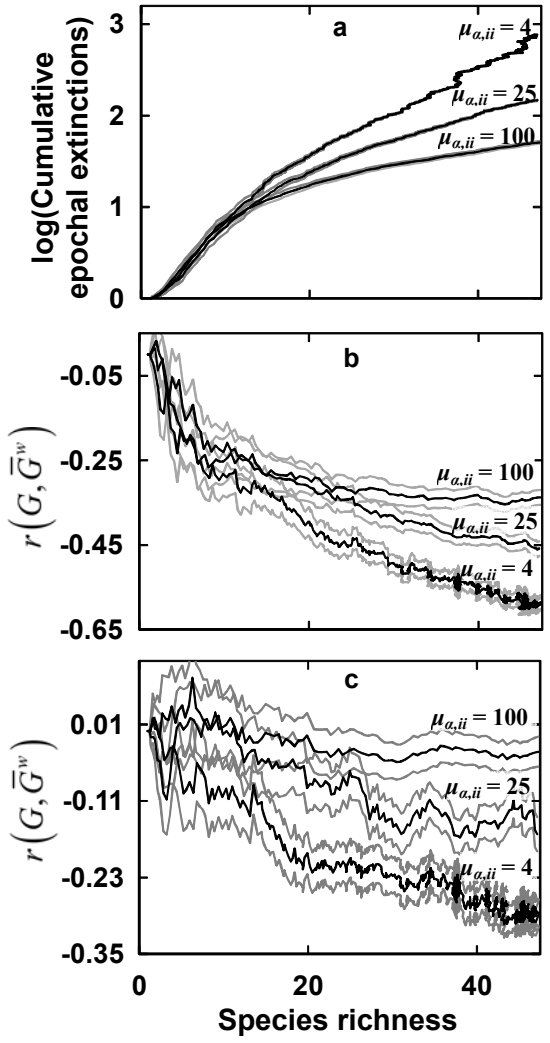

Chapter 3: The effect of species body size variation on community assembly, stability and food web structure

Abstract. Understanding the survival of species within the context of their community is a fundamental challenge in biology. Multispecies systems consist of potentially complex interrelationships between the structure of the interaction network, dynamics of individual species populations, and the stability of the system as a whole. For understanding these interrelationships, and for addressing fundamental questions about the survival of species in nature, the study of food webs is crucial because the most tangible interactions in natural communities are typically those involving consumers and their resources (e.g., predators and prey). In this paper, I use well established allometric relationships between body size and key life history parameters to interlink individual level metabolic constraints, community stability, and food web structure in a Lotka-Volterra type population dynamical model. I show that using this approach, three aspects of communities that have typically been studied in isolation can be interrelated: the body mass distribution of all species in the community, the distribution of consumer-resource (e.g., predator-prey) body mass ratios across trophic links, and certain food web structural features. Some of these features have previously lacked explanatory models. These ostensibly disparate properties are interrelated because individual metabolism and body-size difference between consumers and resources influences interspecific interactions, and the system's stability constraints drive the emergence of certain structural features of food webs that allow coexistence of multiple species' populations. The results yield a suite of testable predictions about food web structure that constitute unequivocal "signatures" of the importance of species interactions in structuring local communities. A survey of the literature shows that most of these signatures have hitherto been reported in various empirical studies, indicating broad support for the theoretical predictions of this study.

3.1 Introduction

Over the last decade or so, the use of species' body sizes to parameterize trophic interactions has emerged as an important tool for studying the feedback between food web structure and community stability. Body size is an important factor in this context because natural communities can consist of species with average body sizes spanning >20 orders of magnitude (Brown et al., 2004; Peters, 1983). Body size constrains interspecific trophic interactions in two distinct ways.

First, the whole organism metabolic rate increases allometrically with body mass according to a remarkably consistent power law relationship (Brown et al., 2004; Kleiber, 1961; Peters, 1983). This in turn determines species life history characteristics such as biomass production, birth, and mortality rates. Second, depending upon the environmental context, the average size difference between individuals of consumer and resource species sets physical limits on the frequency with which the two encounter each other, as well as the rate at which the former can exploit the latter following encounter (Aljetlawi et al., 2004; Dial et al., 2008).

The importance of body size was first considered in the 1950's as a driver of foraging preferences and niche differentiation in communities (Brown and Wilson, 1969; Hutchinson, 1959; Hutchinson and MacArthur, 1959). However, the actual incorporation of the size-metabolism allometry in models of community dynamics appears to have been pioneered by Peters (1983), who used it to parameterize trophic interactions in a simulation model of community assembly. Subsequently, Yodzis & Innes (1992) also used allometric scaling to parameterize the Rosenzweig-MacArthur predator-prey model (Rosenzweig and MacArthur, 1963). Since then, the use of body size in empirical descriptions as well as theoretical models of trophic interactions and food webs community ecology has rapidly increased, especially in the last five years or so (Berlow et al., 2009; Brose et al., 2006a; Brose et al., 2008; Jonsson and Ebenman, 1998; Lewis et al., 2008; Loeuille and Loreau, 2005; Otto et al., 2007; Petchey et al., 2008; Vasseur and McCann, 2005; Virgo et al., 2006; Weitz and Levin, 2006; Woodward et al., 2005a; Woodward et al., 2005b). An important consensus that appears to be emerging from recent theoretical studies in this area is that composition of species in communities is partly driven by the constraints of stable multi-species coexistence (community stability) mediated by their body sizes. In other words, consumer-resource interactions between certain species pairs can destabilize communities because the constraints of their body sizes. This has been demonstrated in multiple ways. For example, Loeuille & Loreau (2005) simulated community assembly and showed that specific food web configurations emerge repeatedly due to repeated speciation (mechanistically equivalent to immigration in their model) and interaction driven extinction events. On the other hand, Emmerson & Raffaelli (2004), Brose et al. (2006a) and Otto et al. (2007) used a combination of mathematical modeling and empirical data to provide evidence that the observed structures of natural food webs are non random, and are at least partly a result of the fact that particular stabilizing predator-prey body mass ratios are favored during community assembly.

In this paper, I study the effect of individual species' body size variation on the interplay between food web structure, and community stability. As will be seen below, this investigation

naturally breaks into three interlinked parts, each of which addresses the origin and population dynamical underpinnings of a distinct community characteristic:

(i) The distribution of species' average body masses

(ii) The distribution of consumer-resource body mass ratio across all trophic links, and

(iii) Food web structural characteristics.

My modeling approach is to extend the Lotka-Volterra type mathematical model (LV model) and its analysis of Chapter 2 (Pawar, 2009) by developing species' body size based parameterizations. While doing so, I pay particular attention towards two key drawbacks of previous studies on body sizes and food webs dynamics. Firstly, I consider the context of community assembly explicitly. As mentioned before, this is important because the pattern of species' immigration can have nontrivial effects on changes in food web structure during community assembly (Pawar, 2009; Virgo et al., 2006). Second, I will attempt to accommodate the entire spectrum of consumer resource relationships into the parameterization of trophic interactions: from cases where consumers are smaller than their resources (e.g., parasite-host interactions) to those where consumers are larger (e.g., many predator-prey interactions). In contrast, most previous food web studies focused mainly on predator-prey interactions (Brose et al., 2006a; Emmerson and Raffaelli, 2004). In part, I am motivated by increasing evidence for the importance of parasites and parasitoids in food web structure (Kuris et al., 2008; Lafferty et al., 2006a; Lafferty et al., 2008; Leaper and Huxham, 2002; Memmott et al., 2000; Thompson et al., 2005; Woodward et al., 2005a). A compelling feature of these new data is preliminary evidence that these hitherto poorly studied interactions are likely to be major channels of energy flow in terrestrial and aquatic communities (Hudson et al., 2006; Lafferty et al., 2006a; Lafferty et al., 2006b; Lafferty et al., 2008).

3.2 Body size based parameterization of the dynamical food web model

To specify body size based parameterizations of the basic LV model (equation 2.1), an obvious starting point is the fundamental allometric scaling relationship between individual metabolic rate (B) and body mass (m), which is of the power-law form $B \propto m^{\beta}$ (Brown et al., 2004; Kleiber, 1961; Peters, 1983). The scaling exponent β is known to be close to ¾ for a wide range of organisms from unicells to plants and animals (> 20 orders of magnitude increase in body mass; Brown et al., 2004). Temperature is an additional factor that influences metabolism (Gillooly et al., 2001), but will not be included in this study because it does not affect the allometric scaling qualitatively, and also because the vast majority of species in food webs tend to be ectotherms. I will also not delve into the

mechanisms underlying metabolic scaling, which have been strongly debated (Brown et al., 2005; Glazier, 2005; Kozlowski and Konarzewski, 2005; O'Connor et al., 2007; West et al., 1997); for the purpose of this study, it is sufficient that the existence of such scaling *per se* is well accepted.

Now, because for mass-specific metabolic rate decreases with mass, i.e., $B/m \propto m^{\beta-1}$, I assume that biomass production (including reproduction) rate for basal (primary producer) species also scale as,

$$b_i = a_{b,i} m_i^{\beta-1} \tag{3.1}$$

where $a_{b,i}$ is a taxon-specific normalization constant and m the species' average adult body mass. Similarly, mass-specific biomass (including mortality) is assumed to scale as (McCoy and Gillooly, 2008),

$$d_i = a_{d,i} m_i^{\beta-1} \tag{3.2}$$

where $a_{i,d}$ is a normalization constant. Both these relationships have good empirical support (Calder, 1984; Charnov, 1993; Peters, 1983; Savage et al., 2004), and have been used previously in similar contexts (e.g., Brose et al., 2006a; Loeuille and Loreau, 2005; Virgo et al., 2006; Weitz and Levin, 2006; Yodzis and Innes, 1992). The intrinsic production rate of consumers should have the same scaling as that of basal species (equation 3.1). Hence I define the mass-specific biomass loss of the i^{th} resource to consumption by the j^{th} consumer species to be,

$$\alpha_{ij} = -a_{b,j} m_j^{\beta-1} \varphi_{ij} , \tag{3.3a}$$

where, $a_{b,j}$ is a normalization constant, and φ_{ij} the consumption rate: the net effect of mass-specific encounter and biomass transfer rates (from the i^{th} resource to the j^{th} consumer) between the two species (encounters/time)x(biomass transferred /encounter). This function can only take values between 0 and 1, and hence represents a normalized rate. Thus from expression 2.1b, the contribution to the j^{th} species' total biomass production (including reproduction) by consumption of the i^{th} species is

$$\alpha_{ji} = a_{b,j} m_j^{\beta-1} e_j \varphi_{ji} \tag{3.3b}$$

I assume that the consumption rate function is unimodal (gaussian) such that it peaks at some ratio of average consumer mass to average resource mass (consumer-resource body mass ratio, or CRBR):

$$\varphi_{ij} = \exp\left(-\left(s\log\left(m_j m_i^{-1}/k\right)\right)^2\right) \tag{3.4}$$

Here s determines how rapidly the function reaches its peak k (the CRBR of maximum consumption intensity). Clearly, this is a substantial simplification of the potentially complex dynamics of consumer-resource encounter and consumption rates in nature. However, expression 3.4 captures an important feature of empirically observed consumption rates (Aljetlawi et al., 2004; Brose et al., 2008; Persson et al., 1998): that they tend to peak at intermediate CRBR values. The main reason for this is that in a finite time step, for a resource species with some given average individual body mass, a small consumer is less capable of extracting biomass (greater handling time) from it than is a relatively larger one due to a combination of physical constraints and handing inefficiency. i.e., $\lim_{m_j m_i^{-1}\to 0} \varphi_{ij} = 0$. Conversely, there is also a reduction in the efficacy with which a consumer can extract the biomass of a much smaller resource, i.e., $\lim_{m_j m_i^{-1}\to \infty} \varphi_{ij} = 0$. The actual values of k and s are expected to vary with type of consumption (foraging) strategy as well as habitat type. For example, in the case of predator-prey interactions, because smaller organisms have greater mass-specific power relative to larger ones (Dial et al., 2008), and can hence handle a larger range of prey sizes, k may be closer 1 (or even <1) for small consumers, and s smaller (a more gradual decline of consumption intensisty at extreme ratios). A meta-analysis of consumer-resource body mass ratios by Brose et al. (2006b) shows that invertebrate consumers do indeed have a k closer to 1 than vertebrates across disparate habitat types, indicating their superior ability to handle prey closer to their own size. In host-parasite and parasitoid interactions on the other hand, k should be < 1 because parasites and parasitoids are selected to adopt strategies that increase effective encounter rate as well as exploitation success of resource species much larger than themselves (Cohen et al., 2005; Raffel et al., 2008). Below (section 3.4) I show that my results are largely insensitive over a wide range of choice of the parameters k and s.

Finally, I specify the intra-specific interaction coefficients α_{ii}. Because α_{ii} represents biomass loss (including individual mortality) resulting from metabolic stress induced by increasing biomass density of conspecifics, it should scale as

$$\alpha_{ii} = -a_{ii} m_i^{-\gamma} \tag{3.5}$$

where a_{ii} is a normalization constant and γ the scaling exponent. Below I show that if γ ranges from ¼ to ½ (which includes the scaling exponent of mass-specific metabolic rate), empirically tenable scaling between body mass and equilibrium biomass abundance across species is seen in model communities. This is similar to the scaling used in a different set of body size parameterizations of the LV model by Virgo *et al*. (also see Lewis et al., 2008; 2006).

This completes the specification of the body size parameterized LV model (BLV model). Table 3.2 provides a summary of the above parameterizations.

3.3 Model analysis

In Chapter 2 (Pawar, 2009) I have shown how food web structure changes in model communities during assembly though a combination of "stable invasions" (establishment of a new immigrant and its trophic links without any extinctions) and "species sorting" (unstable invasion followed by one or more extinctions) (see section 2.2.1). Stable invasions result in gradual changes in food web structure during assembly, whereas species sorting events can cause greater structural upheavals by the extinction of multiple species. In the absence of population dynamical stochasticity (e.g., due to environmental or demographic fluctuations) stable invasions and species sorting events are purely interaction driven, and are determined by the probability of Hurwitz stability (PHS; defined in section 2.2.1) of the invaded community. Eventually, for a given immigration rate, community assembly reaches a quasi-equilibrium where immigrations are approximately balanced by extinctions through failed invasions and species sorting events (immigration-extinction equilibrium, or IEE). At IEE, certain nonrandom food web structural characteristics that have been favored during assembly due to their stabilizing influence are seen. I now proceed to extend these results of Chapter 2 to study the effect of species' body size variation on this feedback between community stability, assembly and food web structure.

3.3.1 Null expectations under relaxed assembly

To understand the effects of stability constraints, we can begin by analyzing the pattern of changes (or lack thereof) in food web structure under relaxed community assembly (assembly with minimal extinctions due to stability constraints). These will serve as "null" hypotheses to

test against for the presence of signatures of stability constraints during and after assembly. In Chapter 2 I have shown that the null expectations about changes in food web structural features are straightforward: under relaxed assembly, certain the stabilizing configurations should fail to emerge (or emerge more slowly) (section 2.3.2). I now derive analogous null expectations about the distributions of species' average adult body masses (SBMs) and CRBRs under relaxed assembly.

I begin by modifying the assumptions in Chapter 2 about assembly patterns to accommodate interspecific body size variation. Assume that the SBM distribution from which immigrants are drawn can be represented as a probability density function over some body mass range. This function does not merely represent the SBM distribution of the region to which the community belongs, but is a convolution of the probability density functions of the regional species pool's SBM and body size-based immigration (assuming a relationship between body size and dispersal ability). Hence I will refer to this SBM as belonging to the "immigrant pool". For reasons explained below, I will assume that the probability density function of the SBMs in the of immigrant pool follows a one parameter Beta distribution, Beta(1,ω) (Springer, 1979) ,

$$f_y(y_i) = \omega(1-y_i)^{\omega-1},\ y_i \in [0,1] \tag{3.6a}$$

rescaled to lie between biologically feasible lower and upper log-SBM (l-SBM) limits ($y'_{\min}$ and $y'_{\max}$) of the immigrant pool:

$$y' = y'_{\min} + \left(y'_{\max} - y'_{\min}\right) y \tag{3.6b}$$

Thus here the random variable $y' = \log(m)$, and distribution 3.6a gives the probability of immigration of any species with respect to its log-transformed body size. Note that the logarithm of body mass is being used here purely for convenience. Using the Beta probability density function here has two main advantages. First, it has finite bounds, which allows a precise allocation of minimum and maximum feasible body masses in the model. Second, depending upon the choice of ω, different types of size structured immigrant pools (e.g., uniform, skewed, etc) can be chosen. The latter factor will be considered in greater detail below (section 3.4.1).

From the immigrant pool, species are assumed to arrive at the local community at a fixed rate. At each immigration event, the i^{th} invader species establishes a trophic link with the j^{th} resident species with some probability, which I assume is independent of the body masses of both

species. Thereafter, whether the new species establishes or goes extinct depends upon the strengths and directions (consumer-resource or vice versa) of the intra- (α_{ii}'s) and interspecific (α_{ij}'s) interaction coefficients in the newly invaded community. Under completely relaxed assembly, the nature of the trophic links only matter to the extent that a species can invade successfully; very few extinctions occur by species sorting. Then the main limitation on species accumulation is immigration rate (ignoring environmental or demographic stochasticity). In this scenario, the l-SBM distribution of the local community is expected to reflect that of the immigrant pool. I will concentrate on two properties of the local l-SBM to measure deviations from this null expectation: its mean and kurtosis. The mean of the local community's l-SBM distribution under relaxed assembly would be approximately,

$$\mu_{\text{l-SBM}} \cong y'_{\min} + \left(y'_{\max} - y'_{\min}\right)\frac{1}{(1+\omega)} \tag{3.7a}$$

(Using the properties of the Beta(1,γ) distribution). In addition, because log-SBM distributions tend to be right skewed to different degrees (Allen et al., 2006b), we are interested in skewness of the community's l-SBM. Again using the properties of the Beta(1,γ) distribution, this is expected to be

$$sk_{l-SBM} \cong \frac{2(\omega-1)\sqrt{\omega+2}}{(\omega+3)\sqrt{\omega}} \tag{3.7b}$$

Expressions 3.7a&b are only approximations for two reasons. First, there is bound to be sampling error during stochastic immigration from the immigrant pool. Second, some extinctions do occur because of failed invasions; if these are non-random with respect to body size, particular body size classes may be systematically underrepresented in the local community.

The nature of the l-CRBR distribution under relaxed assembly can also be inferred as follows. Assuming that the l-SBMs of consumer and resource species follow the same distribution, if trophic links are assumed to be established independent of species body sizes as well as existing links during assembly, the l-CRBR of each trophic link is the random variable $y'_c - y'_r$ (because $\log(m_c/m_r) = \log(m_c) - \log(m_r)$), with the subscripts "c" and "r" denoting consumer and resource species respectively. We do not need to determine the actual form of this distribution because its mean and kurtosis can be directly calculated. Firstly, because given two independent random variables X and Y, $E(X-Y) = E(X)-E(Y)$,

$$\mu_{l-CRBR} \cong 0 \tag{3.8a}$$

Additionally, because the distribution of differences between two independent and identically Beta-distributed random variables is unimodal and symmetric (with upper and lower bounds equal to $y'_{\min} + y'_{\max}$, in our case)[3], again assuming that the SBM distributions of consumers and resources are identical, the l-CRBR distribution must also have approximately zero skewness under relaxed assembly, i.e.,

$$sk_{l-CRBR} \cong 0 \tag{3.8b}$$

Any deviation from these characteristics of local community l-SBM and l-CRBR distributions (expressions 3.7–3.8) can be attributed to nonrandom processes during community assembly (which, following random immigration, bias the success of species towards those with particular body sizes). Below I will show that one such process is nonrandom species extinctions driven by the stability constraints of multi-species stability. For this, we first need to understand how community stability is affected by the body size scaling of interaction strengths.

3.3.2 PHS and the scaling of interaction strengths

The elements of the community matrix $\boldsymbol{C}$, which determines Hurwitz stability, include species' equilibrium biomass abundances ($\hat{x}$'s) (see section 2.2.1). Hence the following analyses would be much simplified if the equilibrium biomasses also followed a scaling relationship with body size, as is typically seen in local communities (Brown and Gillooly, 2003; Leaper and Raffaelli, 1999). In Appendix E I show that while deriving this relationship is analytically intractable for arbitrary n, it can be shown numerically that the above body mass based parameterizations result in equilibrium biomass densities that scale across species as

$$\hat{x}_i = a_{\hat{x}} m_i^{\nu} \tag{3.9a}$$

[3] In fact, this is true for any distribution with finite upper and lower bounds Springer, M.D., 1979. The algebra of random variables. Wiley, New York..

where $\mathfrak{N}$ denotes the set of unique species indices 1, 2,…, n in the n-species community, $a_{\hat{x}}$ is the intercept and depending upon the parameters ω and k,

$$\nu = z\gamma - c \tag{3.9b}$$

with z lying between 0.5 – 0.6 and c between 0.1 – 015 (see Appendix E). Thus if γ lies between 0.25–0.5, ν lies between 0–0.25, which is consistent with data from local communities as well as theory (Brown and Gillooly, 2003; Leaper and Raffaelli, 1999; Marquet et al., 1995; Sheldon et al., 1977). I now show how the scaling of interaction strengths affects PHS. In Chapter 2, I have shown that empirically feasible food web sign structures tend to be interaction strength sensitive (ISS; see section 2.2.2 and Table 2.1), and hence PHS is limited by the "trophic link strengths" (derived in Appendix B), which are defined as (defined originally in expression 2.7),

$$\bar{\underline{c}}_{ij} = |\alpha_{ij}| \sqrt{e_i \hat{x}_i \hat{x}_j}\ , \forall i, j \in \mathfrak{N}\ \text{(where } i \text{ consumes } j\text{)}. \tag{3.10}$$

Each $\bar{\underline{c}}_{ij}$ is the geometric mean of the pair of coefficients associated with each interspecific interaction, and measures the biomass transfer rate from resource to consumer (see section 2.2.2). Now substituting expressions 3.3 and 3.9 into 3.10, we have the approximate scaling of trophic link strengths:

$$\bar{\underline{c}}_{ij} \cong a_{b,i} m_i^{\beta-1} \varphi_{ij}\ a_{\hat{x}} \sqrt{e_i m_i^{\nu} m_j^{\nu}}, \forall i, j \in \mathfrak{N}\ \text{(where } j \text{ consumes } i\text{)} \tag{3.11}$$

However, because PHS is defined relative to the strengths of the diagonal elements of the community matrix $\boldsymbol{C}$ (intraspecific density dependences at biomass equilibrium)(see Appendix A) which also scale with body size, the scaling of the $\bar{\underline{c}}_{ij}$'s in itself does not provide sufficient information to understand their effects on community stability. So we need a measure that considers their effects relative to the diagonal elements of $\boldsymbol{C}$, which I will derive now[4].

The destabilizing effect of the $\bar{\underline{c}}_{ij}$'s is inversely related to the strengths of the diagonal elements (the c_{ii}'s) of the community matrix $\boldsymbol{C}$, which themselves scale as (combining expressions 2.3, 3.5 and 3.9)

[4] Note that this was not required in the analysis of the LV model Chapter 2 because the diagonal elements were assumed to be independent of the off diagonal ones.

$$c_{ii} \cong a_{\hat{x}} a_{ii} m_i^{\nu-\gamma}, \forall i \in \mathfrak{N} \tag{3.12}$$

Then, recalling from section 3.3.2 that PHS is inversely related to the quantity $\sum_{i,j=1}^{n} \bar{c}_{ij}$, the dynamical impact of the j^{th} immigrant consumer during assembly can be measured as the ratio of the sum of the strengths of the new trophic link strengths added to the system, over the new diagonal element (expression 3.12),

$$\frac{\sum_{i\in\mathscr{B}_j} \bar{c}_{ij}}{c_{jj}} \cong \frac{a_{b,j} m_j^{\beta-1} a_{\hat{x}} \sqrt{e_j m_j^{\nu}} \sum_{i\in\mathscr{B}_j} \left(\varphi_{ij} \sqrt{m_i^{\nu}}\right)}{a_{\hat{x}} a_{jj} m_j^{\nu-\gamma}} \tag{3.13}$$

where $\mathscr{B}_j$ is the set of all the resource species of the immigrant. Smaller this ratio, weaker the impact of the new consumer on community stability. The effects of the immigrant's vulnerability (all the new trophic links in which it is the resource) are not included in expression 3.14 because they can be absorbed into the analogous terms of its consumer species. Preliminary insights into the effects of species body sizes on PHS can be gained without explicitly considering assembly dynamics. Simplifying expression 3.13, and substituting $\beta = ¾$ gives,

$$\frac{\sum_{i\in\mathscr{B}_j} \bar{c}_{ij}}{c_{jj}} \cong \frac{a_{b,j} \sqrt{e_j} \sum_{i\in\mathscr{B}_j} \left(\varphi_{ij} m_i^{\nu/2}\right)}{a_{jj} m_j^{\frac{\nu}{2}-\gamma+\frac{1}{4}}} \tag{3.14}$$

Assuming that e_j is at most weakly dependent on body size, expression 3.14 indicates that if $\gamma \geq 0.25+\nu/2$, potentially destabilizing effects of the higher mass-specific trophic link strengths associated with smaller species will be counterbalanced by their stronger intraspecific density dependence. Note here that ν itself also increases as a fraction of γ (expression 3.9b), and hence it is expected to be > 0 for $\gamma \geq 0.25$. If $\gamma = 0.25$, as might be expected from metabolic considerations, the effects of increasing mass-specific biomass acquisition and production rates are canceled out by the biomass loss due to negative intraspecific density dependence. In that case, the denominator of 3.14 *increases* with body mass, and larger species tend to be relatively stabilizing. Also, irrespective of its body mass, the impact of an immigrant is determined by the terms in the numerator in expression 3.14: CRBR's (through the function φ_{ij}) associated with its trophic generality, and provided that $\nu > 0$, the body sizes of its resource species.

Across the range of possible CRBRs over an empirically feasible range of body sizes (see Chapter 4), Fig. 3.1 compares the distribution of the interaction strengths (α_{ij}'s), trophic link strengths ($\underline{\bar{c}}_{ij}$'s) and the ratio 3.14 for two different values of γ. Three salient features of the α_{ij}'s are immediately evident from Fig. 3.1a; (i) they decrease at either extremes of body mass difference, (ii) increase with decrease in body mass of either species (i.e., for a given CRBR, the peak values- the "hottest" zones- lie towards the upper left corner of the figure), and (iii) decrease more rapidly at extreme upper values of CRBRs compared to lower extreme values (the hottest zones lie slightly above the CRBR = 1 line). While (i) is a result of the unimodal symmetry of φ_{ij} (expression 3.4), (ii) and (iii) result from the scaling of intrinsic biomass production rates (expressions 3.1 and 3.3). These features of mass-specific interaction strengths are consistent with previous such body size based models (Brose et al., 2006a; Brose et al., 2008; Yodzis and Innes, 1992). Fig. 3.1b shows that if $v > 0$ (the case of $v = 0.25$ is shown), when the effects of equilibrium biomasses are added to the α_{ij}'s, the resulting trophic link strengths reduce the bias of the interaction strengths towards smaller sized organisms (the hottest zones extend further along the CRBR = 1 line towards the bottom right corner of the figure), while increasing the bias towards extreme upper values of CRBRs (the hottest zones lie further above the CRBR = 1 line). Finally, Fig. 3.1c&d show that as expected from the body size scaling composition of the ratio 3.13, for the two extreme values of γ (0.25 and 0.5), the effects of the mass-specific biomass production scaling are either perfectly negated (Fig. 3.1c), or overwhelmed (Fig. 3.1d) (because v increases with γ). In other words, in the former case, the potentially destabilizing effects of smaller body sized species are negated (the hottest zone becomes a ridge across the entire CRBR = 1 line), while in the latter, larger body sized species actually become more destabilizing (the hottest zone shifts to the bottom right hand corner along the CRBR = 1 line). Moreover, the more rapid decline in interaction strengths and trophic link strengths at extreme upper values of CRBRs compared to lower extreme ones is no longer seen (cooler areas are larger below the CRBR = 1 line in Fig. 3.1a&b are no longer larger).

The following two sections now complete the analysis of the dynamical effects of body size scaling of interaction and trophic link strength on food web structural characteristics by a detailed consideration of community assembly dynamics.

3.3.3 Signatures of stability constraints on body size based food web structural features

Following the establishment of at least one basal species, at the early stages of assembly, because n is small and PHS is high, the success of immigrant consumers is dependent mainly on

their ability to invade (determined by inequality 2.2). By substituting expressions 3.1– 3.3 into 2.2 it is obvious that smaller species tend to have higher mass-specific biomass uptake and production rates, and are hence more likely to invade, provided they are able to establish sufficient number of trophic links. As assembly proceeds, link density (L_D; as defined in section 2.2.2) increases linearly with n, i.e., species' generalities tend to increase (see section 2.3.2 and Fig. 2.5b) (Martinez, 1992; Piechnik et al., 2008). Hence PHS decreases because the numerator in ratio 3.14 overwhelms the denominator. Hence successful invasions are now more often followed by species sorting (see section 2.2.3 and Fig. 2.5), and so while relatively small sized species continue to invade more successfully, the constraints on trophic link strengths have increased. At such a stage, the numerator of the ratio 3.13 has to be mitigated for the growing number of species to coexist stably. In section 2.2.2, this numerator was called the species' "weighted generality" (G^w); i.e., for the i^{th} consumer, (see expression 2.8),

$$\begin{aligned} G_i^w &= \sum\nolimits_{j\in\mathcal{C}_i} \bar{c}_{ij} \\ &= a_{b,i} m_i^{\beta-1} a_{\hat{x}} \sqrt{e_i m_i^{\nu}} \sum\nolimits_{j\in\mathcal{C}_i} \left(\varphi_{ij} \sqrt{m_j^{\nu}}\right) \end{aligned}$$

The mitigation of these G^w's can happen if species with higher generality tend to have relatively lower G^w. As shown in Chapter 2, this actually happens because stable invasion and species sorting events respectively add and eliminate whole structural modules consisting of species and their trophic links. Thus the two signatures of stability constraints of species generality modules that were predicted in chapter 2 can be reiterated here. These are,

(i) *A decrease in species' $\bar{G}^w$ (as well as $\bar{\alpha}_G$) with generality,* and

(ii) *A decrease in species' $\bar{G}^w$ (as well as $\bar{\alpha}_G$) with trophic level*

As shown in Chapter 2, these two relationships can be measured by correlation coefficients (specified below), and will be denoted by $r\left(G, \bar{G}^w\right)$ and $r\left(TL, \bar{G}^w\right)$ respectively. Here, $\bar{G}^w$ is species' trophic generality-averaged weighted generality (expressions 2.11) which using the above body size parameterizations (substituting expressions 3.3a & 3.9 into 2.11) now becomes for the i^{th} consumer,

$$\bar{G}_i^w = \frac{a_{b,i} m_i^{\beta-1} a_{\hat{x}} \sqrt{e_i m_i^{\nu}} \sum_{j\in\mathcal{C}_i} \left(\varphi_{ji} \sqrt{m_j^{\nu}}\right)}{G_i}, \forall i \in \mathfrak{N}, \tag{3.15}$$

while $\bar{\alpha}_G$ is species' generality-averaged interaction strengths (expression 2.12), which measures the contribution of their consumption strategies alone (without the effects of equilibrium biomass abundances) to G^w mitigation. This quantity is now,

$$\bar{\alpha}_{G,i} = \frac{a_{b,i} m_i^{\beta-1} \sum_{j \in \mathfrak{C}_i} \varphi_{ji}}{G_i}, \forall i \in \mathfrak{N} \tag{3.16}$$

Furthermore, the body size parameterizations of interspecific interactions now allow predictions of three additional signatures of dynamically constrained assembly:

(iii) *A positive correlation between species size and trophic generality*. Because larger species tend to have lower mass-specific biomass assimilation and production rates, they are associated with lower mass-specific interaction strengths as well as trophic link strengths. Hence the numerator of the ratio 3.13, and the quantities 3.15 and 3.16 decrease with consumer mass provided that v is not larger than β–1 (this typically the case; see section 3.3.2 and Fig. 3.1). Hence a mechanism for the emergence of signature (i) above is the selection (through stable invasion and species sorting events) of trophic modules consisting of larger species with higher generality.

(iv) *A negative correlation between a consumer's trophic level and its CRBRs*. From the simplified ratio 3.14, it is clear that during assembly, irrespective of the size of the consumer, its G^w can be mitigated by deviation from peak values of the function φ_{ij}, (at CRBR = k) and if $v > 0$ (i.e., at least weak increase of equilibrium biomass with body size) by an decrease in the size of the resource species it feeds on (the terms inside the sum of the numerator). These two conditions can simultaneously be satisfied only if the consumer has trophic links with CRBRs>0. Because their higher invasibility will have favored species in the small end of the spectrum of the immigrant pool's SBM at the earlier assembly stages, CRBRs will inherently tend to increase because the later immigrants will be on average larger than the residents. Thus linked to the increase in species CRBRs with trophic level, another pattern is expected:

(v) *A positive correlation between a species' size and its trophic level*.

Similar to signatures (i) and (ii), the relationships (iii) – (iv) can also be measured by correlation coefficients (specified below), and will be denoted by $r(m, G)$, $r(TL, CRBR)$ and $r(TL, m)$, respectively. Clearly, (iv) and (v) are mechanisms for the emergence of signature (ii) above. Note

that if community assembly is hierarchical, such that later immigrants tend to be consumers rather than resources, occupying higher trophic levels (see section 2.3.1 for a discussion of this aspect of assembly dynamics), signatures (iv) and (v) (and hence (ii)) will be stronger because this will predispose the relatively larger later immigrants towards becoming consumers of resident species. Hence the following interdependences between food web structural signatures of stability constraints are predicted: (i) ↔ (iii) i.e., the decrease in species' generality-averaged weighted generality (and interaction strength , $\bar{\alpha}_G$) with generality (measured by $r\left(G,\bar{G}^w\right)$ and $r\left(G,\bar{\alpha}_G\right)$, respectively) is brought about by an increase in species' generality with body size (measured by $r\left(m,G\right)$), and (ii)↔(iv)↔(v) i.e., decrease in species' generality-averaged weighted generality (and $\bar{\alpha}_G$) with trophic position (measured by $r\left(TL,\bar{G}^w\right)$ and $r\left(TL,\bar{\alpha}_G\right)$ respectively) is strongly linked to increase in consumer species' body size as well as CRBR's with trophic position (measured by $r\left(TL,m\right)$ and $r\left(TL,CRBR\right)$ respectively).

3.3.4 Signatures of stability constraints on SBM and CRBR distributions

I now consider how the BM and CRBR distributions change concurrently with the dynamically driven changes in the above food web structural features. Firstly, as mentioned above, species with small body sizes are expected to invade with greater success because of their inherently superior rate of biomass uptake and production. This is especially true when species richness is low and stability constraints are weak (invasibility constraints dominate community stability constraints). Hence the local l-SBM distribution is expected to deviate from the null one in the direction of small body sizes at the early stages of assembly. In other words, $\mu_{\text{l-SBM}}$ will become increasingly smaller than that in expression 3.7a, and $sk_{\text{l-SBM}}$ higher (more positive, or right skewed) than that in expression 3.7b. At the same time, because trophic link strengths are strongest at CRBR = 1 (Fig. 3.1c–d), species will be more successful in invading by feeding on those similar to them in size, and $\mu_{\text{l-CRBR}}$ and $sk_{\text{l-CRBR}}$ should initially stay around 0 (the null values). As assembly proceeds, because relatively larger species experience increasingly fare better at invading stably (for reasons explained in signature (iv) above), as the community approaches IEE, $\mu_{\text{l-SBM}}$ and $sk_{\text{l-SBM}}$ should decrease at a decreasing rate. Thus the invasibility (energetic requirement for initial establishment) of individual species and the stability requirements of multi-species stable coexistence "pull" the local SBM distribution in opposite

directions during assembly. Thus the following predictions can be made about the signatures of dynamically constrained assembly on community SBM and CRBR distributions:

- *An asymptotic decrease and increase in $\mu_{l\text{-}SBM}$ and $sk_{l\text{-}SBM}$ respectively during assembly, culminating in smaller and larger values respectively of these measures at IEE relative to those of the immigrant pool's SBM distribution.*
- *An asymptotic increase in $\mu_{\text{l-CRBR}}$ during assembly, culminating in a larger value at IEE relative to that of the immigrant pool's CRBR distribution.*

It is important to note that as in the case of the signatures (iv) and (v) above, changes in CRBRs is not independent of assembly pattern. An increase in $\mu_{\text{l-CRBR}}$ is possible because the local $\mu_{\text{l-SBM}}$ progressively decreases relative to that of the immigrant pool; hence if interactions are established more or less randomly with respect to body size, $\mu_{\text{l-CRBR}}$ is bound to increase (because the species arriving from the immigration pool will be on average larger than those in the local community). Obviously, if later immigrants tend to be consumers with greater probability (occupy higher trophic levels), this effect will be magnified. On the other hand, if assembly is completely nonhierarchical such that each immigrant is equally likely to be a consumer or resource, even if an increase in the $\mu_{\text{l-CRBR}}$ is favored by stability constraints, it may change little from the null expectation of 0 (expression 3.8) irrespective of the local l-SBM. As discussed in Chapter 2, current data as well as theory indicate that assembly in natural communities tends to be at least somewhat hierarchical. Also, although the null expectation for $sk_{\text{l-CRBR}}$ is 0 (expression 3.8b), it is difficult to predict the direction in which a deviation from it may be expected; this will be investigated numerically below.

3.4 Community assembly simulations

I now evaluate the above predictions about the emergence of nonrandom food web structural features (signatures) using numerical simulations of community assembly based on the BLV model.

3.4.1 Methods

The community assembly algorithm using the BLV model was identical to the one used for the LV model described in Chapter 2 (section 2.3.1), except that here immigrant species populations were sampled from the Beta(1,ω) distribution introduced above (expression 3.6), and

their inter- and intra-specific interaction parameters were determined by the scaling relationships 3.1–3.5. The ranges for the non-body size related parameters were the same as those used in Chapter 2 (summarized in Table 2.2), except for the following differences.

- p_v was fixed at 0.9 because this is the midpoint of the range [0.75–1] that yields communities with structural and dynamical characteristics similar to that of real ones (similar to the niche model; see section 2.3.2 and Fig. 2.3).
- e_j was fixed at 0.5 for all species; this is the midpoint of the range reported from empirical data (Brown et al., 2004; Peters, 1983).
- The number of basal species was set as a fixed proportion of the total target community size at IEE, instead of just one. Allowing multiple basal species reduced the variability in the characteristics of replicated food webs arising from differences in their body sizes alone.

Varying p_v or e_j within the ranges shown in Table 2.2 does not change the results qualitatively. In addition, body size related parameters were chosen as follows (summarized in Table 3.1):

- ω, which determines the shape of the immigrant pool SBM distribution was varied between 1 (uniform distribution; immigration rate independent of body size) and 2 (power law-like with slope = –2; immigration rate decreases with body mass). This range of ω was chosen with the consideration of two factors: (i) Empirical data show the distributions of SBM's at large spatial scales are right skewed (Allen et al., 2006b), probably partly driven by speciation rate, which appears to follow a negative power law relationship with body size (Dial and Marzluff, 1988; Marzluff and Dial, 1991), and has been linked to metabolic allometric scaling by recent studies (Allen and Gillooly, 2006; Allen and Savage, 2007; Allen et al., 2006a) and, (ii) dispersal ability appears to increase with body size (depending upon locomotion mode; Peters, 1983). Only considering (i) means that ω should be > 1; choosing $\omega = 2$ sets a reasonably high upper limit to this bias. Considering (ii) means that the effect of (i) may be somewhat negated due to dispersal ability. However, because speciation within the local community also adds to the effective bias towards immigration by smaller species and because data on dispersal ability itself is biased towards larger organisms (cf. Peters, 1983), it is unlikely that (ii) can overwhelm the effects of (i). Hence $\omega = 1$, which yields the uniform distribution expected if the effects of (i) and (ii) exactly cancel out, is a reasonable lower limit to the immigration rate bias.
- The log-body mass range $[\, y'_{\min}, y'_{\max} \,]$ was chosen to be [–12,12] because this is approximately the range of species' log-body masses observed across empirical communities (Brose et al., 2005) (also see Chapter 4).

- β was chosen to be 0.75, which is well supported empirically, especially across species differing in body size by orders of magnitude (Brown et al., 2004).
- k was chosen to vary randomly between 10^{-3} and 10^{3} with uniform probability (consumers 1000 times smaller to 1000 times larger than resources), which covers most of the range considered to be "optimal" (in the sense of viable, or evolutionarily stable strategy for the consumer) in previous studies on consumer-resource interactions (Cohen et al., 2005; Weitz and Levin, 2006), and accommodates potential differences in k across the most common trophic interaction types seen in food webs (i.e., predator-prey, herbivore-plant and parasitoid-host) (Brose et al., 2005).
- s was set to 0.1; however, varying it between a wide range (0.05–0.5) did not change the results.
- The allometric constants a_b and a_d were chosen to be 1 and 0.002, respectively (Brown et al., 2004; Peters, 1983).
- The constant a_{ii} was chosen according to the target mean n at IEE; larger values give larger feasible communities.

3.4.2 Results

Signatures on other food web structural features. Fig. 3.3 shows changes during assembly in a fundamental signature of stability constraints on food web structure: the correlation between trophic generality and $\bar{G}^w$ as well as $\bar{\alpha}_G$. Clearly, the emergence of signatures of stability constraints on species' trophic generality based food web structural features are almost indistinguishable between the two values of ω in terms of their strength (measured by the spearman rank correlation coefficients $r\left(G,\bar{G}^w\right)$ and $r\left(G,\bar{\alpha}_G\right)$). The shape of the relationship between G and $\bar{G}^w$ in communities at IEE is similar to the ones found with the LV model (Fig. 2.4), and is not shown here.

Signatures of dynamically constrained assembly on SBM and CRBR distributions. Fig. 3.3 shows the changes in characteristics of the local l-SBM and l-CRBR distributions during assembly, Fig. 3.4 shows representative examples of these distributions of the resulting communities at IEE, and Table 3.2 (last three rows) summarizes their characteristics across replicated communities at IEE. Changes in other, non-body size related food web structural features were similar to those seen during assembly based on the LV model (Fig. 2.5), and are not

shown here. For both extremes of shapes of the regional l-SBM distributions (ω = 1 or 2; profiled by the dashed lines in Fig. 3.4a&c), Fig. 3.3a&b show that as expected, both $\mu_{\text{l-SBM}}$ and $sk_{\text{l-SBM}}$ deviate from the null values rapidly, respectively increasing and decreasing asymptotically. Also, because immigration is strongly dominated by small bodied species for ω = 2, these deviations are proportionally higher. This proportional difference in deviation may be regarded as the "neutral" component of the l-SBM distribution (i.e., under fully relaxed assembly, the relative difference between the two distributions would be the same, even if their absolute $\mu_{\text{l-SBM}}$ and $sk_{\text{l-SBM}}$ values were different from those under dynamically constrained assembly).

In the case of the l-CRBR distribution as well, the effects of dynamically constrained assembly were as expected. Fig. 3.3c shows that on average, $\mu_{\text{l-CRBR}}$ increases asymptotically. For ω = 2, $\mu_{\text{l-CRBR}}$ starts off well below the null value (dotted line). This is because the success of the first few basal species is independent of their body size as they lack consumers (assuming there is no competition between basal species). However, the invasibility of the first consumers feeding on these basal species decreases with body size. For ω = 2, there is already a bias towards migration of small species, and hence $\mu_{\text{l-CRBR}}$ will tend to < 0 initially. Even after the early stages of assembly however, $\mu_{\text{l-CRBR}}$ values for ω = 2 remain below those seen for ω = 1, which, as in the case of the SBM distribution, indicates that sufficiently strong immigration bias can overwhelm stability constraints. In the case of $sk_{\text{l-CRBR}}$ on the other hand, both ω values result in a similarly weak negative deviation from the null value of 0 (note that this null value will be the same irrespective of ω), indicating that $sk_{\text{l-CRBR}}$ may not carry a strong signature of dynamically constrained assembly. Note that with reference to Fig. 3.1c, the increase in $\mu_{\text{l-CRBR}}$ during assembly indicates an overall shift of CRBRs away from the hottest zones lying along the CRBR = 1 line towards the cooler zones below the line.

Table 3.2 summarizes the incidence and strengths of the various food web structural signatures predicted in section 3.3.3. In most features, a high incidence (high percentage values) of the expected signatures is seen for either value of ω. Moreover, even in the case where the incidences were low, trends in the opposite direction were not seen. For example, in the case of increase in body size with trophic level ($r(TL,m)$), although only 48% of the communities shows the expected relationship, none of the remaining ones showed a significant relationship in the opposite direction (decrease in body mass with trophic level). Finally, Fig. 3.5a–c shows that the interdependencies between the various signatures (see section 3.3.3) are as expected. Furthermore, Fig. 3.5d shows that the increase in trophic generality with body size ($r(m,G)$) is largely independent of the increase in body size with trophic level (measured by $r(TL,m)$),

indicating that the observed $r(m,G)$ is indeed a result of stability constraints and not an artifact of the fact that larger species have a larger pool of resource species as they tend to occupy higher trophic levels during assembly.

3.5 Discussion

Using species' average adult body size to constrain the magnitudes of biomass-specific trophic interactions in a Lotka-Volterra type model, I have studied the interrelationship between community assembly, stability and food web structure. The results show that under biologically feasible assumptions about metabolic allometric constraints and community assembly patterns, certain nonrandom configurations of food web structural features are likely to emerge due to the constraints of multi-species stable coexistence. These configurations are thus "signatures" of stability constraints on food web structure. Because these structural features are related to species' body sizes, which are relatively easy to measure in the field, their measurement offers a reasonable method to gauge the importance of non-neutral processes underlying the assembly and persistence of real communities. In Chapter 4, I will evaluate some of the theoretical predictions of this study using food web data from multiple terrestrial and aquatic communities.

To the best of my knowledge, this is the first study to explore the interrelationships between food web structural features as well as SBM and CRBR distributions of local communities within a single theoretical framework. Hitherto these features have been studied using different, often disparate models, as will be discussed below.

The predicted increase in SBMs with trophic level due to stability constraints is a pattern that is widely observed in natural communities, especially aquatic ones (Hildrew et al., 2007) also see Chapter 4). This study appears to be the first to show that stability constraints can contribute to this aspect of food web structure. Previous models have mainly invoked species' metabolic constraints and principles of biomass transfer across trophic levels, without the explicit consideration of population stability consequences of trophic interactions (Brown and Gillooly, 2003; Brown et al., 2004; Cohen, 2008). Similarly, the increase in species' trophic generality with size is a commonly seen empirical pattern (Jonsson et al., 2005; Memmott et al., 2000). Here again, I am unaware of any mechanistic model that predicts this pattern (but see Otto et al., 2007). An indirect explanation may be attributed to Schoener (1989), who argued that species' generalities are bound to increase trophic level because the number of potential prey species increases. Then, if body size also increases along trophic level (presumably for some other reason), a positive correlation between size and generalty is expected. However, here I have

shown that stability constraints can directly favor such a pattern. Fig. 3.5d demonstrates this; the increase in trophic generality with body size in model communities is largely independent of the increase in body size with trophic level.

The distribution of CRBRs along trophic levels is another signature of stability constraints. In particular, an increase of CRBRs with trophic level is expected. This result differs from that of Jonsson & Ebenman (1998), who concluded that CRBR ratios should *decrease* with trophic level due to stability constraints. Our result differs from theirs for two reasons; they only studied predator prey interactions with CRBRs >1, and they did not consider the context of community assembly. Both these factors act together to result in a gradual increase in CRBRs during assembly, as predicted in section 3.3.4, and demonstrated numerically in section 3.4.2. Furthermore, Jonsson & Ebenman (1998) claim that their result is supported empirically. In Chapter 4 I will show that this is not the case; across a set of food webs of relatively high resolution, I find that CRBRs typically increase with trophic level.

This study strengthens the main results of Chapter 2 about two signatures of stability constraints on species' trophic generality characteristics: a negative correlation between species' generalities and generality-averaged weighted generalities ($\bar{G}^w$), and a negative correlation between species' trophic level and $\bar{G}^w$. However a striking difference between the emergence of this signature in assembly based on the simpler Lotka-Volterra model of Chapter 2 and the BLV models of this study, is that the latter involves a much larger contribution of species' generality-averaged interaction strength ($\bar{\alpha}_G$) to their generality-averaged weighted generality ($\bar{G}^w$) (compare Fig. 3.4 and 2.5f). This means species' foraging strategies themselves, excluding the effect of equilibrium biomasses of the interacting species (compare expressions 3.15 and 3.16), are strongly "selected" by stability constraints on stability. This is an important result because it strengthens the conclusion drawn from the results of Chapter 2 that species foraging characteristics need not be determined solely by their energetic requirements (as predicted by optimal foraging theory; Stephens and Krebs, 1986) (also see Abrams, 1991). This conclusion is in strong contrast to that of some recent papers (Beckerman et al., 2006; Petchey et al., 2008), which have claimed that community assembly rules based upon species' optimal foraging considerations alone are sufficient to predict food web structure. In part, this contradiction may be explained by the measures of food web structure used in this study and theirs; they use purely qualitative measures of food web structure (presence and absence of trophic interactions, not their strengths), whereas here I have focused on measures related to strengths of interactions.

Finally, this study shows how SBM and CRBR distributions are related to community stability. Irrespective of the distribution of immigration probability with respect to body size, a

right-skewed unimodal l-SBM distribution emerges through species invasion and extinction dynamics driven by interspecific trophic interactions. The skewness and unimodality of this distribution is a result of the tradeoff between the higher invasibility of smaller body sized consumer species at early stages of assembly due to their higher mass-specific metabolic rate, and the stabilizing effects (in terms of Hurwitz stability of the community) of invasion by larger sized species during later stages. That such a unimodal, right-skewed l-SBM distribution, which is often reported in the empirical literature (e.g., Jonsson et al., 2005; Leaper et al., 2001; Siemann et al., 1999; Stead et al., 2005) (also see Chapter 4), emerges due to stability constraints is an intriguing result. The origin of the local community's SBM distribution is an enduring problem in biology, and a variety of explanatory models have been proposed in the past (only a small subset of these include interspecific interactions; see review by Allen et al., 2006b). The model developed in this chapter combines the features of three classes of previous SBM distribution models that exclusively consider, (a) metabolic restrictions of resource use by species' individuals (e.g., Brown et al., 1993), (b) size-based constraints on speciation & dispersal (e.g., Etienne and Olff, 2004), and (c) interspecific interactions (e.g., Hutchinson and MacArthur, 1959). To the best of my knowledge, no other published SBM distribution model merges these features.

The CRBR distribution emerges concurrently with that of the SBMs. The interest in the effect of stability constraints on the distribution of CRBRs in local communities as a whole appears to have arisen relatively recently (Brose et al., 2006a; Emmerson and Raffaelli, 2004; Jonsson and Ebenman, 1998; Otto et al., 2007), perhaps partly due to increasing availability of food web datasets with body size information (Brose et al., 2005). This study and a few other existing ones mentioned above differ from other CRBR studies in that they consider the feedback between individual trophic links and stability of the community as a whole. These other CRBR studies have mainly focused on CRBRs that maximize the fitness or persistence of consumer-resource species pairs (Vasseur and McCann, 2005; Weitz and Levin, 2006; Yodzis and Innes, 1992) without scaling up to more complex systems where multi-species coexistence stability becomes an important factor. Indeed, this study supports the results of previous ones that the CRBR distribution evolves during community assembly partly because of community stability constraints (Brose et al., 2006a; Emmerson and Raffaelli, 2004; Jonsson and Ebenman, 1998). However, it differs from them in that it includes a larger spectrum of CRBRs < 1, such as those between parasitoids or parasites and their hosts (but see Otto et al., 2007). This is a nontrivial issue because recent data suggest that such interactions are ubiquitous and may even dominate food web structure and energetics (Kuris et al., 2008; Lafferty et al., 2006a; Lafferty et al., 2008;

Leaper and Huxham, 2002; Memmott et al., 2000; Thompson et al., 2005; Woodward et al., 2005a). In terms of the dynamical underpinnings of the CRBR distribution, the results of this study are in broad agreement with those of Brose *et al*. (2006a) and Otto *et al*. (2007) even though they have used different mathematical models from the one here. The fundamental mechanism that interlinks CRBRs to community dynamics identified by those studies and this one are the same (the stabilizing effect of the relatively weaker mass-specific interaction strengths associated with larger CRBRs). However, this study shows that because the CRBR distribution is tightly linked to that of the community's SBMs, it is difficult to separate the feedback between CRBRs *per se* and community stability. For example, assuming that trophic linking probability (p_c) is independent of body sizes, changes in the CRBR distribution will partly reflect the realized trophic linking due to differences in the SBMs of the immigrant pool and the local community.

3.5.1 Caveats

Metabolic allometric scaling assumptions. The fact that I have used $\beta = ¾$ throughout this study might suggest that this scaling exponent relationship is truly universal. This if definitely not the case, and deviations from this exponent can be found within many taxonomic groups (Glazier, 2005; Peters, 1983). However, this relationship does hold well across taxonomic groups spanning large orders of magnitude variation in body sizes, which is typically how local communities are composed (Brose et al., 2005; Brown et al., 2004)(also see Chapter 4 of this dissertation). Accordingly, the analysis of the BLV model above also encompasses > 20 orders of magnitude variation in body size. I have also not included body temperature-dependence into the allometry of metabolism for parameterizing the LV model (Gillooly et al., 2001). This can be justified to some extent because the vast majority of species in local communities belong to the same metabolic category (ectotherms). However, as far as ectotherms are concerned, environmental temperature is particularly important. Hence a more realistic body size based interaction network model should include temperature dependence to account for climatic variation across space, or the effects of temporal climate change.

Another potential problem is the assumption that species' intraspecific density dependence scales with mass according to expression 3.5. I am unaware of any empirical data on the actual scaling of intraspecific density dependence with body mass. The values ¼ – ½ for γ were chosen because they yield empirically feasible values for the scaling exponent of equilibrium biomasses (see section 3.3.2 and Appendix E). Hence until relevant empirical data become available, the model developed in this study should be viewed for what it is: a possible set of mechanisms for

the emergence of biomass scaling in local communities (for examples of alternative interaction based models, see Loeuille and Loreau, 2006; Rossberg et al., 2008). Note also that as long as equilibrium biomasses in local communities scale with v between 0 and 0.25 (empirical data strongly support this; see Brown and Gillooly, 2003; Leaper and Raffaelli, 1999), the main results of this study remain unchanged.

Effects of body size specific scaling of encounter rates. I have chosen a rather simple model for scaling consumption rate as a function (φ_{ij}) of CRBRs. φ_{ij} subsumes both encounter rate and handling efficiency, and assumes that the overall effect of these two factors is unimodal. The unimodality of handing handling stems from the physical limitations that consumers face while exploiting resource that are too much smaller or too larger than themselves, and is supported empirically (Aljetlawi et al., 2004; Brose et al., 2008; Persson et al., 1998). On the other hand, establishing a general body mass dependent scaling of encounter rate is a difficult problem because of paucity of empirical data combined with the wide variation in physical properties of environments (for example, terrestrial vs. aquatic), organismal sensory channels (e.g., visual vs. chemical signals), and foraging strategies (e.g., sit-and-wait vs. active). As mentioned before, the task of proposing an appropriate scaling of encounter rates is made harder in this study because unlike previous body size based parameterizations which have focused mainly on interactions where consumers tend to be larger than resources (cf. Loeuille and Loreau, 2005; Petchey et al., 2008; Weitz and Levin, 2006), this one includes the entire spectrum of biologically feasible CRBRs.

Because variation in encounter rates can effectively change the location of the peak (k) of the consumption intensity finction φ_{ij}, I have allowed six orders of magnitude variation in k, and found that it does not change the main results of this study. Nevertheless, the potential scaling of encounter rates with body size needs further work. I argue that this work has to be empirical to begin with, because there is almost no data upon which to base encounter rate scaling models (The study by Aljetlawi et al., 2004 is a rare example). I will illustrate this with an example. In a related study on modeling predator prey dynamics, Weitz & Levin (2006) assume that if consumers are much larger than their prey, a relatively higher encounter rate on a per capita basis is more likely than vice versa, mainly because larger consumers can cover larger areas. However, when CRBRs < 1 are taken in to consideration, additional biological considerations come into play. For example, host-parasite and parasitoid interactions are typically characterized by some level of evolutionarily stable trophic specialization (such as that between a parasite or parasitoid and its host), which increases effective encounter rate (Raffel et al., 2008). Hence the CRBR

based consumption rate function used in this paper is nothing but a minimal model that should be extended to accommodate variation in different types of consumer-resource interactions in future work. Whether this minimal model succeeds in predicting the characteristics of real community food webs will be evaluated in the next chapter.

Tables

Table 3.1. Parameters of the BLV model of community food web dynamics and their numerical values.

Parameter	Description	Dimensions	Scaling	Parameter values
β	Scaling exponent for mass-metabolism allometry	-	-	0.75
b_i	Mass-specific biomass production rate of the i^{th} basal species	$time^{-1}$	$m_i^{\beta-1}$	-
d_i	Mass-specific intrinsic death rate	$time^{-1}$	$m_i^{\beta-1}$	-
α_{ij}	Mass-specific biomass loss rate of i^{th} species to the j^{th} one	$time^{-1}$	$m_j^{\beta-1}, m_j/m_i$	-
$a_{b,i}$	Scaling constant for b_i	$mass^{1-\beta}$ x $time^{-1}$	-	1
	Scaling constant for d_i	$mass^{1-\beta}$ x $time^{-1}$	-	0.002
k	Location parameter for the function φ	-	-	0.001–1000
s	Scale parameter for the function φ	-	-	0.01–0.1
α_{ii}	Mass-specific intraspecific density dependent biomass loss rate	$time^{-1}$	m_i^{γ}	-
γ	Scaling exponent for α_{ii}	-	-	0–0.25
a_{ii}	Scaling constant for α_{ii}	$mass^{\gamma}$ x $time^{-1}$	-	Depending upon target n at IEE

Table 3.2. Various food web structural signatures of stability constraints in body size structured communities at IEE. The mean species richness (±SD in parentheses) at IEE for each assembly type is shown in the header row. For each structural feature, the tabulated values give the percentage of 150 model food webs that showed the expected relationship, along with the mean value (±SD) of the measure in parentheses. For the measures that are correlation coefficients (rows 1–7) (Spearman's rank correlation coefficient), the signature was considered significant if p <0.01 (two-tailed). For the measures that are SBM and CRBR distribution characteristics (rows 8–10), the signature of stability constraints was considered significant if a deviation in the expected direction from the null value (section 3.3.4 and expressions 3.7–3.8) was seen.

Signatures of stability constraints	**Assembly type (distribution of the immigrant SBM)**	
	$\omega = 1$ (n(IEE) = 43.12±5.6)	**$\omega = 2$** (n(IEE) = 40.1±5.0)
$r\left(G, \bar{\bar{G}}_w\right)$	100% (–0.73±0.08)	97.3% (–0.68±0.09)
$r\left(G, \bar{\alpha}_G\right)$	99.3% (–0.71±0.10)	92.7% (–0.66±0.11)
$r\left(m, G\right)$	99.3% (0.70±0.09)	94% (0.66±0.11)
$r\left(TL, \bar{\bar{G}}_w\right)$	68% (–0.56±0.09)	73.3% (–0.57±0.1)
$r\left(TL, \bar{\alpha}_G\right)$	54% (–.53±0.09)	46.7% (–0.56±0.10)
$r\left(TL, m\right)$	48% (0.54±0.09)	48% (0.56±0.1)
$r\left(TL, CRBR\right)$	68% (0.31±0.10)	84% (0.31±0.13)
$\mu_{\text{l-SBM}}$	100% (–5.63±1.29)	100% (–7.69±1.11)
$sk_{\text{l-SBM}}$	100% (1.07±0.36)	100% (1.58±0.47)
$\mu_{\text{l-CRBR}}$	100% (3.06±1.08)	93 .3% (1.56±0.15)

Figures

Figure 3.1. The body size dependence of interspecific trophic interaction characteristics across twelve orders of magnitude variation in consumer and resource species' body masses: the possible distribution of interaction strengths (α_{ij}) (expression 3.3) (a), trophic link strengths ($\overline{c}_{ij}$) (expression 3.10) for $v = 0.25$ (b), and the ratio 3.14 (assuming generality of 1 for each consumer) for $v = 0$ and 0.25 (corresponding approximately to $\gamma = 0.25$ and 0.5, respectively, based upon expression 3.9 b) (c & d). All variables are shown in the log scale to facilitate visual interpretation. These figures are for $k = 1$ and $s = 0.1$; changing the former would change the location of the CRBR =1 line, while increasing (decreasing) the latter would increase (decrease) the spread of the interaction strengths around k. The values of the allometric scaling constants $a_{b,i}$, and a_{ii} are largely irrelevant and were arbitrarily set to 1, and of the parameter e_i to 0.5.

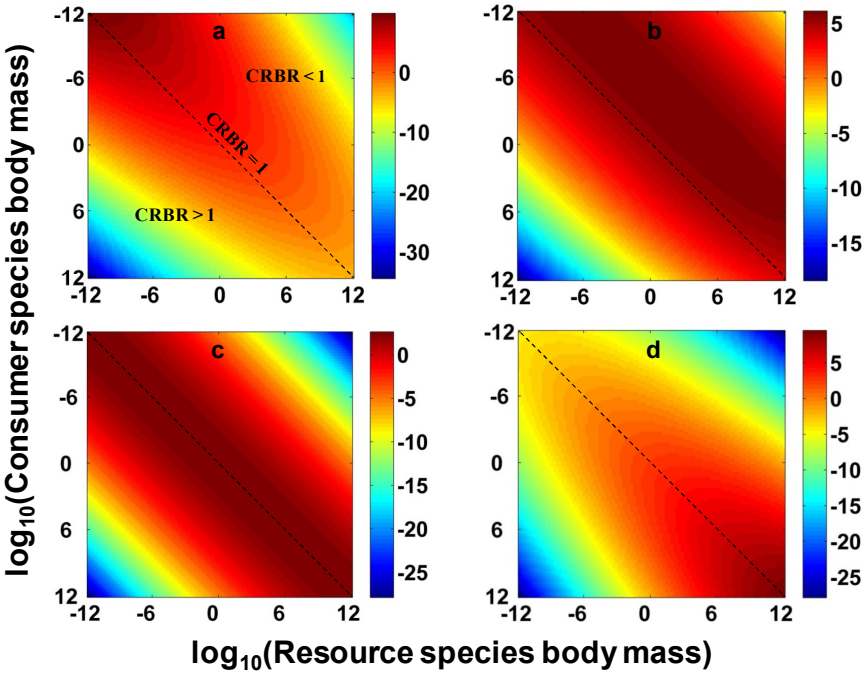

Figure 3.2. Changes in characteristics of trophic generality modules during assembly in communities assembled using the BLV model for the two extreme values of ω; 1 (a) and 2 (b). Mean values with 99% confidence intervals (grey lines) across 150 simulation runs over 400000 time steps are shown for the correlation coefficient between generality and $\bar{G}^w$ ($r\left(G,\bar{G}^w\right)$) (lower lines) as well as $\bar{\alpha}_G$ ($r\left(G,\bar{\alpha}_G\right)$) (upper lines). The patterns of changes in other, non-body size based community characteristics (such as link density) were similar to those seen in Fig. 2.5, and are not shown here. The values of n achieved at IEE for the two different settings of ω are shown in Table 3.2. All assembly algorithm runs had the same connectance probability (p_c = 0.3), and began with five basal species (~10% of n at IEE, which was 43.12 for ω = 1 and 40.1 for ω = 2; see Table 3.2). These trends do not change qualitatively for assembly with fewer or more basal species than this. They are also insensitive to a wide range of variation in other parameter values as well (see section 3.4.1).

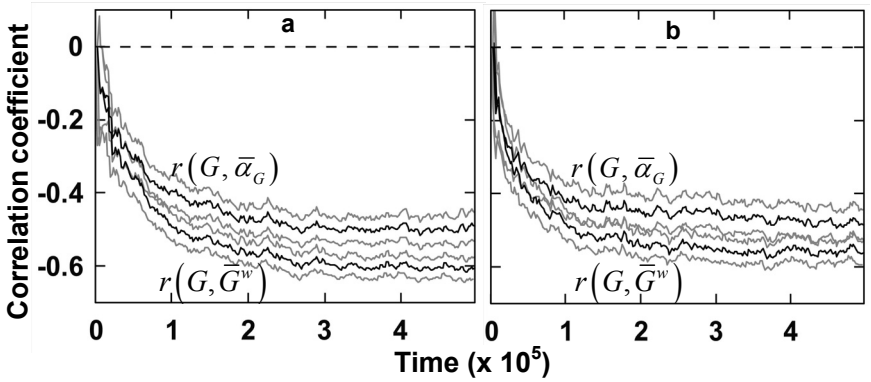

Figure 3.3. Changes in the l-SBM and l-CRBR distributions of model communities during assembly. Mean values with 99% confidence intervals (grey lines) across 150 simulation runs over 400000 time steps are shown for mean (a) and skewness (b) of the l-SBM well as the CRBR distributions (c & d). Each plot compares the trajectories for the two extreme values of ω, with the dotted lines showing the null values of distributional characteristics (section 3.3.4 and expressions 3.7–3.8). These trends are for the same communities shown in Fig. 3.2.

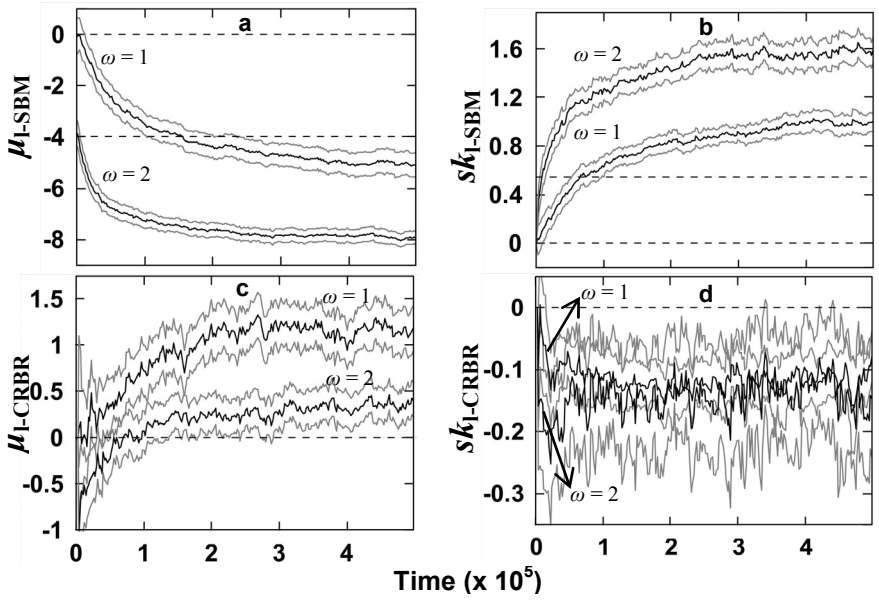

Figure 3.4. SBM (a,c) and the associated CRBR (b,d) distributions in two different model communities at IEE assembled with $\omega = 1$ (upper panel) and 2 (lower panel). The dotted lines in the SBM distribution plots show the expected distribution expected if assembly was fully relaxed and there was no sampling error (see section 3.3.4).

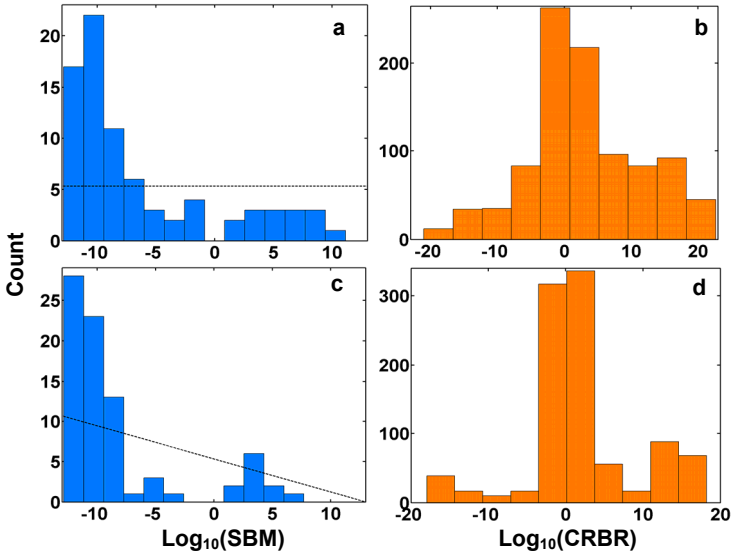

Figure 3.5. The interdependence between food web structural signatures of dynamically constrained assembly in 150 model communities at IEE. These results are for communities assembled at $\omega = 1$; the incidences and strengths of these signatures across the model communities are summarized in Table 3.2 (second column). The relationships a–c are strong and highly significant ($p < 0.0001$; $R^2 = 0.91$, 0.95, and 0.68 respectively), while d is significant but weak ($p = 0.0002$, $R^2 = 0.09$).

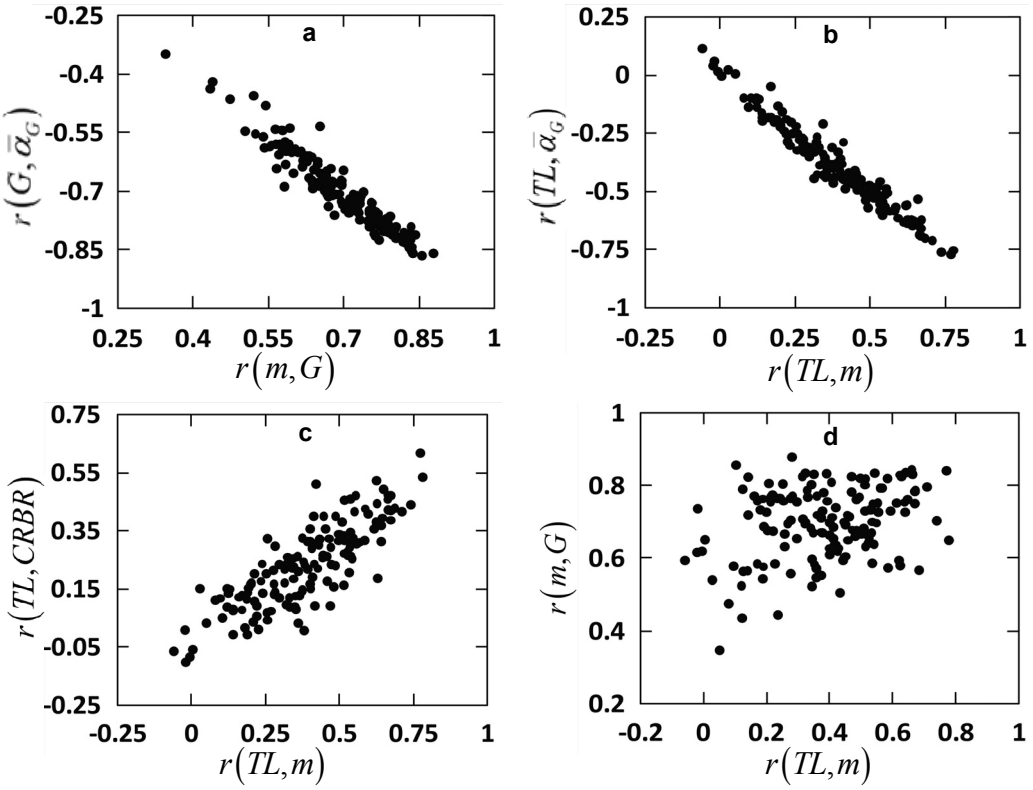

Chapter 4: Signatures of stability constraints on food web structure in natural communities

Abstract. To understand the persistence of natural species-rich communities, a major challenge is to quantify the relationship between their stability and the structure of the underlying food web. Building on the theoretical results of a previous study, in this paper I address two interrelated questions: first, whether the food web structure of real communities show some predicted signatures of dynamically constrained assembly, and second, whether species-level foraging properties are constrained (and in turn constrain) community stability. I address these questions using data from nine communities across a range of terrestrial and aquatic food webs, using species' body sizes to constrain the strengths of interspecific interactions. The results provide strong evidence that the food web structure of natural communities do indeed exhibit signatures of stability constraints, and that a relatively simple Lotka-Volterra type mathematical model (see chapter 3) with body size based parameterizations is successfully able to predict a number of empirically observed food web structural features. In particular, I find that five food web structural characteristics are influenced by constraints on community stability: (i) A decrease in consumer species' trophic generality-averaged interaction strengths ($\bar{\alpha}_G$) (a measure of their average biomass uptake rate), (ii) increase in their trophic generality with body size, (iii) decrease in their $\bar{\alpha}_G$ with trophic position, (iv) increase in their body size with trophic position, and (v) increase in the ratios of body sizes of consumers and their resources with trophic level. While some of these features were already known in the literature, this is the first study to compare the prevalence of these features across multiple local communities, and to propose a single explanatory model for them. I also find strong evidence that species foraging strategies are determined not just by their optimal foraging requirements (maximization of biomass uptake), but also by constraints placed by community stability. In particular, species with high biomass uptake rate tend to destabilize the community, and can even be driven extinct by feedbacks through the food web.

4.1 Introduction

An important challenge in contemporary biology is to understand how food web structure and the persistence of species rich communities are interrelated. This issue is rendered all the more interesting because of the very presence of neutral biogeographic models for community

structure, which ignore the effects of interspecific interactions, and empirical data supporting them (Hubbell and Borda-De-Agua, 2004; MacArthur and Wilson, 1967).

A major advance towards interlinking food web structure and community stability, beginning with seminal studies by May (1973; 1974) and Levins (1974; 1975), has been the development of mathematical models that elucidate the effects of particular food web structural motifs (such as trophic chains or network modules resulting from omnivory) on community stability, and the mechanisms by which stabilizing configurations of these features emerge during assembly (McCann et al., 1998; Neutel et al., 2007; Neutel et al., 2002; Pawar, 2009; Pimm and Lawton, 1977; Yodzis, 1981). A consensus emerging from these studies is that certain regularities seen in food web structure are likely to be signatures of stability constraints on the stable coexistence of multiple species. For example recently, building on the work of Levins (1974; 1975), Neutel et al. (2007; 2002) have shown theoretically how community stability is limited by strengths of interactions along trophic loops (a series of trophic links beginning and ending at the same species node without visiting any other node more than once). Moreover, they provide compelling empirical evidence that stabilizing configurations of trophic chains and omnivorous interaction modules emerge during secondary succession of the community. However, Neutel et al.'s study is an exception; while theoretical studies continue to advance our knowledge of the potential mechanisms and the particular non-random food web structures that are likely to emerge due to dynamical stability constraints, empirical research lags far behind in confronting the theory with data (May, 2006; Pimm, 1982). This is not surprising because the complexity of natural communities rivals that of most other biological as well as non biological systems (May, 2006; Newman, 2003; Proulx et al., 2005), and quantifying interactions between multiple species is no trivial task (Berlow et al., 2004; Wootton and Emmerson, 2005). This study aims to make a contribution by addressing two questions:

(i) Do natural communities show signatures of dynamical stability constraints on their food web structure? and,

(ii) How do species-level foraging strategies affect community stability, and *vice versa*?

The first, fairly broad question addresses the issue of whether limitations of community stability do indeed drive the emergence of particular, stabilizing food web structures in natural communities. Thus addressing it will shed further light on whether food web structure and species interactions are important to species diversity and community structure in local assemblages (McCann et al., 1998; Neutel et al., 2007; Neutel et al., 2002; Yodzis, 1981; Yodzis, 2000). The second question addresses an important issue that has been largely ignored in the past: the mechanisms by which particular food web structures may emerge due to stability constraints.

This issue is conceptually challenging; any suggestion that groups of species interacting in a particular way can be "selected" is problematic because natural selection typically operates at a much lower level of organization- to enhance the fitness of individuals in populations (Webb, 2003). Decades ago, this problem was considered by Levins (1974; 1975), who theoretically studied the interrelationships between levels of food web organization, natural selection, and community stability, and concluded that, "…*mendelian selection in a single species may stabilize or destabilize the community as a whole, may introduce oscillations, and may affect community stability in ways that are not intuitively obvious.*" (Levins, 1975). In other words, strategies that are good for single species (i.e., which maximize their mean population fitness) may not be beneficial to the community (in terms of the persistence of multiple species) as a whole. However, these conclusions and this issue appear to have been largely overlooked in community ecology until recently (Webb, 2003). In fact, some recent authors have suggested that species-level foraging strategies alone are adequate for understanding food web structure (Beckerman et al., 2006; Petchey et al., 2008). In the words of Petchey et al. (words in parentheses are mine): "*Although such theories* [about stability constraints on food web structure] *are interesting, theoretically attractive and may play a part in structuring networks, our results suggest that building food webs from the bottom-up, by modeling the behavioral decisions of individuals, is a simple and promising alternative framework.*". If this conclusion is correct, understanding not just how food web structure changes, but even the more general issue of the maintenance of species rich communities can be boiled down to species-level traits alone. This issue begs further investigation because recent studies have, on the other hand, shown empirical evidence for the relationship between food web structural features involving species' foraging strategies (such as degree distributions and omnivory) and stability of the community as a whole (Berlow et al., 2009; Neutel et al., 2007; Neutel et al., 2002; Otto et al., 2007).

To address the above two questions, I will test some of the theoretical predictions of a previous study (Chapter 3). In that study, using a species' body size-constrained Lotka-Volterra type model of community structure and dynamics (BLV model), it was shown that a combination of assembly dynamics (the pattern of species' immigrations and extinctions into a local community) and the constraints of multi-species stable coexistence should result in the emergence of certain non-random food web structural features. The incidence and strength of these features are hence signatures of stability constraints, and can be used to gauge the importance of species interactions and food web structure to the assembly and persistence of local communities. To test these theoretical predictions, I will use interspecific trophic interaction and species' body size data from nine communities across a range of habitats and geographical localities. The use of

body size in this study is also a matter of necessity. Body size provides a means to map individual-level biological constraints onto population- and community-level dynamics in an empirically tractable way (body size is relatively easy to measure in nature). This mapping is possible because body size constrains interspecific trophic interactions in two ways. First, the whole organism metabolic rate increases allometrically with body mass according to a consistent power law relationship (Brown et al., 2004; Kleiber, 1961; Peters, 1983). This in turn determines species life history characteristics such as biomass production, birth, and mortality rates. Second, depending upon the environmental context, the average size difference between individuals of consumer and resource species sets physical limits on the frequency with which the two encounter each other, as well as the rate at which the former can exploit the latter following encounter (Dial et al., 2008). An increasing number of studies are now using both these effects of body size in empirical and theoretical studies of trophic interactions (Berlow et al., 2009; Brose et al., 2006a; Brose et al., 2008; Jonsson and Ebenman, 1998; Lewis et al., 2008; Loeuille and Loreau, 2005; Otto et al., 2007; Petchey et al., 2008; Vasseur and McCann, 2005; Virgo et al., 2006; Weitz and Levin, 2006; Woodward et al., 2005a; Woodward et al., 2005b).

4.2 Methods

4.2.1 Food web data

Of all the available community food web datasets, sixteen relatively high quality ones were initially chosen using the criteria described in Chapter 2 (see section 2.2.2, and Table 2.1). The justification and application of these criteria, as well as the methods of preliminary data processing are described in Appendix C. Essentially, these data selection criteria ensure that only those communities which have a relatively well-resolved tropic interaction structure were chosen. In particular, these criteria eliminated communities that had been subjected to substantial *a priori* taxonomic aggregation. Nor did we perform an aggregation of taxa into "trophospecies", wherein taxa with highly similar or identical sets of consumer and resource species are treated as the same functional unit for convenience (i.e., two or more network nodes are collapsed into one) (Yodzis, 1988). Apart from the fact that developing objective criteria for trophospeices is a difficult task (Yodzis and Winemiller, 1999), the use of this approach in the current study in undesirable for two reasons. Firstly, the trophospecies approach has been used mainly in "static" structural studies of food webs wherein only the presence-absence of trophic links are studied, and not the associated interaction strengths (e.g., see Allesina et al., 2008 and references therein). In contrast,

this study is focused on the effects of food web structure on dynamical stability; hence even if two species have identical consumers and resources, they are unlikely to have identical strengths of interactions across the links, and hence are not dynamically equivalent. Secondly, the complete structure of the quantified food web is necessary for analyzing the stability of the community, and collapsing nodes into trophospecies can give a distorted view of the community's dynamical characteristics.

Sixteen food webs met the initial criteria (listed in Table 2.1), of which only nine had data on body sizes of all taxa. These are listed in Table 4.1, along with salient features and the sources of trophic link and body size data. In the case of the GC community, only one of the six subcommunities ("Clmown1") was chosen because they all had similar food web structural properties (connectance, average trophic degree, and food chain length were more similar between these communities than between them and others).

Because body mass is the species size variable of interest here, whenever only data on a species' body length was available, it was converted using allometric relationships of the form: mass = a (length)^b. The parameters a and b were varied according to broad taxonomic groups (typically at the level of class and order) (Niklas and Enquist, 2001; Peters, 1983). Table 4.2 lists these values across different plant and animal groups. In the case of certain groups such as worms and coelenterates, no meta-analyses were available. In these cases, the parameters of groups with similar body form and mass density were used (for example, legless herpetofauna for worms). Of the community datasets that had body mass (instead of length) data to begin with, most consisted of at least a few species whose mass information was derived by the original authors using such length-to-mass conversions. The EW community consists of 391 taxa including a number of animal groups for whom length-mass scaling information are unavailable, and whose body forms preclude the use of scaling parameters of other groups (e.g., coelenterates and anthozoans) (Brose et al., 2005). Hence length, instead of mass data, was used for this community.

Clearly, taxonomic class- or order-wide use of the same length-mass scaling parameter is bound to increase the inherent noise in such data; this is exacerbated by the substitution of parameters for groups without information. However, as will be discussed further below, across local communities, > 20 orders of magnitude interspecific body mass variation is seen, with each local community having been sampled for at least six orders of magnitude variation (see Fig. 4.3). Hence these errors are expected to be somewhat mitigated by this wide variation.

4.2.2 Food web structural measures and theoretical predictions

The predicted food web structural signatures that will be tested for are summarized in Fig. 4.1. In Chapter 3 (also see Chapter 2 and Pawar, 2009) it was shown that given some fairly general and biologically reasonable assumptions about the probability of immigration of species into a local community with respect to their body sizes, these signatures emerge through immigration-extinction dynamics, with extinctions driven partly by dynamical stability constraints. In particular, a key food web structural property that is subjected to these constraints is species' "generality-averaged interaction strengths" ($\bar{\alpha}_G$), which for the j^{th} consumer species is defined to be (see section 3.3.3 of chapter 3):

$$\bar{\alpha}_{G,j} = \frac{\sum_{i \in \mathcal{B}_j} |\alpha_{ij}|}{G_j} \tag{4.1}$$

where $\mathcal{B}_j$ the set of its resource species and G_j the number of species in this set (its trophic generality or niche width). The broad conclusion drawn from the previous study was that species with high values of $\bar{\alpha}_G$, which is essentially a measure of biomass uptake rate, tend to destabilize the community, which results in the signatures shown in Fig. 4.1. Furthermore, it was also shown that these signatures were interlinked; in particular, the decrease in species' generality-averaged interaction strength ($\bar{\alpha}_G$) with generality (measured by $r\left(G, \bar{\alpha}_G\right)$) is brought about by an increase in species' generality with body size (measured by $r\left(m, G\right)$), while decrease in species' $\bar{\alpha}_G$ with trophic position is strongly linked to increase in consumer species' body size as well as CRBR's with trophic position (measured by $r\left(TL, m\right)$ and $r\left(TL, CRBR\right)$ respectively).

Note that three of the signatures predicted in Chapter 3 (sections 3.3.3 & 3.3.4), i.e., decline of species' generality-averaged weighted generality ($\bar{G}^w$; defined in expression 2.11) with generality ($r\left(G, \bar{G}^w\right)$), decline of $\bar{G}^w$ with trophic level (TL)($r\left(TL, \bar{G}^w\right)$), and the mean of the distribution of logarithmically transformed species' body masses ($\mu_{\text{l-SBM}}$) are not being considered here for the following reasons. Firstly, in the case of $r\left(G, \bar{G}^w\right)$ and $r\left(TL, \bar{G}^w\right)$, measuring $\bar{G}^w$ requires information about species' equilibrium biomasses, information on which are not available for most food web datasets. Moreover, examining $r\left(G, \bar{\alpha}_G\right)$ and $r\left(TL, \bar{\alpha}_G\right)$ instead allows insights into the importance of stability constraints on species' consumption strategies alone (without the effects of biomasses). Secondly, the local community's $\mu_{\text{l-SBM}}$ cannot be examined meaningfully as a signature of stability constraints because, as shown in Chapter 3

(section 3.3.4), its deviation from the null expectation requires knowledge of the immigration pool and assembly pattern.

4.2.3 Data analyses

The various parameters and their values used in the following data analysis are shown in Table 4.3.

Detecting food web structural signatures. The tests used to evaluate the presence and significance of each of the structural signatures are also summarized in Fig. 4.1. For the signatures that are bivariate relationships (rows 1–5 of Fig. 4.1), the strength of the pattern was calculated using the Spearman rank correlation coefficient (with standard parametric two-tailed p values). A stronger measure (such as a linear or nonlinear regression model fit) was not used because though the numerical simulations of Chapters 2 & 3 provide insights into the actual shapes of the relationships $r(G,\bar{\alpha}_G)$, $r(m,G)$, $r(TL,\bar{\alpha}_G)$, $r(TL,m)$ and $r(TL,CRBR)$ that emerge during assembly, there is currently no theoretical basis for expecting any particular form for them.

In all the signatures except $sk_{\text{l-SBM}}$, the significance of the observed pattern was also tested by comparing it with those of randomized communities. Randomizations were performed in two ways: full and partial. Under full randomization, species' body masses were randomly permuted while keeping the food web structure intact. This is easily done by permuting body masses across species. Under partial randomization, body masses were randomly permuted only within basal and non basal species (i.e., trophic level 1 vs. all others). This additional, conservative method of randomization was used because it maintains the body mass ranges of basal and non-basal species, which have been found to show consistent patterns within habitat types, and may be driven by historical and environmental factors rather than the internal dynamics of the system (Brown and Gillooly, 2003; Hildrew et al., 2007). 2000 randomizations of each type were performed.

Calculation of interaction strengths. The mass-specific interspecific interaction strength coefficients α_{ij} needed for calculating the food web structural signatures were obtained using the expressions (originally defined in section 3.2 of Chapter 3),

$$\alpha_{ij} = e_j a_{b,j} m_j^{\beta-1} \varphi_{ij} \tag{4.2a}$$

and

$$\varphi_{ij} = \exp\left(-\left(s\log\left(m_j m_i^{-1}/k\right)\right)^2\right) \quad (4.2b)$$

(where j consumes i). Here, $a_{b,i}$ is a taxon-specific normalization constant, m_i the species' average adult body mass and β the scaling exponent of metabolic allometry. φ_{ij} is a consumption intensity function, the shape of which, across a given range of consumer-resource body mass ratios, $m_j m_i^{-1}$ (CRBR's), is determined by the parameters s & k. Thus assuming that $\beta = ¾$ (see section 3.2), of all the parameters of the BLV model (Tables 2.2 and 3.1), the ones needed for calculating the food web structural features (rows 4–7 of Fig. 4.1) are a_b, e, k, and s. These were determined as follows.

a_b was chosen to be 1 based upon extensive empirical data (Brown et al., 2004; Peters, 1983). Consumption efficiency e was fixed at 0.5 for all species; this is the approximate midpoint of the range reported from empirical data (Brown et al., 2004; Peters, 1983). As discussed in Chapter 3 (section 3.2), the values of the parameters k (the CRBR at which the consumption intensity peaks) and s (the steepness with which consumption intensity peaks with respect to CRBR's) are expected to vary with type of consumption (foraging) strategy as well as habitat type. For example, in the case of predator-prey interactions, because smaller organisms have greater mass-specific power relative to larger ones (Dial et al., 2008), and can hence handle a larger range of prey sizes, k may be closer 1 (or even <1) for small consumers, and s smaller (a more gradual decline of consumption intensity at extreme ratios). A meta-analysis of CRBR's by Brose et al. (2006b) shows that invertebrate consumers do indeed have a k closer to 1 than vertebrates across disparate habitat types, indicating their superior ability to handle prey closer to their own size. In host-parasite and parasitoid interactions on the other hand, k should be < 1 because parasites and parasitoids are selected to adopt strategies that increase effective encounter rate as well as exploitation success of resource species much larger than themselves (Cohen et al., 2005; Raffel et al., 2008). Hence it is desirable to adjust k and s for calculating empirical interaction strengths according to interaction type. However, because of the paucity of data on actual CRBR dependence of functional constraints and consumption intensity across biotic groups (see Aljetlawi et al., 2004 for two rare examples of such data; Brose et al., 2008), it is currently difficult to develop a model to select these parameters. Hence I chose to fix k at 1 (maximum consumption intensity when consumers and resources are equal in size). The value of s was chosen as follows. The function φ_{ij} approaches zero more and more rapidly as s increases. As $s \rightarrow$

0.1, consumption intensity falls to zero within the range of the CRBRs observed across the nine real communities (Fig. 4.2; cf. Fig. 4.3); hence larger values larger than this are unfeasible because if a CRBR is observed, no matter how extreme, it *must* be associated with some level of consumption. On the other hand the consumption intensity function becomes flat as $s \to 0$, and the effects of CRBRs on trophic link strengths are eliminated. Hence s was set at 0.05, the midpoint of these two extreme values of s.

In Appendix F I show two things. First, the results of this study are remarkably robust to variation in k and s. Second, as has been suggested above, an interaction-type specific choice of k results in stronger values of food web structural signatures, indicating that this may indeed be an appropriate approach. Note that in Chapter 3 I have also shown that the theoretical results themselves are also robust to considerable variation in k and s.

Evaluation of community stability properties. I also tested whether the observed communities were indeed organized in a manner that enhanced their stability, by examining whether the observed system was more likely to be Hurwitz stable than randomized counterparts. As defined in section 2.2.1, a community is Hurwitz stable if the maximum of the real parts of the eigenvalues of the Jacobian ("Community matrix", $\boldsymbol{C}$) is negative; i.e.,

$$\lambda_{\max}\left(\boldsymbol{C}\right) < 0\,, \tag{4.3}$$

where $\lambda_{\max}\left(\boldsymbol{C}\right) \equiv \max\left\{\mathrm{Re}\left(\lambda_i\left(\boldsymbol{C}\right)\right)\right\} \forall\ i \in \mathfrak{N}$. Under the assumptions of the BLV model, $\boldsymbol{C}$ can be calculated using species' body mass and trophic interaction information alone by substituting expression 4.2, intraspecific density dependences (originally defined in section 3.2 of Chapter 3),

$$\alpha_{ii} = -a_{ii} m_i^{-\gamma} \tag{4.4}$$

and the scaling of equilibrium biomasses (section 3.3.2 of Chapter 3)

$$\hat{x}_i = a_{\hat{x}} m_i^{\nu}\,, \tag{4.5}$$

into the elements of the community matrix (originally defined in section 2.2.1),

$$c_{ij} = \alpha_{ij} \hat{x}_i \tag{4.6}$$

Thus the additional parameters $a_{\hat{x}}$, v, a_{ii} and γ are now needed, which were determined as follows. The scaling exponent for equilibrium biomass v was chosen to range between 0 and 0.25, which is consistent with data from local communities (Leaper and Raffaelli, 1999; Sheldon et al., 1977) as well as the range of exponents predicted by current theories that combine size-metabolic scaling with trophic interactions (Brown and Gillooly, 2003; Loeuille and Loreau, 2006; Marquet et al., 1995; Rossberg et al., 2008; Chapter 3 of this dissertation). The constant $a_{\hat{x}}$ merely rescales all the elements of $\boldsymbol{C}$ and was arbitrarily chosen to be 1. The parameter γ, which determines the scaling of mass-specific biomass loss rate due to intraspecific interactions, was also chosen to lie between 0 and 0.25, which accommodates density dependence ranging from being independent of species body-masses ($\gamma = 0$), to that expected from the scaling of mass-specific metabolic rate ($\gamma = 0.25$) (also see sections 3.2 and 3.3.2 of Chapter 3). Finally, for each combination of values of v and γ, the value of the scaling constant a_{ii} was chosen to be the minimum value across species that would guarantee that the system was Hurwitz stable (any nontrivial community matrix can be rendered so by increasing the magnitudes of the negative diagonal elements; see Chapter 2 and Appendix A). This was done by first calculating $\boldsymbol{C}$ and assigning a value of c_{ii} that was arbitrarily large (such that the system was Hurwitz stable). The value of c_{ii} was then gradually decreasing it until $\lambda_{\max}(\boldsymbol{C})$ became positive, thus giving the minimal value needed to make the system Hurwitz stable. This minimal value of c_{ii} was then used across the community matrices of the randomized counterparts of the community.

Comparisons with maximal foraging communities. To address the second question of this study, i.e., the effects on food web structure of constraints from dynamical stability need to be weighed against those from species' optimal foraging requirements. To this end I constructed a counterpart of each observed community by rearranging the trophic links such that some function of species' energy uptake was maximized. These counterparts were then compared with the observed communities.

Under classical optimal foraging theory (OFT) (Stephens and Krebs, 1986), resource species are allocated to each consumer using a function that considers the net energy gained by consumption of an individual of the potential resource species, the encounter rate with it, and handling time. Recent papers seeking to predict food web structure using OFT have used these parameters to rank potential resource species of consumers, and allocating them until an optimal energy intake function is maximized (e.g., Beckerman et al., 2006; Petchey et al., 2008). In the BLV model of this study, encounter rate and handling efficiency are subsumed under a single

consumption intensity function (see section 3.2). Therefore a species' optimal foraging strategy under the BLV model would be the maximization (under suitable constraints) of its total biomass uptake and production which is (given the set of its potential resource species $\mathcal{C}_j$),

$$U_j \equiv \sum_{i \in \mathcal{C}_j} \left(\alpha_{ij} e_j \hat{x}_i \right) \tag{4.7a}$$

which upon substituting expression 4.2 and 4.5 becomes,

$$U_j = e_j a_{\hat{x}} a_{b,j} m_j^{\beta-1} \sum_{i \in \mathcal{C}_j} \left(m_i^{\nu} \exp\left(-\left(s \log\left(m_j m_i^{-1} / k \right) \right)^2 \right) \right), \tag{4.7b}$$

Because this model is very different from the traditional OFT framework, I will call it a "maximal foraging" strategy. Obviously, some constraints need to be placed on U_j so that species' generalities don't grow boundlessly as this function is maximized. Here I choose to restrict species' generalities such that the overall structure of the food web is maintained. This will allow a direct comparison of the food web configurations of observed and maximal foraging communities. The determination of the maximal foraging counterpart of each community was implemented as follows. For each community, the location of species' in the interaction network were permuted until the proportion of species that had achieved a better biomass uptake and production than the observed web (U_{new}–$U_{obs} > 0$) (let this proportion be denoted by n_{MF}) and the foraging index (*FI*),

$$FI = \sum_n \left(U_{i,new} - U_{i,obs} \right) \tag{4.8}$$

were simultaneously maximized. This was the "maximal foraging counterpart" (MFC) of the observed community. A simple algorithm was used to find the MFC; species' body masses were first permuted iteratively (using the more conservative partial randomization method described above) until a maxima for n_{MF} was found (ideally, ~1). Then the suite of restructured communities with this maximum value of n_{MF} was screened for one that has the maximal *FI* value. If more than one community satisfied this condition, the body masses were iterated further until a single MFC was found. The calculation of expression 4.7 either requires data on species' equilibrium biomasses of a reasonable assumption about the size-biomass scaling exponent *v*.

Because data on equilibrium biomasses were not available for most of the communities, I determined MFCs for both the extreme values of v: 0 and 0.25.

4.3 Results

4.3.1 Stability of observed vs. size-randomized communities

Table 4.4 summarizes the Hurwitz stability properties of the nine communities (proportion of 2000 size-randomized food webs that had $\lambda_{max}(\boldsymbol{C})$ smaller than that of the observed one). As might be expected, the $\lambda_{max}(\boldsymbol{C})$ of the observed communities deviates more strongly from those of fully randomized webs compared to the partially randomized ones. Overall, irrespective the scaling of equilibrium biomasses (parameter v) or the intraspecific density dependence (γ), the observed body size structures of the empirical food webs clearly tend to endow some measure of stability. Moreover, most of the cases where the stability of observed webs is no better or worse than random (values ≥ 0.5), appear when equilibrium biomasses are assumed to scale strongly with body mass ($v = 0.25$). This value of v is expected under the energetic equivalence rule, but is rarely observed in real communities (Brown and Gillooly, 2003; Leaper and Raffaelli, 1999; Marquet et al., 1995; Marquet et al., 2005; Sheldon et al., 1977). Thus overall, these results provide strong evidence that the observed food web structures are nonrandom, and tend to impart stability to the community. We can now examine the predicted signatures of dynamical stability constraints on food web structure.

4.3.2 Signatures of dynamical stability constraints

Signatures on food web structural features. Figure 4.3 graphs the relevant food web structural characteristics across the nine communities, while Table 4.5 summarizes the incidences and significance of structural signatures. Although the significance of these signatures was tested using both full and partial randomizations, only the results for the more conservative partial randomizations is shown; full randomizations yielded consistently stronger significances, as might be expected. Columns 1–5 of Table 4.5 show that most food webs do indeed show the expected signatures (summarized in Fig. 4.1) of stability constraints. In particular, $r\left(G, \overline{\alpha}_G\right)$ and its coupled characteristic $r\left(m, G\right)$ are consistently negative and positive respectively, across communities. The significance of both these signatures is also consistently strong except in the

case of the BS and YE communities. In the case of $r(TL, \bar{\alpha}_G)$ and its coupled signatures $r(TL, m)$ and $r(TL, CRBR)$, the expected correlations are seen less consistently, and in two cases, even opposite trends are seen (in the MS and SB communities). This is not surprising because these features are strongly dependent on hierarchical assembly, wherein later species are more likely to be consumers than resources. Moreover, in the case of the MS community, trophic link sampling appears to be poor, with only the average trophic level value being only 1.2 (see Table 4.1). Below I will consider the issue of sampling adequacy in greater detail. In the case of the SB community on the other hand, the observed pattern suggests a fundamentally different organization, as suggested by the fact that it belongs to a terrestrial community based on a single primary producer species, and has the largest proportion of parasitoid-host links among the nine communities.

The interdependencies between structural signatures predicted in Chapter 3 (section 3.3.3) are shown in Fig. 4.4a–c, and are consistent with the patterns seen in simulated model communities (compare with Fig. 3.5a–c). Furthermore, Fig. 4.4d shows that the increase in trophic generality with body size (measured by $r(m, G)$) is largely independent of the increase in body size with trophic level (measured by $r(TL, m)$), indicating that the observed $r(m, G)$ is a result of stability constraints and not an artifact of the fact that larger species have a larger pool of resource species because they tend to occupy higher trophic levels during assembly (cf. Fig. 3.5d).

Signatures on species' body size and consumer-resource body mass ration distributions. The penultimate column of Table 4.5 shows that the expected right skew of l-SBM distributions is seen in only two communities. Fig. 4.3 shows that the nine communities in fact show a variety of l-SBM distributions, including two that are clearly bimodal (YE and MS). The third column of Table 4.5 shows that as expected from the predictions of Chapter 3 the mean of the l-CRBR distributions tends to be > 0 (biased towards CRBRs > 1). Moreover, the communities show a $\mu_{\text{l-CRBR}}$ that is higher than that expected by (partially) random trophic linking given the observed SBM. Interestingly, the mean $\mu_{\text{l-CRBR}}$ values of most of the communities lie within or close to the range seen for the model communities assembled using the BLV model (i.e., 3.06 (±1.08 SD) and 1.56 (±0.15 SD) depending upon the parameter ω ; see Table 3.2). Also, all the observed l-CRBR distributions show at most weak left skewness, as can be seen in Fig. 4.3, with the skewness values ranging from -1.9 (MS community) to 0.81 (SP community). As shown in Chapter 3, the skewness of the l-CRBR distribution is expected to show a weak signature of stability constraints.

4.3.3 Species' optimal foraging vs. community dynamical stability constraints

Table 4.6 shows the characteristics of MFCs of the nine communities assuming $v = 0$. The results for the $v = 0.25$ are not shown because they were found to be stronger and hence the following conclusions apply irrespective of the choice of v. Also, only the features $r\left(G, \overline{\alpha}_G\right)$ and $r\left(TL, \overline{\alpha}_G\right)$ are shown because as predicted, they were found to be tightly linked to the three others (see Fig. 4.4a–c). The second column of Table 4.6 shows that in all communities the computational algorithm was able to find MFC's with high a proportion of species having improved biomass uptake and production (n_{MF}). Clearly, the food web structural signatures indicative of dynamically constrained assembly are lost in all the MFCs, with the pattern even being significantly reversed in many cases. This means that using optimal foraging principles alone to construct food webs does not account for the distribution of species' with particular body masses across the interaction network. Furthermore, when the $\lambda_{\max}(\boldsymbol{C})$'s of the MFCs were examined (using the methods described in section 4.2.3 above), in most cases they were found to be dynamically unfeasible (not Hurwitz stable), indicating that species optimal foraging requirements can in fact prevent community stabilization during assembly.

4.3.4 A tale of missing links?

As mentioned previously, it is important to gauge whether and to what extents the above results are affected by sampling inadequacies. This is bound to be an important factor because collecting trophic interaction data is an extremely difficult and time labor intensive task, and at best it is possible to quantify only a subset of the interaction network of any local community (Berlow et al., 2004; Goldwasser and Roughgarden, 1997; Martinez et al., 1999). Errors in community food web datasets arise from two main sources: lack of taxonomic sampling, and lack of adequate trophic link sampling. As discussed above, the former probably affects the observed shapes of SBM and CRBR distributions, and potentially, food web structural features as well. However, quantifying this source of error is beyond the scope of this study because it would require sampling effort and species accumulation data from each of the local communities. Quantifying sampling inadequacies in trophic link data is a somewhat more tractable proposition, especially because given a sample of species from a local community, the potential distribution of trophic links can be estimated. Furthermore, certain biases in trophic link data are well documented. For example, recent studies have shown that most food web data sets have an

underrepresentation of parasite-host interactions, as well as all trophic interactions where both consumers and resources are small in size (Kuris et al., 2008; Lafferty et al., 2006a; Lafferty et al., 2008; Leaper and Huxham, 2002; Memmott et al., 2000; Thompson et al., 2005; Woodward et al., 2005a). Hence here I will consider the effect of trophic link sampling bias on the above results.

A number of food web structural features are known to be especially sensitive to inadequate sampling of interactions (Goldwasser and Roughgarden, 1997; Martinez et al., 1999). To obtain a measure of sampling inadequacy across communities, I selected a suite of food web structural characteristics were found to be sensitive to sampling effort by Goldwasser & Roughgarden (1997). These features are connectance (C_T), average generality of consumers ($\overline{G}$), average trophic chain length ($\overline{T_c}$), and omnivory degree (O_{deg}). O_{deg} is the mean of the standard deviations of each consumer species' trophic height (standard deviation of the lengths of all the paths to the species from its basal species (Goldwasser and Roughgarden, 1993)). Other features such as the number and maximum of trophic chain lengths are also sampling sensitive, but are directly related to one or more of these selected measures, and were not included. Nevertheless, the selected features are still (albeit indirectly) interdependent (for example, O_{deg} will typically increase with $\overline{T_c}$); hence I used a Principal Component Analysis (PCA) (Jongman et al., 1995) to combine them, ideally into a single pseudo-variable that can be used as an index of sampling sensitivity. The correlation of strengths of the ostensible signatures of stability constraints across communities with this index would then provide insights into the effects of sampling error. If the signatures become stronger with increasing values of the index, it would suggest that the above results would have been stronger with better sampling. On the other hand, if the signatures become weaker, it would suggest the above results are an artifact of sampling bias.

Data normality is a central assumption of PCA; because the distributions of these food web structural features across communities were somewhat skewed, the data were square-root transformed, which resulted in approximately normal distributions of all four variables (determined using the Lilliefors test). The PCA did indeed result in a single significant component accounting for 86% of variance (with loadings in the following order: $\overline{T_c} > O_{deg} > C_T > \overline{G}$). The scores of this first component were thereafter used as an index of trophic link sampling inadequacy, with which the correlations of observed strengths of the two key signatures of stability constraints, $r(G, \overline{\alpha}_G)$ and $r(TL, \overline{\alpha}_G)$, were calculated using the spearman rank coefficient. Both the correlations were weakly negative ($R^2 = 0.2$ and 0.15 respectively), but insignificant ($p > 0.1$). At the very least, this indicates that the above results are not an artifact of sampling bias.

Furthermore, I also examined the correlation of $\mu_{\text{l-CRBR}}$ with trophic link sampling inadequacy. Recall that stability constraints are expected to increase the community's $\mu_{\text{l-CRBR}}$, which should therefore be positively correlated with link sampling inadequacy index if sampling bias decreases the observed strength of this signature. However, this correlation was found to be weakly negative ($R^2 = 0.34$) but insignificant ($p > 0.1$). Nevertheless, this suggests that unlike the food web structural signatures, the observed fit of the $\mu_{\text{l-CRBR}}$ to theoretical predictions may in fact be affected by sampling bias. In other words, while the observed $\mu_{\text{l-CRBRs}}$ are qualitatively consistent with theoretical predictions, their actual values may be overestimated because of an underrepresentation of links with CRBRs < 1 (typically observed in the form of parasite-host, parasitoid-host, or herbivore-plant interactions). This is further supported by the fact that that the skewness of the l-CRBR distribution is also positively and significantly correlated ($R^2 = 0.67$, $p = 0.009$) with the link sampling inadequacy index. Because a higher positive skewness means an inordinately high concentration of values at the right half of the distribution (where CRBRs > 1) this indicates that the sampling bias may in fact be against CRBRs ≤ 1, as has been suggested in recent studies highlighting the lack of data on host-parasite links (Hudson et al., 2006; Lafferty et al., 2006a; Lafferty et al., 2006b; Lafferty et al., 2008). This is also supported by the fact that an overwhelming majority (~90%) of links across the nine communities were of predator-prey interactions (which typically have CRBRs > 1). Thus this study is indeed in part a story of missing links.

4.4 Discussion

Using food web and species' body size data from nine communities across a range of terrestrial and aquatic habitats, I have addressed two questions: whether real the food web structure of real communities show signatures of stability constraints, and whether species-level foraging strategies are affected by (and in turn affect) community stability. The results, which are summarized in Fig. 4.1, show strong support for both; the observed structures of food webs shows configurations that are indicative of dynamically constrained assembly, and maximization of biomass uptake (maximal foraging) across species is constrained due to stability constraints. I now revisit these two issues in detail.

4.4.1 Signatures of dynamical stability constraints in natural community food webs

Signatures on food web structural features. The results provide a remarkable degree of support for the theoretical predictions about food web structural signatures. All communities show at least one of the two main food web signatures to a significant degree: $r\left(G,\bar{\alpha}_G\right)$ (decrease in species' generality-averaged interaction strength ($\bar{\alpha}_G$) with their generality) and $r\left(TL,\bar{\alpha}_G\right)$ (decrease in species' $\bar{\alpha}_G$ with their trophic level). Moreover, the significance of these patterns was tested using a conservative scheme of food web randomization (partial body size randomization); the results were much stronger if a less conservative (full body size randomization) method was used. Furthermore, as shown in Appendix F the results of this study are remarkably robust to variation in the parameters *k* and *s*, which are key parameters determining the strengths of interspecific interactions with respect to body sizes differences between interacting species. The signatures linked to $r\left(G,\bar{\alpha}_G\right)$ and $r\left(TL,\bar{\alpha}_G\right)$, i.e., $r\left(m,G\right)$ (increase in species' trophic generality with body size), $r\left(TL,m\right)$ (increase in species' body size with their trophic level), and $r\left(TL,CRBR\right)$ (increase in consumers' CRBRs with their trophic level) showed similarly significant patterns.

The observed increase in species' body sizes with trophic level is a pattern widely observed in natural communities, especially in aquatic ones (Hildrew et al., 2007). This study appears to be the first to show that stability constraints can contribute to this aspect of food web structure. Previous models have mainly invoked species' metabolic constraints and principles of biomass transfer across trophic levels without the explicit consideration the population stability consequences of trophic interactions (Brown and Gillooly, 2003; Brown et al., 2004; Cohen, 2008).

The increase in species' trophic generality with size is also a commonly seen empirical pattern (Jonsson et al., 2005; Memmott et al., 2000). This study shows that this pattern is indeed quite general, and that it is in fact driven community stability constraints on species foraging characteristics. This result is in agreement with that of Otto et al. (2007), who also found that the increase in generality with body mass in real communities is driven by stability constraints (the overall pattern is termed "allometric degree distributions" by Otto et al.). No previous quantitative model has been able to predict this pattern. An earlier, qualitative explanation can be attributed to Schoener (1989), who argued that species' generalities are bound to increase with trophic level because the number of potential prey species increases. Then, if body size also increases along trophic level (presumably for some other reason), a positive correlation between size and generalty is expected. However, here I have shown that stability constraints can directly

favor such a pattern. Fig. 4.4d supports this; the increase in trophic generality with body size in empirical communities is largely independent of the increase in body size with trophic level.

The predicted increase in CRBRs with consumers' trophic level was also observed in most communities. This contrasts with the study of Jonsson & Ebenman (1998), who showed theoretically that CRBR ratios should *decrease* with trophic level due to stability constraints, and suggested that this was empirically supported. Only one (MS) community in this study showed a significant decline in CRBRs.

In general, while the incidences of these different signatures (in terms of the percentage of communities showing the expected patterns in each feature) were consistent with those seen in model communities (cf. Table 3.2), their strengths (values of the correlation coefficients) lay at or beyond the lower ends of those of model communities. This is not surprising, given the multiple sources of noise inherent in community datasets, combined with the fact that the model communities were assembled without spatial or temporal environmental variation, both of which are expected to have strong effects on real communities. It is also possible that there is a greater influence of biogeographically neutral processes such as immigration and stochastic extinction (which would weaken signatures of interaction driven stability constraints on food web structural features) than what was simulated in the theoretical study of chapter 3. I also tested for the possibility that some or all of the observed signatures were artifacts of trophic link sampling bias. I found that this was not the case; in fact, there was some evidence that the strengths and incidences of the observed signatures may actually be underestimated due to sampling bias.

Signatures on species' body size and consumer-resource body mass ration distributions. I found little support for a predominance of right-skewness in empirical l-SBM distributions, which should be the result of the same processes that drive the emergence of the weighted generality-based food web structural signatures. I argue that this lack of right-skewness can be partly attributed to inadequate taxonomic sampling; there is strong evidence that SBMs become more right skewed as the inherent taxonomic bias towards larger organisms is mitigated (Blackburn and Gaston, 1994). Indeed studies on local communities that have high taxonomic resolution typically find a right-skewed l-SBM distribution (Allen et al., 2006b) (these could not be included in this study due to lack of trophic interaction data). Also, as shown in Chapter 3, the local SBM is dependent upon the SBM of the immigration "pool", and other factors such as the body-size dependence of speciation and immigration rate. It is currently difficult to determine whether these differ across the different communities studied here. But then why do taxonomic sampling biases also not render the signatures $r\left(G,\bar{\alpha}_G\right)$ and $r\left(TL,\bar{\alpha}_G\right)$ (or the related ones $r\left(m,G\right)$, $r\left(TL,m\right)$, and

$r(TL, CRBR)$) undetectable? This is not surprising because taxonomic sampling *per se* does not affect trophic link structure detection as much (Goldwasser and Roughgarden, 1997; Martinez et al., 1999).

While I did find support for the effect of stability constraints on the CRBR distribution, I also found evidence that these apparent fits to the theoretical predictions were *overestimated* by trophic link sampling biases against CRBRs ≤ 1. Such a bias is understandable because of the practical difficulties associated with detecting interactions wherein consumers are much smaller than their resources (such as parasites and parasitoids). Nevertheless, biases in current food web datasets may seriously hinder our understanding of community stability dynamics because a spectrum of potentially important trophic interactions (mainly with CRBRs < 1) remains undersampled.

4.4.2 Optimal foraging vs. population stability constraints

A particularly interesting aspect of this study's results is those pertaining to its second main question. Individual consumer species' foraging characteristics in real communities, in terms of the intensity with which they exploit their resource species, appears to be determined not just by their optimal (or maximal) energetic requirements, but also by the constraints of stable multi-species coexistence. In the light of this result, it is interesting to revisit Levins' (1974; 1975) seminal work on this issue. As mentioned in the introduction above, Levins concluded that foraging strategies that are ostensibly stable evolutionarily for single species may eventually destabilize the community and even drive the species itself extinct through feedbacks though the food web (interaction network). While this study and in the previous theoretical one (Chaper 3) do ignore heritable trait or generic variation within species, the dynamics of interaction driven species extinctions and probabilistic invasions qualitatively reproduce evolution-like dynamics across the system such that a non-random composition of species and interspecific interactions emerges.

Thus an important general conclusion that can be drawn from this study, in contrast to those of some recent studies (Beckerman et al., 2006; Petchey et al., 2008), is that there is no simple relationship between species' optimal foraging strategies and food web organization; species that achieve superior foraging performance are also likely to go extinct because of their effect on community wide stability (e.g., through trophic "cascades"). Moreover, across fifteen empirical communities Petchey *et al.* (2008) found that an algorithm that combines species' body-size data with optimal foraging theory to predict food web structure performed rather poorly, with only

>50% links being correctly predicted for only 3 of the communities. In particular, they found that the algorithm performed worst in communities with a significant number of links of CRBRs < 1 (such as the SB community, which has a large proportion of host-parasitoid links). In contrast, although this study did not aim to predict individual trophic links correctly, it did find consistent support for the dynamical basis of certain food web structures, including those of the SB community. This can partly be attributed to the fact that BLV model of this study was designed to accommodate CRBRs < 1. But more importantly, the results of this study suggest that the addition of rules that reflect stability constraints to models that seek to predict food web structure may improve their performance.

4.5 Conclusions

Overall, this study offers a single theoretical framework that successfully predicts multiple structural properties of community food webs. To summarize, I have shown that,

(a) The structure of the tropic interaction network, i.e., the food web of real communities shows distinct features that are signatures of assembly under dynamical stability constraints. Most of these signatures are in fact patterns that can and have been observed in nature, and many of them have previously lacked a predictive model.
(b) Food web structure is strongly determined by species' body sizes, partly because of size influences metabolic rate, and partly because interactions between species are influenced by their size differences.
(c) The trophic characteristics of individual species are not determined solely by their energetic requirements, but also by their effect on the community's dynamics.

This study is also a step towards modeling the dynamics of individuals and populations in the context of their community in empirically meaningful way. Body size allows individual level properties to be mapped on to population interaction network structure and dynamics, providing fresh insights into the organization of natural communities. This is particularly important because the use of species body size data provides a valuable tool to decipher the rather daunting complexity of natural communities.

Tables

Table 4.1. The empirical community datasets used to test theoretical predictions about signatures of stability constraints of food web structural characteristics. The abbreviation of each community's name used in subsequent tables and figures are shown in parentheses. The last four columns some key food web structural characteristics (the characteristics and their symbols were defined in Table 2.1). Body mass is expressed in grams throughout this chapter.

Community Name	General habitat	Description	Trophic link method[a]	Body mass data method[b]	Data sources	Food web characteristics				
						n	C_T	$\overline{G}$	$\overline{T}_c$	O_{deg}
Broadstone stream (BS)	Aquatic (freshwater)	Spring-fed acidic headwater stream, Sussex, UK	1, 2	2	(Brose et al., 2005; Woodward et al., 2005a)	28	0.37	15.3	4.6	0.81
Caribbean sea (CS)	Aquatic (marine)	Benthic and pelagic communities from surface to 100 m depth	3	2, 3	(Bascompte et al., 2005)	248	0.11	13.5	4.6	0.45
Eastern Weddell Sea (EW)	Aquatic (marine)	Antarctic shelf	1, 2	2, 3	(Brose et al., 2005)	391	0.02	9.5	2.9	0.21
Grand Cariçaie marsh (GC)	Terrestrial	Marsh dominated by *Cladietum marisci*, Lake Neuchâtel, Switzerland	1 ,3 ,4	1, 2, 3	(Brose et al., 2005; Cattin et al., 2004)	163	0.16	24.0	4.8	1.05
Mill Stream (MS)	Aquatic (freshwater)	Lowland chalk stream, Dorset, UK	2	2	(Brose et al., 2005)	74	0.14	8.2	1.2	0.03
Scotch Broom (SB)	Terrestrial	Community on *Cytisis scoparius*, Berkshire, UK	1, 2	1, 2, 3	(Brose et al., 2005; Cohen et al., 2005; Memmott et al., 2000)	153	0.03	10.2	3.2	0.14
Skipwith pond (SP)	Aquatic (freshwater)	Large acidic pond, North Yorkshire, UK	1, 2, 3	1, 2	(Brose et al., 2005; Warren, 1989)	33	0.61	17.8	4.1	0.58
Tuesday lake (TL)	Aquatic (freshwater)	Small, mildly acidic lake, Michigan, USA	1, 2	1, 2	(Brose et al., 2005; Cohen et al., 2003; Jonsson et al., 2005)	72	0.15	12.3	3.8	0.18
Ythan estuary (YE)	Estuarine	Ythan river mouth, Scotland	1, 3, 4	1, 2, 3	(Hall and Raffaelli, 1991; Leaper and Huxham, 2002)	79	0.09	5.7	3.2	0.56

[a] 1: Direct observations (lab or field), 2: Gut/stomach content analysis (typically, predators), feeding trials (typically, predators) or rearing (typically, parasitoids), 3: Published account, 4: Unpublished sources (including dissertation theses and internet sites).

[b] 1: Direct measurement, 2: Length-mass regression (see Table 4.2), 3: Published account, 4: Unpublished sources (including dissertation theses and internet sites).

Table 4.2. Parameter values used for converting length (meters) to wet mass (grams) using scaling models of species in different taxonomic groups across communities. In the case of animals, the scaling for snout-vent length was used. In groups for which the scaling parameters were substituted from those of other groups with similar body form, the latter is shown in parentheses.

General taxonomic category	*a*	*b*	Reference
Plants	27	3.79	(Niklas and Enquist, 2001)
Fish	10600	2.57	(Peters, 1983)
Worms (legless herpetofauna)	720	3.02	-
Mammals	14000	3.23	(Peters, 1983)
Birds	7390	2.74	(Peters, 1983)
Legless herpetofauna	720	3.02	(Peters, 1983)
Legged lizards	28000	2.98	(Peters, 1983)
Frogs	181000	3.24	(Peters, 1983)
Arachnids (Insects)	8800	2.62	-
Crustaceans (Insects)	8800	2.62	-
Insects (terrestrial and aquatic)	8800	2.62	(Peters, 1983)
Planktonic crustaceans	80	2.1	(Peters, 1983)
Algae	5.8	1.9	(Peters, 1983)
Other planktonic invertebrates (Planktonic crustaceans)	80	2.1	-

Table 4.3. Parameters values used for calculating food web structural characteristics of empirical communities.

Parameter	Description	Value
β	Scaling exponent for mass-metabolism allometry	0.75
$a_{b,i}$	Scaling constant for intrinsic rate of biomass production	1
k	Location parameter for the function φ_{ij}	0.001–1000
s	Scale parameter for the function φ_{ij}	0.01–0.1
γ	Scaling exponent for mass-specific intraspecific density dependent biomass loss rate (α_{ii})	0–0.25
a_{ii}	Scaling constant for α_{ii}	Arbitrary
v	Scaling exponent for equilibrium biomass density	0–0.25
$a_{\hat{x}}$	Scaling constant for equilibrium biomass	1

Table 4.4. The proportion of 2000 randomized community food webs that were more stable than the empirically observed one (had smaller $\lambda_{max}(\boldsymbol{C})$), given various values of the scaling exponents ν (mass-biomass scaling) and γ (scaling of mass-specific intraspecific density dependent biomass loss).

Randomization	γ	ν	Community								
			BS	CS	EW	GC	MS	SB	SP	TL	YE
Part	0	0	0	0.04	0.01	0	0	0.38	0	0	0.05
		0.25	0	0.64	0.13	0	0.008	0.47	0	0	0.67
	0.25	0	0.20	0.001	0.36	0.40	0.20	0.25	0.12	0.32	0.51
		0.25	0.58	0.13	0	0.49	0.53	0	0.15	0.02	0.93
Full	0	0	0	0.03	0.004	0	0	0.29	0	0	0.001
		0.25	0	0.55	0.08	0	0.005	0.37	0	0	0.19
	0.25	0	0.06	0	0.39	0.35	0.03	0.08	0.06	0.33	0.14
		0.25	0.35	0.19	0	0.48	0.60	0	0.10	0.002	0.86

Table 4.5. Food web structural signatures of stability constraints in real communities. The tabulated present the following measures of fit of the observed food web characteristics to theoretical predictions: $r(TL,m)$, $r(m,G)$ & $r(TL,CRBR)$ – rank correlation coefficient and two-tailed p value (in parentheses); $r(G,\bar{\alpha}_G)$ & $r(TL,\bar{\alpha}_G)$ – rank correlation coefficient, two-tailed p value (first pair of parentheses), and proportion of 2000 size-randomized (partial randomization) communities that had a correlation coefficient more negative than the observed one (second pair of parentheses); $sk_{\text{l-SBM}}$–skewness of the l-SBM distribution; $\mu_{\text{l-CRBR}}$– mean of the l-CRBR distribution and proportion of 2000 size-randomized communities that had a greater mean than that of the original community (in parentheses) (see section 3.3.4). Only the results for partial randomizations are shown because the less-conservative full randomizations yielded consistently stronger significances. Significant signatures are flagged (*). Except for $sk_{\text{l-SBM}}$, a measure was considered significant either if p< 0.05, or the proportion of (partially) randomized communities with a stronger than the observed signature was < 0.05. In the case of $sk_{\text{l-SBM}}$, a positive value of the quantity was deemed significant.

Community	Signatures of stability constraints						
	$r(G,\bar{\alpha}_G)$	$r(m,G)$	$r(TL,\bar{\alpha}_G)$	$r(TL,m)$	$r(TL,CRBR)$	$sk_{\text{l-SBM}}$	$\mu_{\text{l-CRBR}}$
BS	-0.34 (0.38) (0.17)	0.34 (0.38)	-0.98* (<0.001) (0)	0.98* (<0.001)	0.58* (<0.001)	-0.07	1.07* (0.0005)
CS	-0.24* (<0.001) (0)	0.39 * (<0.001)	-0.35* (<0.001) (0)	0.53* (<0.001)	0.09* (<0.001)	-1.17	2.02* (0)
EW	-0.21* (<0.001) (0)	0.28 * (<0.001)	-0.30* (<0.001) (0)	0.34* (<0.001)	0.20* (<0.001)	-0.1	1.61* (0.01)
GC	-0.24* (0.03) (0.02)	0.27* (0.01)	-0.15 (0.17) (0.09)	0.16 (0.14)	-0.08 (<0.001)	2.32*	0.74* (0.0025)
MS	-0.25 (0.10) (0.06)	0.29 (0.06)	0.25 (0.09) (0.88)	-0.10 (0.52)	-0.26 (<0.001)	-0.49	5.53* (0.0045)
SB	-0.37* (<0.001) (0)	0.39* (<0.001)	0.12 (0.14) (0.82)	-0.07 (0.42)	-0.03 (0.60)	-1.03	0.09* (0.1290)
SP	-0.76* (<0.001) (0)	0.79* (<0.001)	-0.72* (<0.001) (0.0005)	0.75* (<0.001)	0.28* (<0.001)	-1.19	0.99* (0.0005)
TL	-0.55* (<0.001) (0.001)	0.57* (<0.001)	-0.73* (<0.001) (0)	0.76* (<0.001)	-0.01 (0.84)	1.69*	3.38* (0.0050)
YE	-0.18 (0.19) (0.07)	0.19 (0.18)	-0.61* (<0.001) (0)	0.65* (<0.001)	0.13* (0.04)	-0.38	3.36* (0)

Table 4.6. The values for two structural signatures of stability constraints in MFC counterparts of the nine empirical communities. The second column shows the proportion of species in the MFC that achieved better energy uptake and production than in the original community. Columns 5 – 8 show the maximum eigenvalue of the community matrix under various assumptions about the scaling of biomasses (v) and intraspecific density dependence (γ).

Community	n_{MF}	$r(G,\bar{\alpha}_G)$	$r(TL,\bar{\alpha}_G)$	$\lambda_{\max}(\boldsymbol{C})$			
				$\gamma = 0$		$\gamma = 0.25$	
				$v = 0$	$v = 0.25$	$v = 0$	$v = 0.25$
BS	0.87	0.83 (0.008)	0.12 (0.78)	0.21	0.03	0.08	0.005
CS	0.92	0.12 (0.07)	0.24 (<0.001)	0.03	0.06	0.03	0.04
EW	0.84	0.07 (0.20)	0.12 (0.04)	0.02	0.06	-0.00007	-0.00002
GC	0.95	0.25 (0.02)	0.21 (0.05)	0.20	0.03	0.05	-0.002
MS	1	0.16 (0.30)	0.11 (0.48)	0.01	0.0004	-0.0004	-0.0003
SB	0.75	0.06 (0.45)	0.11 (0.20)	5.30	1.44	1.18	0.44
SP	0.90	0.32 (0.20)	0.25 (0.39)	0.10	0.05	0.05	0.02
TL	0.94	0.35 (0.05)	0.22 (0.23)	0.48	0.22	0.05	0.01
YE	0.79	0.24 (0.08)	0.11(0.42)	0.06	0.03	0.04	-0.0005

Figures

Figure 4.1. A graphical overview of the predicted signatures of dynamically constrained community assembly on food web structural characteristics (see sections 2.2.3, 3.3.4, and 3.3.3), and the observed fits. The term "null expectation" in the third column refers to the values of characteristics expected under purely random trophic linking. Each filled circle in a figure indicates a single consumer species' node in the food web, with arrows indicating their trophic links (with their resources). The size of a circle and the thickness of an arrow represent respectively, species body mass and interspecific interaction strength. In the summary of the results (fourth column), the observed correlation coefficient was deemed to be significantly fitting the theoretical prediction either if its $p < 0.05$, or the proportion of 2000 randomized communities with a stronger than the observed coefficient was < 0.05. In the case of the l-SBM distribution, a positive value of skewness ($sk_{\text{l-SBM}}$) was deemed significant. For the l-CRBR distribution, a proportion of 2000 size-randomized communities that had a mean ($\mu_{\text{l-CRBR}}$) greater than that of the original community < 0.05 was deemed significant.

Description of signature	Prediction	Test of fit to prediction	Proportion of communities fitting prediction
Decrease in species' generality-averaged interaction strength ($\bar{\alpha}_G$) with generality	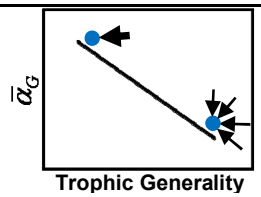	Sign and significance of rank correlation $r(G, \bar{\alpha}_G)$	6/9 (strongly) 3/9 (weakly)
Increase in species' generality with body size	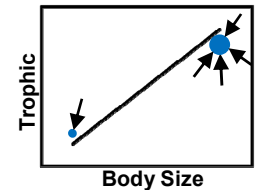	Sign and significance of rank correlation $r(m, G)$	6/9 (strongly) 2/9 (weakly)
Decrease in species' $\bar{\alpha}_G$ with trophic position	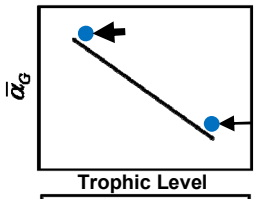	Sign and significance of rank correlation $r(TL, \bar{\alpha}_G)$	6/9 (strongly)
Increase in species' body size with trophic position	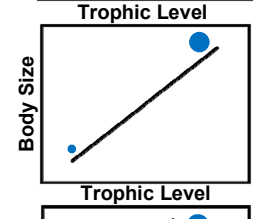	Sign and significance of rank correlation $r(TL, m)$	6/9 (strongly) 1/9 (weakly)
Increase in consumers' CRBR's with trophic position	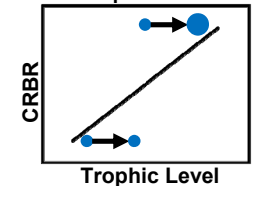	Sign and significance of rank correlation $r(TL, CRBR)$	5/9

Right skewed distribution of species' log-transformed body masses	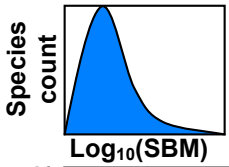	Degree of right skewness of the distribution	2/9
Weakly skewed distribution of log-transformed CRBR's with mean > null expectation	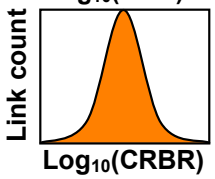	Degree to which mean of observed distribution is higher than null expectation.	9/9

Figure 4.2. The shape of consumption intensity (function φ_{ij}; expression 3.4) for different values of s (shown next to the respective curves) across the range of possible CRBRs given the range of body masses across nine real communities (approximately 10^{-12}–10^{12}; see Fig. 4.3). The vertical dashed lines show the limits of the actually observed CRBRs across the communities (Fig. 4.3).

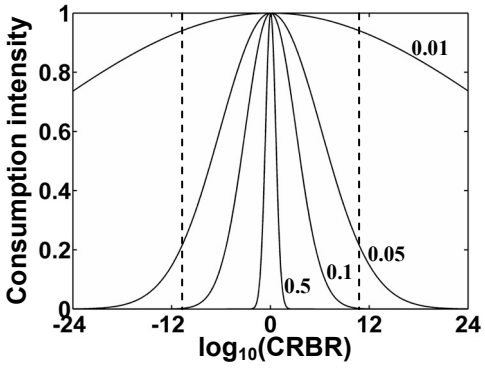

Figure 4.3. (continued on next page). Dynamically relevant food web characteristics across nine empirical communities, each row representing a different feature (rows are in the same order as Fig. 4.1). Histograms embedded in the third and fifth rows figures show the location of the correlation coefficients $r(G,\bar{\alpha}_G)$ & $r(TL,\bar{\alpha}_G)$ with respect to the distribution of the coefficients from 2000 size-randomizations of the community. The fits of observed patterns to theoretical predictions are summarized in Table 4.5. For the EW community, body size measure shown is length.

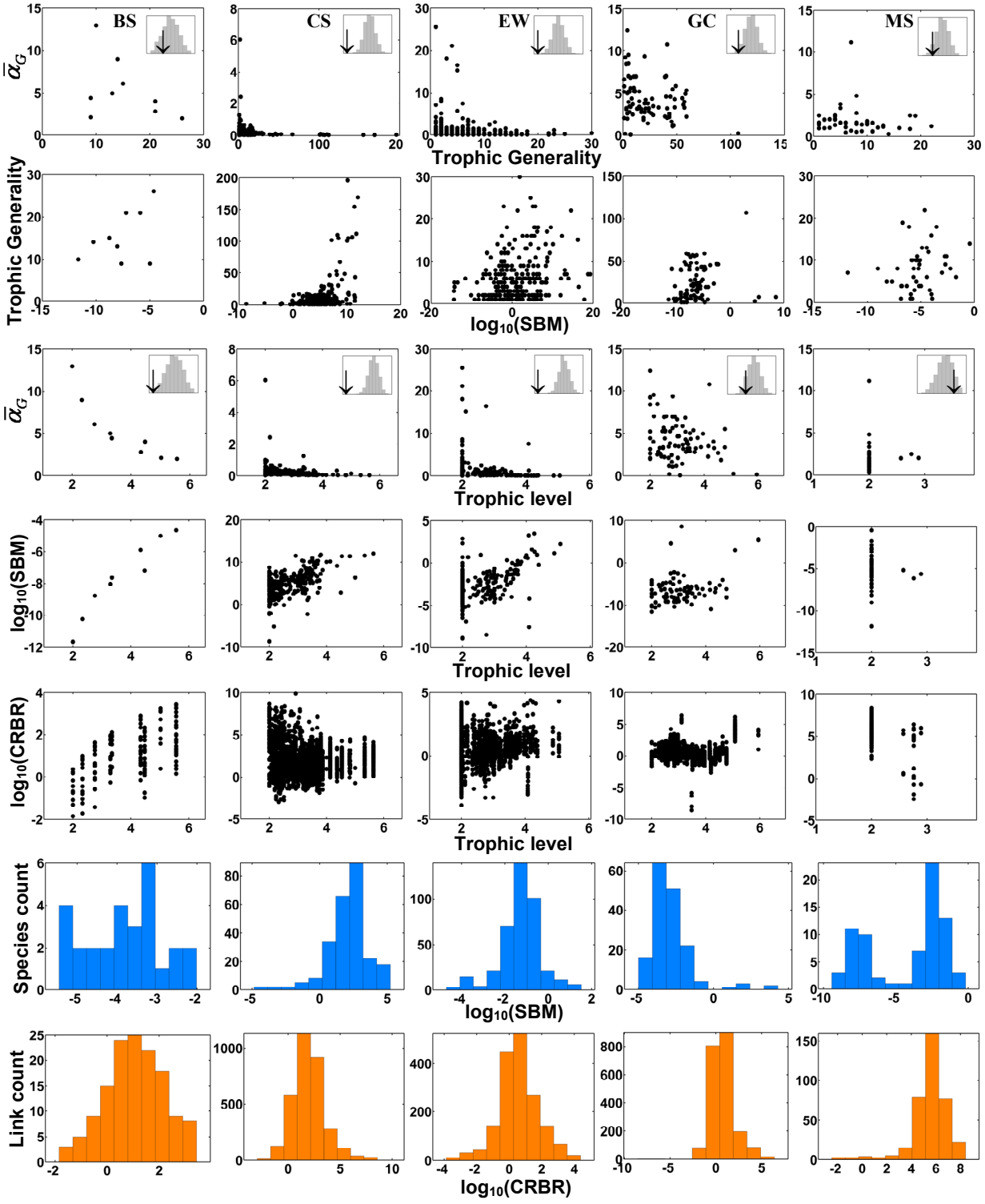

Figure 4.3. (continued)

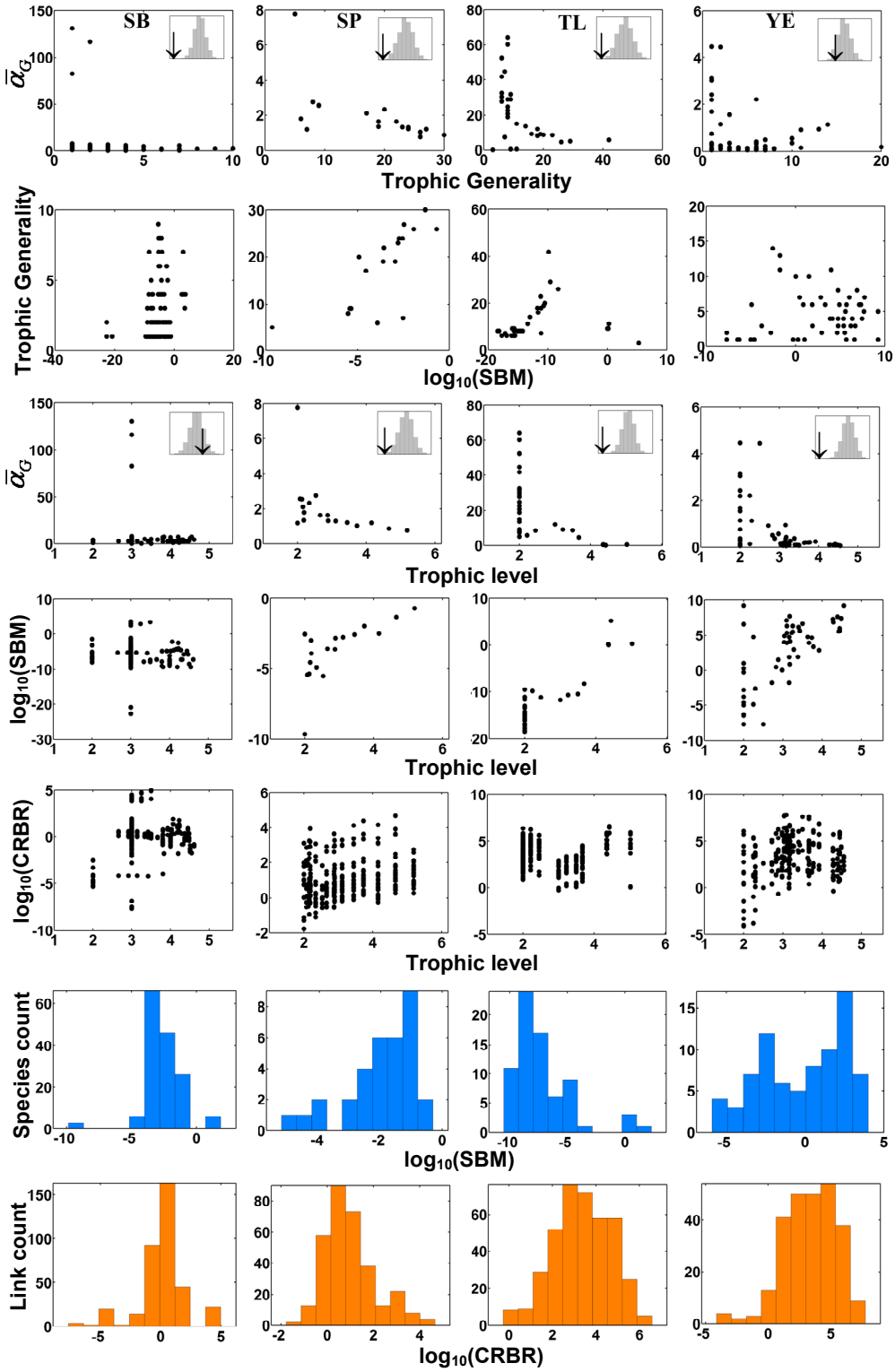

Figure 4.4. The interdependence between food web structural signatures of stability constraints across nine real communities. The incidences and strengths of these signatures across the communities are summarized in Table 4.5. The relationships a–c are significant ($p < 0.0001$ & $R^2 = 0.94$, $p < 0.0001$ & $R^2 = 0.98$, and $p < 0.02$ & $R^2 = 0.63$ respectively), while d is not ($p = 0.32$ & $R^2 = 0.14$).

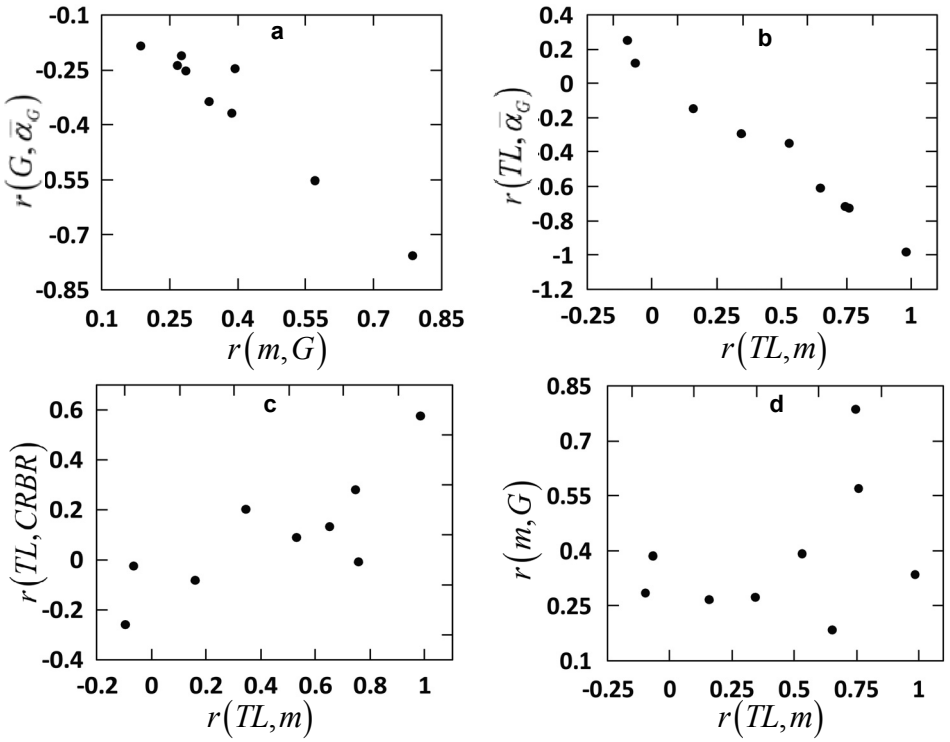

Appendices

Appendix A: The relationship between $\rho(\underline{C})$ and probability of Hurwitz stability

Here, I will first show that Neutel et al.'s (2007; 2002) use of $\rho(\underline{C})$ (expression 2.6 of the main text) as a measure of distance from global stability is mathematically incorrect, and then that $\rho(\underline{C})$ can nevertheless be related to PHS in communities with certain interaction sign structures. Neutel et al.'s (2002) approach towards relating food web structure to stability is to use the fact that given a $n \times n$ community matrix $\boldsymbol{C}$ (see section 2.2.1 of the main text), the dynamical system resulting from the Lotka-Volterra type equations is globally stable if a vector $\boldsymbol{q}$ of n positive constants $q_1, q_2, \ldots q_n$ exists such that the inequality

$$q_i c_{ii} > \sum_{i \neq j}^{n} q_j \mid c_{ij} \mid, \ \forall \ i \in \mathfrak{N}$$

holds. Such globally stable systems are termed quasi-diagonally dominant (qdd) (Hofbauer and Sigmund, 1998; Logofet, 1993). Now, provided $\underline{C}$ is primitive, the Perron-Frobenius theorem guarantees that $\rho(\underline{C}) > 0$, with an associated strictly positive eigenvector $\boldsymbol{v}$ (Horn and Johnson, 1985). Neutel et al. (2002) suggest that $\boldsymbol{v} = \boldsymbol{q}$, and hence that $\rho(\underline{C})$ is the minimum value needed to be added to the diagonal elements of $\boldsymbol{C}$ to render the system qdd. Thus stabilization of the system is essentially a matter of the mitigation of $\rho(\underline{C})$. The utility of such a relationship is obvious; any food web structural feature that determines $\rho(\underline{C})$ can then be related to stability. However, it can be easily shown that Neutel et al.'s conjecture is wrong[5]. Suppose that the system is already qdd. This implies that its $\rho(\underline{C})$ must = 0. However, this is impossible because $\rho(\underline{C})$ is bound to be > 0 for non-trivial community matrices from the Perron-Frobenius Theorem! Thus the mitigation of $\rho(\underline{C})$ does not guarantee global stability.

I now turn to a second conjecture of Neutel et al. (2007; 2002), which can still allow $\rho(\underline{C})$ to be related to Hurwitz stability: that $\lambda_{max}(\boldsymbol{C})$ increases monotonically with $\rho(\underline{C})$ for a given set of diagonal elements of $\boldsymbol{C}$. If this were true, it would mean that given some levels of negative density dependence across species in the community, $\lambda_{max}(\boldsymbol{C})$ is bound to become positive (and Hurwitz stability lost) as $\rho(\underline{C})$ increases, irrespective of $\boldsymbol{C}$'s sign structure. In other words, PHS would be inversely related to $\rho(\underline{C})$. Moreover, because we are no longer interested in the strict positivity of the eigenvector $\boldsymbol{v}$, $\rho(\underline{C})$ can now be related to stability across all community types (instead of only the ones that satisfy the condition of primitivity of $\underline{C}$), because $\rho(\underline{C}) > 0$ even under the weaker condition that each row of matrix $\underline{C}$ has at least one interaction coefficient (all species have at least one trophic interaction) (e.g., see corollary 8.1.25 in Horn and Johnson, 1985). However, the very existence of sign stable (Logofet, 1993; May, 1974) and "quasi-sign stable" (in the sense of Allesina and Pascual, 2008) communities precludes the possibility of a general, monotonically increasing relationship between $\lambda_{max}(\boldsymbol{C})$ and $\rho(\underline{C})$. In such communities,

[5] This problem originally was pointed out to me by Dimitrii Logofet.

$\lambda_{max}(\boldsymbol{C})$ either does not increase and cross the critical boundary even if $\rho(\underline{\boldsymbol{C}})$ increases infinitely (strictly sign-stable), or is relatively insensitive to changes in $\rho(\underline{\boldsymbol{C}})$ (quasi-sign stable). Nevertheless, for a given community size it is always possible to find a nontrivial sign structure that renders $\lambda_{max}(\boldsymbol{C})$ sensitive to $\rho(\underline{\boldsymbol{C}})$. For example, consider the community matrix,

$$\boldsymbol{C} = \begin{bmatrix} -1 & 0 & -1 \\ 0 & -1 & c \\ c & -1 & -1 \end{bmatrix}, \text{ which means that } \underline{\boldsymbol{C}} = \begin{bmatrix} 0 & 0 & 1 \\ 0 & 0 & c \\ c & 1 & 0 \end{bmatrix}$$

The eigenvalues of $\boldsymbol{C}$ are $-1, -1+\sqrt{-2c}$, and $-1-\sqrt{-2c}$, and $\rho(\underline{\boldsymbol{C}}) = \sqrt{2c}$. Thus while $\rho(\underline{\boldsymbol{C}})$ increases with c, $\lambda_{max}(\boldsymbol{C})$ remains constant (–1), and the system remains Hurwitz stable. Now let us make a change to the sign structure of $\boldsymbol{C}$ by adding one more trophic link such that,

$$\boldsymbol{C} = \begin{bmatrix} -1 & c & -1 \\ -1 & -1 & c \\ c & -1 & -1 \end{bmatrix}, \text{ and } \underline{\boldsymbol{C}} = \begin{bmatrix} 0 & c & 1 \\ 1 & 0 & c \\ c & 1 & 0 \end{bmatrix}$$

Now the eigenvalues of $\boldsymbol{C}$ are $c-2, 0.5\left(-1+\sqrt{3}i\right)(c+1)$, and $-0.5\left(1+\sqrt{3}i\right)(c+1)$, while $\rho(\underline{\boldsymbol{C}}) = c+1$. Now, as $\rho(\underline{\boldsymbol{C}})$ increases (with c), so does $\lambda_{max}(\boldsymbol{C})$. I call this property of community sign structure, "interaction strength sensitivity" (ISS). The ISS of a community can be gauged from the correlation coefficient between $\lambda_{max}(\boldsymbol{C})$ and $\rho(\underline{\boldsymbol{C}})$ (r_{ISS}) across randomly generated food webs that have the same sign structure, but random interaction strength configurations (IS-randomized; see below for numerical methods) (two contrasting empirical examples of this measure are shown in Fig. 2.1). In Table 2.1, the ISS of sixteen empirical communities is shown. Fig. 2.3 shows that model communities assembled using fairly general rules too have consistently high ISS.

Numerical method for IS-randomization: To generate each IS-randomized version of a given community, I generated the off-diagonal elements of the community matrix $\boldsymbol{C}$ by sampling the element c_{ij} (if j eats i) from a half-normal distribution (distribution of the absolute value of a normally distributed random variable with mean 0 and variance σ^2), which has a cumulative density function,

$$F_Y(y;\sigma) = \int_0^y \frac{1}{\sigma}\sqrt{\frac{2}{\pi}} \exp\left(-\frac{z^2}{2\sigma^2}\right) dz$$

and expectation and variance that scale with σ as $\sigma\sqrt{2/\pi}$ and $\sigma^2\left(1-(2/\pi)\right)$, respectively. The corresponding element c_{ji} was also sampled from the half-normal distribution, and then multiplied by 10^{κ}, with κ sampled from a uniform distribution over the interval [a, b]. Thus the choice of [a, b] determines the degree of asymmetry of the interactions in each trophic link (effect of consumer on resource (c_{ij}) vs. resource on consumer (c_{ji})), and the right-skewness of the interaction strength distribution. Empirical data show that this asymmetry is typically high (e.g., Jonsson and Ebenman, 1998; Neutel et al., 2002; Ruiter et al., 1995), with a strongly right-skewed (log-normal like) interaction strength distribution (Wootton and Emmerson, 2005). The diagonal elements of $\boldsymbol{C}$ (all negative) were sampled from a uniform distribution with range C_{ii}. The results for ISS in

Table 2.1, Fig. 2.1 and Fig. 2.2 are for $\sigma = 1$, $[a, b] = [-2, 2]$, and $C_{ii} = [0, 1]$. Using other combinations of parameter values, or different distributions for sampling parameters (such as uniform or log-normal) alters the strengths of the estimated ISS of communities, but not the differences between their ISS.

Appendix B: The relationship between species' weighted generality and $\rho(\underline{\boldsymbol{C}})$

Here I will establish the relationship 2.9 of the main text. We begin by defining the symmetric matrix $S(\underline{\boldsymbol{C}})$ with elements,

$$\overline{\underline{c}}_{ij}\left(=\overline{\underline{c}}_{ji}\right)=\sqrt{\underline{c}_{ij}\underline{c}_{ji}}\ ,\ \forall i,j\in\mathfrak{N} \tag{B.1}$$

and the symmetry measure on $\underline{\boldsymbol{C}}$:

$$S_{\underline{C}}\equiv\sum_{i,j=}^{n}\left|\underline{c}_{ij}-\overline{\underline{c}}_{ij}\right|$$

Then, from the main result of Schwenk (1986) it follows that,

$$\lim_{S_{\underline{C}}\to 0}\left(\rho(\underline{\boldsymbol{C}})-\rho\left(S(\underline{\boldsymbol{C}})\right)\right)=0 \tag{B.2}$$

i.e., $\rho\left(S(\underline{\boldsymbol{C}})\right)$ approaches $\rho(\underline{\boldsymbol{C}})$ from below as $\underline{\boldsymbol{C}}$ increases in symmetry (also see Kolotilina, 1993). Converting $\underline{\boldsymbol{C}}$ to the symmetric matrix $S(\underline{\boldsymbol{C}})$ makes it easier to interlink food web structure and community stability because the coefficients c_{ij} and c_{ji} of each trophic interaction are reduced to a single entity $\overline{\underline{c}}_{ij}$ that contributes to the overall biomass transfer rate between species (see expression 2.10 in the main text). Expression B.2 implies that $\rho(\boldsymbol{C})\cong\rho\left(S(\underline{\boldsymbol{C}})\right)$ if the pairs of the off-diagonal elements $\underline{c}_{ji}$ and $\underline{c}_{ij}$ are sufficiently close to each other in magnitude such that species' biomasses are somewhat balanced, i.e., $\hat{x}_i\cong e_j\hat{x}_j\ ,\ \forall i,j\in\mathfrak{N}$ (using expression 1b from the main text). In fact, it can be shown that even if $S_{\underline{C}}$ is low (interactions are typically very asymmetric), the structural symmetry of $\boldsymbol{C}$ (i.e., $c_{ji}\neq 0$ iff $c_{ij}\neq 0$) is in itself sufficient to guarantee that $\rho\left(S(\underline{\boldsymbol{C}})\right)$ is a tight lower bound of $\rho(\underline{\boldsymbol{C}})$ (Schwenk, 1986). Now, because $S(\underline{\boldsymbol{C}})$ is symmetric, $\rho\left(S(\underline{\boldsymbol{C}})\right)$ is itself bounded below by the Rayleigh quotient (Horn and Johnson, 1985, p. 176),

$$\frac{\boldsymbol{z}^t S(\underline{\boldsymbol{C}})\boldsymbol{z}}{\boldsymbol{z}^t\boldsymbol{z}}\leq\rho\left(S(\underline{\boldsymbol{C}})\right)$$

where $\boldsymbol{z}=(1,1,...,1)^t$. And because

$$\frac{\boldsymbol{z}^t S(\underline{\boldsymbol{C}})\boldsymbol{z}}{\boldsymbol{z}^t\boldsymbol{z}}=\frac{1}{n}\sum_{i,j=1}^{n}\overline{\underline{c}}_{ij}\ ,$$

we have,

$$\frac{1}{n}\sum_{i,j=1}^{n}\overline{\underline{c}}_{ij}\leq\rho\left(S(\underline{\boldsymbol{C}})\right) \tag{B.3}$$

which from expression B.2 means that

$$\frac{1}{n}\sum_{i,j=1}^{n}\underline{\overline{c}}_{ij} \leq \rho(\underline{\boldsymbol{C}}) \qquad \text{(B.4)}$$

Now, the sum in expression B.4 can be partitioned into species' weighted generalities (as defined in expression 2.8 of the main text),

$$\sum_{i,j=1}^{n}\underline{\overline{c}}_{ij} = 2\sum\nolimits_{n} G_i^w = 2G_{tot}^w ,$$

and hence bound 2.9 of the main text follows.

Appendix C: Food web data for assessment of interaction strength sensitivity

I chose the following communities for which the food web structure has been published in the literature[6]: Bridge Brook Lake (Havens, 1992), Broadstone Stream (Brose et al., 2005), Caribbean Sea (Bascompte et al., 2005), Carpinteria Salt Marsh (Lafferty et al., 2006b), Company Bay Mudflat (Thompson et al., 2005), Dempster's Tussock Stream (Townsend et al., 1998), Eastern Weddell Sea (Brose et al., 2005), Grand Caricaie Marsh (Brose et al., 2005; "clmown1"), Little Rock Lake (Martinez, 1991), Martins Stream (Thompson and Townsend, 2003), Mill Stream (Brose et al., 2005), North Carolina Pine Logs (Cohen, 1989; Web 182), Scotch Broom (Memmott et al., 2000), Skipwith Pond (Brose et al., 2005), Tuesday Lake (Cohen et al., 2003), and Ythan Estuary (Huxham et al., 1996). Only local communities, i.e., which had been sampled from one site or a cluster of adjacent sites were considered. For example, this excluded the UK Grassland "community", which is based upon data from >20 localities across England and Wales (Martinez et al., 1999). Of the available local communities, the criterion for selecting these particular ones was taxonomic resolution: Firstly, communities with >80% of taxa resolved to at least genus level were chosen. From these, only those that had >80% of basal taxa and primary consumers (those that fed on basal taxa) also resolved taxonomically up to at least genus level were chosen. The reason for this rather strongent criterion was twofold. First, it excluded food webs that have been subjected to a priori classification into functional groups (e.g., the El Verde (Reagan and Waide, 1996) and Coachella valley (Polis, 1991) communities) which have been used in previous analyses of food web structure. Second, it excluded webs that had a strong taxonomic bias towards taxa at higher trophic levels. This is an important consideration because across ecosystems, lower trophic levels are typically the most taxon rich, and poor taxonomic resolution at those levels is hence likely to exclude important details of interaction structure. Before analysis, each food web dataset was modified in two ways:

- Bidirectional links, where in two taxa are known to consume each other at different life history stages were converted to ordinary ones by assuming that taxon which consumed more life history stages of the other was the effective consumer. For example, many dragonfly species' nymphs consume larvae of a frog species, but the adult frogs then become the consumers of the adult as well as larval dragonflies. In this case, the frog would be considered an effective consumer of the dragonfly because it predates on two life history stages of the latter. If both taxa consume equal number of life history stages of the other, the one with larger adult body size was considered the effective consumer. If neither of these criteria could be applied, one of the two species was chosen at random to be the consumer.
- Separate food web nodes representing different life history stages of the same taxon (for example, juvenile and adult of a fish species) were collapsed into one (by combining their trophic links).

[6] Many of these cited data sources are secondary because the original publications did not include the actual interaction data. In addition, I would like to thank Jennifer Dunne for providing me with many of these datasets.

Appendix D: Calculating trophic levels

A number of methods have been used to estimate the trophic level (*TL*) of each species in a community (Williams and Martinez, 2004). Williams and Martinez (2004) recommend the use of shortest path-weighted, prey-averaged *TL* because it reflects actual energy flow rates across nodes more accurately. But the calculation of prey-averaged *TL* becomes problematic when cycles (wherein a trophic path begins and ends at the same node) are present (Levine, 1980). For example in Fig. D1, the trophic path 4→2→3→4 is a cycle. The presence of cycles can be detected by calculating the maximum eigenvalue of the food web's adjacency matrix (Borrett et al., 2007). An adjacency matrix consists of a 1 at the i x j^{th} position if species j is a consumer of species i (and a zero in the corresponding j x i^{th} position) (e.g., Fig. D1). If the real part of its maximum eigenvalue is 0, there are no cycles; if it equals 1, there is at least one cycle; if it is greater than 1, there is more than one cycle in the food web.

To be able to calculate *TL* consistently across communities with or without cycles, I used the chain-averaged *TL*, which as the name suggests, is the mean of all the chain lengths from a consumer to basal species. The calculation of chain-averaged *TL* too poses problems in cyclic food webs because each cyclic path is effectively infinite in length. To circumvent this, I curtailed cyclic paths as soon as a node was repeated. For example in figure S2, the cyclic path 1→2→3→4→2 can be curtailed at the edge 4→2. Furthermore, the calculation of trophic chain lengths rapidly becomes computationally intractable with increasing community size (n) for a given connectance because the number of paths increases exponentially with path lengths (see Borrett et al., 2007 and references therein), which in turn increase with n. To circumvent this problem, I designed the following algorithm, which maintains computational tractability by finding a representative sample of unique paths originating at basal species in a community with n species:

(i) Choose k, the number of paths to be sampled in each iteration of the algorithm.

(ii) Initialize a null set $\mathcal{P}_u$ that will contain unique paths. Unique paths have a sequence of species indices $\{i_1, i_2, \ldots i_l : l \le n\}$ that is not an ordered subset of any other path in $\mathcal{P}_u$ of length $\ge l$.

(iii) Choose a node by sampling with replacement from the set of basal node indices.

(iv) Starting at the basal species, perform a random walk through connected nodes till either a top consumer or a repeated node (indicating the beginning of a cycle) is reached.

(v) Repeat (iii) and (iv) till k paths (not necessarily mutually unique) have been found.

(vi) Calculate T, which is,

$$T \equiv \frac{P_{u,i}}{P_u}$$

where $P_{u,i}$ is the number of paths from the current sample that are unique with respect to those in $\mathcal{P}_u$, while P_u is the number of paths already in $\mathcal{P}_u$.

(vii) Check if $T < T_{thr}$, where T_{thr} is a predetermined threshold value.

(viii) If $T < T_{thr}$, terminate the algorithm; if not, add the unique paths from the current sample found in step (vi) to $\mathcal{P}_u$ and perform another iteration of steps (iii) – (viiii).

The parameters k and T_{thr} together determine how exhaustive the path search is. Firstly, k has to be high enough to sample sufficient portions of the space all paths in the community in each iteration. Given a value of k, T_{thr} then determines how many iterations will be performed to search for additional unique paths. Thus simultaneously increasing k and decreasing T_{thr} increases the exhaustiveness of the path search. Optimal combinations of the two parameters were determined separately for each community food web by choosing increasing values of k and executing

repeated algorithm runs with a stepwise decrease in T_{thr} for each. The number of unique paths discovered was then plotted against T_{thr}. The optimal T_{thr} is then the value where the detection of unique paths approached an asymptote, while the optimal k was the value that yielded the largest number of paths at the asymptote. Note that in very large communities (such as the Eastern Weddell Sea community; Table 2.1), such an asymptote may not be reached within reasonable computational time. However, this did not happen in any of the sixteen communities chosen for ISS evaluation. The Matlab implementation of the algorithm can be made available upon request.

Figure D1. A cyclic food web and its adjacency matrix. The arrows connecting species' nodes (grey circles) represent the direction of biomass flow across trophic links. Species 1 is basal.

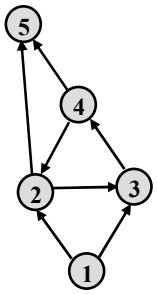

$$\begin{bmatrix} 0 & 1 & 1 & 0 & 0 \\ 0 & 0 & 1 & 0 & 1 \\ 0 & 0 & 0 & 1 & 0 \\ 0 & 1 & 0 & 0 & 1 \\ 0 & 0 & 0 & 0 & 0 \end{bmatrix}$$

Appendix E: The body size scaling of species' equilibrium biomass abundances

The vector of equilibrium biomass densities $\hat{\boldsymbol{x}}$ can be found by solving the system

$$-\boldsymbol{A}\boldsymbol{x} = \boldsymbol{b} - \boldsymbol{d} \tag{E.1}$$

where $\boldsymbol{x}$ is the vector of biomasses (x_i), $\boldsymbol{b}$ of the biomass production rates, $\boldsymbol{d}$ of the density-independent biomass loss rates, and $\boldsymbol{A}$ the n x n matrix of interaction coefficients, as defined in the specification of the basic LV model (equation 2.1). Using Cramer's rule to solve equation E.1, the equilibrium density of the i^{th} species' population can be expressed as a ratio of determinants,

$$\hat{x}_i = -\frac{\det(\boldsymbol{A}_i)}{\det(\boldsymbol{A})} \tag{E.2}$$

where $\boldsymbol{A}_i$ is the is the matrix formed by replacing the i^{th} column of $\boldsymbol{A}$ with the vector $\boldsymbol{b}$–$\boldsymbol{d}$. Now, Leibniz's formula states that for any n x n matrix $\boldsymbol{Z}$,

$$\det(\boldsymbol{Z}) = \sum_{\sigma \in \mathcal{G}_n} \operatorname{sgn}(\sigma) \prod_{i=1}^{n} z_{i\sigma(i)} \tag{E.3}$$

where $\mathcal{G}_n$ is the set of all possible permutations of the integers 1 to n , and sgn(σ) denotes the signature of the permutation product σ. Thus while the solution to equation E.1 is analytically tractable, deciphering the body size scaling of the $\bar{G}_i^w$'s for an arbitrary community size (n) is not, because both the numerator as well as denominator of expression E.2 consist of sums and differences of the n! different permutations of elements (taken n at a time) of the matrices $\boldsymbol{A}_i$ and $\boldsymbol{A}$, respectively! Hence instead, I attempted to determine the relationship numerically by examining the biomass abundances of species in model communities at IEE. The results are shown in Fig. E1. In general, there is a tight linear relationship between v and γ of the form $v = z\gamma + c$ with z lying between 0.5 – 0.6 and c between 0.1 – 015, depending upon the choice of the parameter k (l-CRBR at which consumption intensity peaks). There appears to be no strong dependence of the scaling between v and γ on the choice of ω (the distribution of body sizes in the immigrant pool). Variation in other nonallometric model parameters (the parameters and their ranges are listed in table 2.2) did not change the linearity of this scaling or the range of z and c (results not shown).

Figure E1. The body size dependence of species' equilibrium biomass abundances ($\hat{x}$'s) in model communities. Each plot shows changes in average v with increasing values of γ. Each value of average v (shown with 99% confidence intervals) for a given γ was calculated from 100 replicated communities at IEE. The least-squares regression line and the associated equation are shown for each plot. All the regressions are highly significant ($p < 0.0001$). Plots a–c are for ω =1 but with orders of magnitude increase in k (10^{-3}, 1, and 10^{3}, repectively i.e., CRBRs for peak consumption intensity ranging from .001 to 1000), and d–f for $\omega = 2$ and the same range of k. Assembly simulation methodology is described in section 3.4.1.

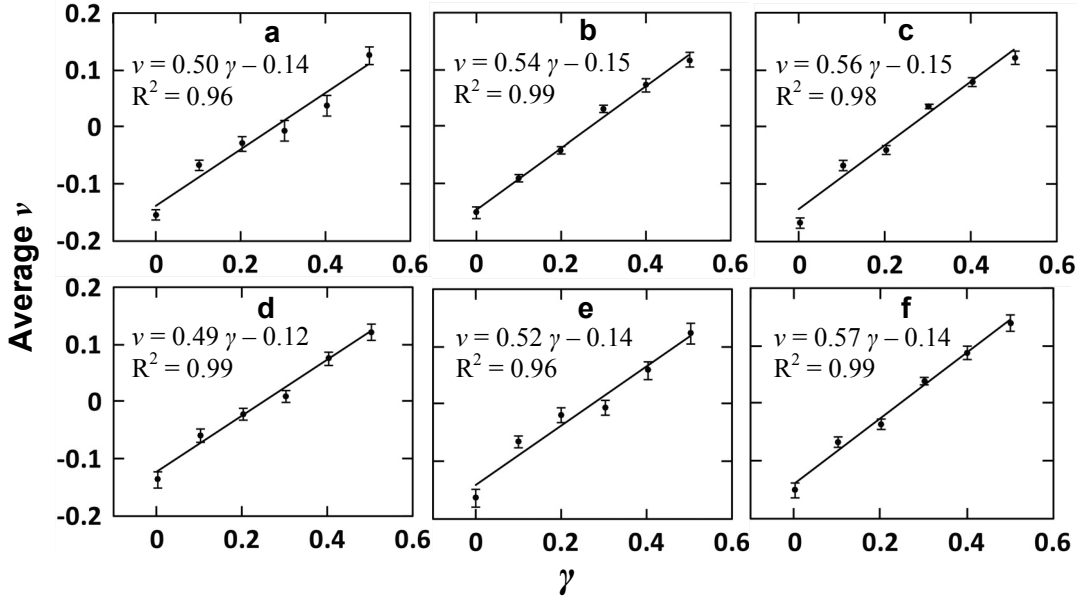

Appendix F: Sensitivity of empirically observed food web structural signatures of stability constraints to variation in the parameters *k* and *s*.

Here I consider the sensitivity of the results of Chapter 4 to variation in values of the two parameters (*k* and *s*) of the CRBR based interspecific mass-specific consumption intensity function φ_{ij} (expression 3.4). In section 4.2.3, I explained the reasons for fixing *k* (the CRBR at which consumption intensity peaks) and *s* (the speed with which consumption intensity declines away from *k*) at 1 and 0.05 respectively, instead of varying them according to the type of trophic interaction, habitat, or the types of organisms involved. To examine the sensitivity of the observed signatures of stability constraints on food web structure to variation in these parameters, I examined the measures $r(m,G)$ and $r(TL,\bar{\alpha}_G)$. The other three network structural signatures (Fig. 4.1) are tightly linked with these two (See section 3.3.3, Fig. 3.5 and Fig. 4.4). The parameter sensitivity was evaluated as follows. Using the methods described in section 4.2.3, I recalculated the measures $r(m,G)$ and $r(TL,\bar{\alpha}_G)$ for each of 100 logarithmically spaced values for *k* between 10^{-3} and 10^{3} (consumer 1000 times smaller to 1000 times larger than resource) and 100 linearly placed values for *s* between 0.01 and 0.1. This range for *k* covers most of the CRBRs considered to be "optimal" (in the sense of viable or evolutionarily stable strategies for consumers) in previous studies on body-size based consumer-resource interactions (Cohen et al., 2005; Weitz and Levin, 2006), and accommodates potential differences in *k* across the most common trophic interaction types seen in food webs (i.e., predator-prey, herbivore-plant and parasitoid-host) (Brose et al., 2005). The upper range for *s* (0.1) was chosen because as $s \rightarrow 0.1$, consumption intensity falls to zero within the range of the CRBRs observed across the nine real communities (Fig. 4.2; cf. Fig. 4.3). Hence values larger than this are unfeasible because if a CRBR is observed, no matter how extreme, it *must* be associated with some level of biomass acquisition by the consumer. The lower limit of *s* (0.01) was chosen as some value arbitrarily higher than 0 because φ_{ij} becomes flat as $s \rightarrow 0$ and the effects of CRBRs on trophic link strengths are eliminated (Fig. 4.2).

Fig. F1&F2 show the resulting variation in the strengths of the signatures $r(m,G)$ and $r(TL,\bar{\alpha}_G)$ respectively. Clearly, both these signatures are particularly robust to changes in *k*, with the correlation coefficient remaining similar across its entire range, as long as $s < 0.05$ or so. As $s \rightarrow 0.1$ however, the signatures either become stronger or weaker, depending upon the community and the value of *k*. This is the effect of elimination of the trophic links associated with extreme CRBRs (because φ_{ij} becomes zero; see Fig. 4.2), which strongly biases the interaction data towards trophic links with CRBRs close to *k*. However, in none of the cases is the sign of the relationship reversed, and the value of the correlation coefficient remains within a narrow range across the entire parameter space. Also, in both the signatures, the SB community shows a different pattern from the others; whereas the detectability of signatures becomes weaker as *k* decreases all the others, it in fact peaks at $k = 10^{-3}$ in the SB community. This is because this is the only community with a significant number of host-parasitoid interactions; this supports the conjecture made in section 4.2.3 that changing *k* according to the interaction type is appropriate (*k* should in fact be << 0 in host-parasitoid interactions). Similarly, *k* is typically ≥ 0 in predator-prey interactions, which dominate all communities other than SB, thus explaining why strengths of the signatures increase towards $k = 10^{3}$ in them. Thus overall, the strengths of the observed signatures, and the main conclusions of this study would be much stronger if trophic-link specific values for *k* were used. Another community that stands out is EW, where the strengths of both signatures peak at $k = 1$ ($\log_{10}(k) = 0$ in the figures); this is it is the community with the most balanced CRBR distribution (in terms of the representation of CRBRs < 1; see Fig. 4.3).

Figure F1. The effect of variation in the parameters *k* and *s* on the strength of the measure $r(G,\bar{\alpha}_G)$ (a food web structural signature of dynamically constrained assembly) across nine empirically observed communities.

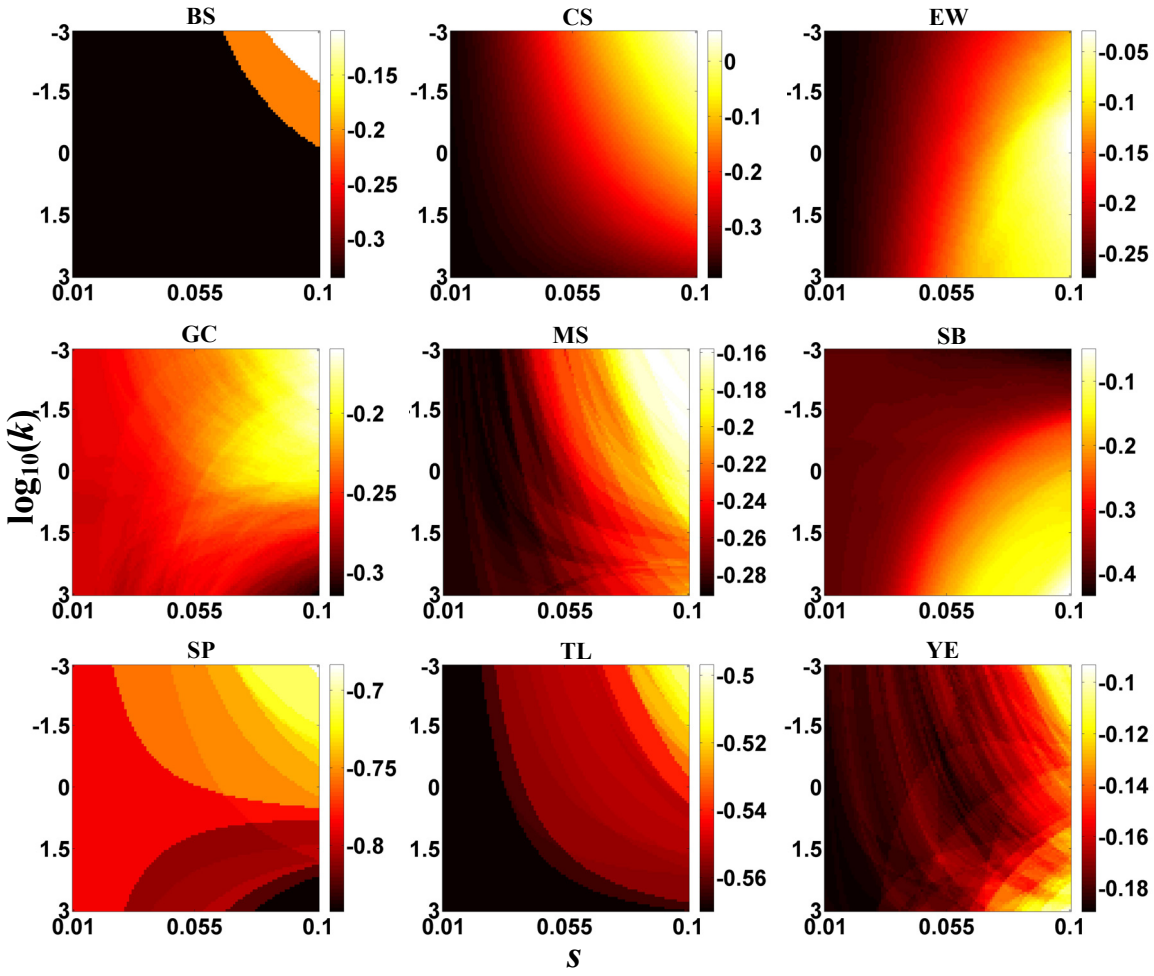

Figure F2. The effect of variation in the parameters *k* and *s* on the strength of the measure $r(TL, \bar{\alpha}_G)$ (a food web structural signature of dynamically constrained assembly) across nine empirically observed communities.

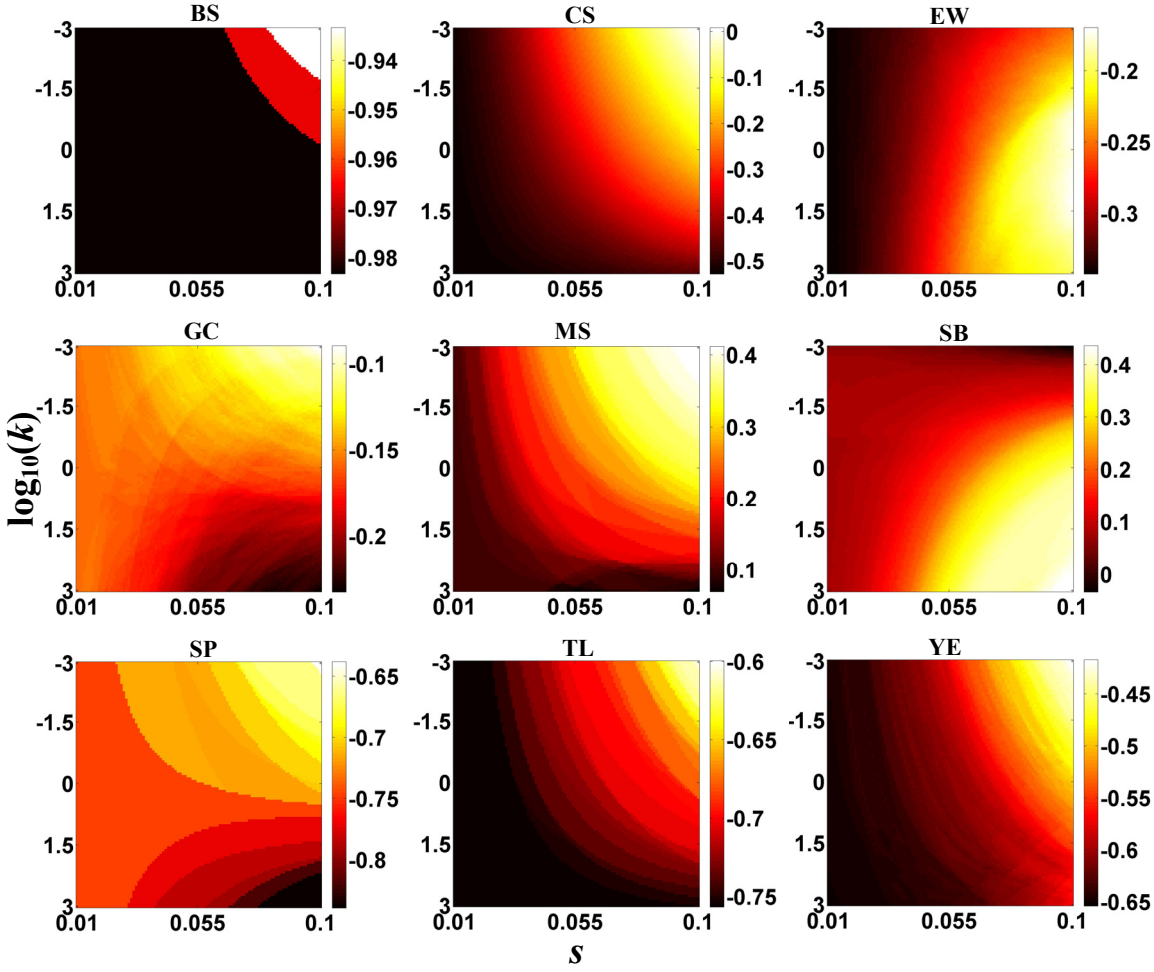

Glossary

Basal species: Species that sequester energy from inorganic or inorganic sources which then flows through the community's food web. Autotrophic basal species are typically called "primary producers". Another example of a basal species is a detritivore.

Dynamically constrained community assembly: Community assembly wherein species interactions strongly determine extinction dynamics following immigration.

Food web: The network of "who-eats-whom", or trophic interactions, with species represented by nodes and the trophic interactions between them by edges (links).

Immigration-extinction equilibrium (IEE): The quasi-equilibrium species richness maintained by an approximate balance between immigration of species into the local community and extinctions of resident ones.

Interaction sign structure: The distribution of interspecific interactions between species, without consideration of the strengths of those interactions.

Interaction strength sensitivity (ISS): The sensitivity of a community's stability to the pattern of absolute magnitudes of interaction strengths.

Probability of Hurwitz stability (PHS): The probability of a randomly chosen community matrix from the space of all possible matrices with the same species richness, sign structure, and statistical properties of the intra- and interspecific interaction strengths being Hurwitz (local asymptotic) stable.

Relaxed community assembly: Community assembly wherein species interactions play little or no role in determining the immigration-extinction dynamics.

Sign stability: A property of the interaction network structure of a community that guarantees Hurwitz (local asymptotic) stability irrespective of the magnitudes of the interaction strengths.

Species sorting: The extinction of one of more species due to an unstable trophic interaction network pattern.

Stable invasion: The successful invasion of an immigrant species during assembly without the loss of any resident.

Trophic generality (*G*): The number of resource species of a consumer, also known as "niche width" in the literature.

Trophic level (*TL*): The network topological distance of a consumer species node from a basal (typically, a primary producer) one.

Trophic vulnerability: The number of consumer species of a resource.

Weighted trophic generality (G^w): A measure of a consumer species' generality weighted by strengths of the trophic links involved (formally defined in expression 2.8).

Bibliography

Abrams, P.A., 1991. Strengths of indirect effects generated by optimal foraging. Oikos 62, 167-176.

Agrawal, A.A., Underwood, N., and Stinchcombe, J.R., 2004. Intraspecific variation in the strength of density dependence in aphid populations. Ecol. Entomol. 29, 521-526.

Aljetlawi, A.A., Sparrevik, E., and Leonardsson, K., 2004. Prey-predator size-dependent functional response: derivation and rescaling to the real world. J. Anim. Ecol. 73, 239-252.

Allen, A.P., and Gillooly, J.F., 2006. Assessing latitudinal gradients in speciation rates and biodiversity at the global scale. Ecol. Lett. 9, 947-954.

Allen, A.P., and Savage, V.M., 2007. Setting the absolute tempo of biodiversity dynamics. Ecol. Lett. 10, 637-646.

Allen, A.P., Gillooly, J.F., Savage, V.M., and Brown, J.H., 2006a. Kinetic effects of temperature on rates of genetic divergence and speciation. Proc. Natl. Acad. Sci. U. S. A. 103, 9130-9135.

Allen, C.R., Garmestani, A.S., Havlicek, T.D., Marquet, P.A., Peterson, G.D., Restrepo, C., Stow, C.A., and Weeks, B.E., 2006b. Patterns in body mass distributions: sifting among alternative hypotheses. Ecol. Lett. 9, 630-643.

Allesina, S., and Pascual, M., 2008. Network structure, predator–prey modules, and stability in large food webs. Theoretical Ecology 1, 55–64.

Allesina, S., Alonso, D., and Pascual, M., 2008. A general model for food web structure. Science 320, 658-661.

Armstrong, R.A., and McGehee, R., 1980. Competitive exclusion. Am. Nat. 115, 151-170.

Bascompte, J., Melian, C.J., and Sala, E., 2005. Interaction strength combinations and the overfishing of a marine food web. Proc. Natl. Acad. Sci. U. S. A. 102, 5443-5447.

Bastolla, U., Lassig, M., Manrubia, S.C., and Valleriani, A., 2005. Biodiversity in model ecosystems, II: species assembly and food web structure. J. Theor. Biol. 235, 531-539.

Beckerman, A.P., Petchey, O.L., and Warren, P.H., 2006. Foraging biology predicts food web complexity. Proc. Natl. Acad. Sci. U. S. A. 103, 13745-13749.

Berlow, E.L., Dunne, J.A., Martinez, N.D., Stark, P.B., Williams, R.J., and Brose, U., 2009. Simple prediction of interaction strengths in complex food webs. Proceedings of the National Academy of Sciences 106, 187-191.

Berlow, E.L., Neutel, A.M., Cohen, J.E., de Ruiter, P.C., Ebenman, B., Emmerson, M., Fox, J.W., Jansen, V.A.A., Jones, J.I., Kokkoris, G.D., Logofet, D.O., McKane, A.J., Montoya, J.M., and Petchey, O., 2004. Interaction strengths in food webs: issues and opportunities. J. Anim. Ecol. 73, 585-598.

Blackburn, T.M., and Gaston, K.J., 1994. Animal body-size distributions change as more species are described. Proc. Roy. Soc. Lond. B. 257, 293-297.

Borrett, S.R., Fath, B.D., and Patten, B.C., 2007. Functional integration of ecological networks through pathway proliferation. J. Theor. Biol. 245, 98-111.

Brose, U., Williams, R.J., and Martinez, N.D., 2006a. Allometric scaling enhances stability in complex food webs. Ecol. Lett. 9, 1228-1236.

Brose, U., Ehnes, R.B., Rall, B.C., Vucic-Pestic, O., Berlow, E.L., and Scheu, S., 2008. Foraging theory predicts predator-prey energy fluxes. J. Anim. Ecol. 77, 1072–1078.

Brose, U., Jonsson, T., Berlow, E.L., Warren, P., Banasek-Richter, C., Bersier, L.F., Blanchard, J.L., Brey, T., Carpenter, S.R., Blandenier, M.F.C., Cushing, L., Dawah, H.A., Dell, T., Edwards, F., Harper-Smith, S., Jacob, U., Ledger, M.E., Martinez, N.D., Memmott, J., Mintenbeck, K., Pinnegar, J.K., Rall, B.C., Rayner, T.S., Reuman, D.C., Ruess, L., Ulrich, W., Williams, R.J., Woodward, G., and Cohen, J.E., 2006b. Consumer-resource body-size relationships in natural food webs. Ecology 87, 2411-2417.

Brose, U., Cushing, L., Berlow, E.L., Jonsson, T., Banasek-Richter, C., Bersier, L.-F., Blanchard, J.L., Brey, T., Carpenter, S.R., Blandenier, M.F.C., Cohen, J.E., Dawah, H.A., Dell, T., Edwards, F., Harper-Smith, S., Jacob, U., Knapp, R.A., Ledger, M.E., Memmott, J., Mintenbeck, K., Pinnegar, J.K., Rall, B.C., Rayner, T., Ruess, L., Ulrich, W., Warren, P.H., Williams, R.J., Woodward, G., Yodzis, P., and Martinez, N.D., 2005. Body sizes of consumers and their resources. Ecology 86, 2545-2545.

Brown, J.H., and Gillooly, J.F., 2003. Ecological food webs: High-quality data facilitate theoretical unification. Proc. Natl. Acad. Sci. U. S. A. 100, 1467-1468.

Brown, J.H., Marquet, P.A., and Taper, M.L., 1993. Evolution of body-size: consequences of an energetic definition of fitness. Am. Nat. 142, 573-584.
Brown, J.H., West, G.B., and Enquist, B.J., 2005. Yes, West, Brown and Enquist's model of allometric scaling is both mathematically correct and biologically relevant. Funct. Ecol. 19, 735-738.
Brown, J.H., Gillooly, J.F., Allen, A.P., Savage, V.M., and West, G.B., 2004. Toward a metabolic theory of ecology. Ecology 85, 1771-1789.
Brown, W.L.J., and Wilson, E.O., 1969. Character displacement. Syst. Zool. 5, 49-64.
Bystrom, P., and Garcia-Berthou, E., 1999. Density dependent growth and size specific competitive interactions in young fish. Oikos 86, 217-232.
Calder, W.A., 1984. Size, function, and life history. Harvard University Press, Cambridge, Mass.
Cattin, M.F., Bersier, L.F., Banasek-Richter, C., Baltensperger, R., and Gabriel, J.P., 2004. Phylogenetic constraints and adaptation explain food-web structure. Nature 427, 835-839.
Charnov, E.L., 1993. Life history invariants: some explorations of symmetry in evolutionary ecology. Oxford University Press, Oxford England.
Cohen, J.E., 1989. Ecologists' cooperative web bank. Version 1.00. The Rockefeller University, New York.
Cohen, J.E., Body sizes in food chains of animal predators and parasites, in: Hildrew, A. G., et al., Eds.), Body size: the structure and function of aquatic ecosystems, Cambridge University Press, Cambridge, UK. 2008, pp. 306-325.
Cohen, J.E., and Newman, C.M., 1985. When will a large complex system be stable. J. Theor. Biol. 113, 153-156.
Cohen, J.E., Jonsson, T., and Carpenter, S.R., 2003. Ecological community description using the food web, species abundance, and body size. Proc. Natl. Acad. Sci. U. S. A. 100, 1781-1786.
Cohen, J.E., Luczak, T., Newman, C.M., and Zhou, Z.M., 1990. Stochastic structure and nonlinear dynamics of food webs: qualitative stability in a Lotka-Volterra cascade model. Proc. Roy. Soc. Lond. B. 240, 607-627.
Cohen, J.E., Pimm, S.L., Yodzis, P., and Saldana, J., 1993. Body sizes of animal predators and animal prey in food webs. J. Anim. Ecol. 62, 67-78.
Cohen, J.E., Jonsson, T., Muller, C.B., Godfray, H.C.J., and Savage, V.M., 2005. Body sizes of hosts and parasitoids in individual feeding relationships. Proc. Natl. Acad. Sci. U. S. A. 102, 684-689.
Connor, E.F., and Simberloff, D., 1983. Interspecific competition and species co-occurrence patterns on islands: null models and the evaluation of evidence. Oikos 41, 455-465.
Connor, E.F., Simberloff, D.S., and Strong, D.R., Neutral models of species' co-occurrence patterns, Ecological Communities: Conceptual Issues and the Evidence, Princeton University Press, New Jersey 1984, pp. 316-331.
Darwin, C., 1859. On the origin of species by means of natural selection, or the preservation of favoured races in the struggle for life. P. F. Collier & Son co., New York.
Dial, K.P., and Marzluff, J.M., 1988. Are the smallest organisms the most diverse. Ecology 69, 1620-1624.
Dial, K.P., Greene, E., and Irschick, D.J., 2008. Allometry of behavior. Trends Ecol. Evol. 23, 394-401.
Drossel, B., Higgs, P.G., and McKane, A.J., 2001. The influence of predator-prey population dynamics on the long- term evolution of food web structure. J. Theor. Biol. 208, 91-107.
Drossel, B., McKane, A.J., and Quince, C., 2004. The impact of nonlinear functional responses on the long-term evolution of food web structure. J. Theor. Biol. 229, 539-548.
Dunne, J.A., Brose, U., Williams, R.J., and Martinez, N.D., Modeling food-web dynamics: complexity-stability implications, in: Belgrano, A., et al., Eds.), Aquatic Food Webs: An Ecosystem Approach, Oxford University Press, New York 2005, pp. 117-238.
Elton, C.S., 1927. Animal ecology. Sidgwick & Jackson, ltd, London.
Emmerson, M.C., and Raffaelli, D., 2004. Predator-prey body size, interaction strength and the stability of a real food web. J. Anim. Ecol. 73, 399-409.
Etienne, R.S., and Olff, H., 2004. How dispersal limitation shapes species-body size distributions in local communities. Am. Nat. 163, 69-83.
Gardner, M.R., and Ashby, W.R., 1970. Connectance of large dynamic (cybernetic) systems: critical values for stability. Nature 228.
Gause, G.F., 1934. The struggle for existence. The Williams & Wilkins company, Baltimore.
Geman, S., 1986. The spectral radius of large random matrices. Ann. Prob. 14, 1318-1328.
Gillooly, J.F., Brown, J.H., West, G.B., Savage, V.M., and Charnov, E.L., 2001. Effects of size and temperature on metabolic rate. Science 293, 2248-2251.

Gilpin, M.E., 1979. Spiral chaos in a predator-prey model. Am. Nat. 113, 306-308.
Gilpin, M.E., Diamond, J.M., and Strong, D.R., Are species co-occurrences on islands non-random, and are null hypotheses useful in community ecology ?, Ecological Communities: Conceptual Issues and the Evidence, Princeton University Press, New Jersey 1984, pp. 297-315.
Glazier, D.S., 2005. Beyond the '3/4-power law': variation in the intra- and interspecific scaling of metabolic rate in animals. Biological Reviews 80, 611-662.
Goldwasser, L., and Roughgarden, J., 1993. Construction and analysis of a large Caribbean food web. Ecology 74, 1216-1233.
Goldwasser, L., and Roughgarden, J., 1997. Sampling effects and the estimation of food-web properties. Ecology 78, 41-54.
Grimm, V., and Wissel, C., 1997. Babel, or the ecological stability discussions: An inventory and analysis of terminology and a guide for avoiding confusion. Oecologia 109, 323-334.
Hall, S.J., and Raffaelli, D., 1991. Food-web patterns: Lessons from a species-rich web. J. Anim. Ecol. 60, 823-842.
Harrison, G.W., 1979. Stability under environmental stress: resistance, resilience, persistence, and variability. Am. Nat. 113, 659-669.
Harvey, P.H., Colwell, R.K., Silvertown, J.W., and May, R.M., 1983. Null models in Ecology. Annu. Rev. Ecol. Syst. 14, 189-212.
Hastings, H.M., 1982. The May-Wigner stability theorem. J. Theor. Biol. 97, 155-166.
Havens, K., 1992. Scale and structure in natural food webs. Science 257, 1107-1109.
Hildrew, A.G., Raffaelli, D.G., and Edmonds-Brown, R., 2007. Body size: the structure and function of aquatic ecosystems. Cambridge University Press, Cambridge ; New York.
Hofbauer, J., and Sigmund, K., 1988. The theory of evolution and dynamical systems: mathematical aspects of selection. Cambridge University Press, Cambridge [England] ; New York.
Hofbauer, J., and Sigmund, K., 1998. Evolutionary games and population dynamics. Cambridge University Press, Cambridge ; New York, NY.
Holling, C.S., 1959. The components of predation as revealed by a study of small-mammal predation of the European pine sawfly. Can. Entomol. 91, 293-320.
Horn, R.A., and Johnson, C.R., 1985. Matrix Analysis. Cambridge University Press, Cambridge.
Hubbell, S.P., 2001. The unified neutral theory of biodiversity and biogeography. Princeton University Press, Princeton, NJ.
Hubbell, S.P., and Borda-De-Agua, L., 2004. The unified neutral theory of biodiversity and biogeography: Reply. Ecology 85, 3175-3178.
Hudson, P.J., Dobson, A.P., and Lafferty, K.D., 2006. Is a healthy ecosystem one that is rich in parasites? Trends Ecol. Evol. 21, 381-385.
Hutchinson, G.E., 1959. Homage to Santa Rosalia or why are there so many kinds of animals? Am. Nat. 93, 145-159.
Hutchinson, G.E., and MacArthur, R.H., 1959. A theoretical ecological model of size distributions among species of animals. Am. Nat. 93, 117-125.
Huxham, M., Beaney, S., and Raffaelli, D., 1996. Do parasites reduce the chances of triangulation in a real food web? Oikos 76, 284-300.
Ikeda, M., and Siljak, D.D., 1982. Lotka-Volterra equations: decomposition, stability, and structure, Part II: Nonequilibrium analysis. Nonlinear Analysis, Theory, Methods & Applications 6, 487-501.
Ives, A.R., and Carpenter, S.R., 2007. Stability and diversity of ecosystems. Science 317, 58-62.
Jongman, R.H.G., Ter Braak, C.J.F., and Van Tongeren, O.F.R., 1995. Data analysis in community and landscape ecology. Cambridge University Press, Biddles.
Jonsson, T., and Ebenman, B., 1998. Effects of predator-prey body size ratios on the stability of food chains. J. Theor. Biol. 193, 407-417.
Jonsson, T., Cohen, J.E., and Carpenter, S.R., 2005. Food webs, body size, and species abundance in ecological community description. Adv. Ecol. Res. 36, 1-84.
Kingsland, S.E., 1985. Modeling nature episodes in the history of population ecology. University of Chicago Press, Chicago.
Kleiber, M., 1961. The fire of life: an introduction to animal energetics. Wiley, New York,.
Kolotilina, L.Y., 1993. Lower bounds for the Perron root of a nonegative matrix. Linear Algebra Appl. 180, 133-151.

Kondoh, M., 2003. Foraging Adaptation and the Relationship Between Food-Web Complexity and Stability. Science 299, 1388-1391.
Kondoh, M., 2006. Does foraging adaptation create the positive complexity-stability relationship in realistic food-web structure? J. Theor. Biol. 238, 646-651.
Kondoh, M., 2007. Anti-predator defence and the complexity-stability relationship of food webs. Proc. Roy. Soc. Lond. B. 274, 1617-1624.
Kozlowski, J., and Konarzewski, M., 2005. West, Brown and Enquist's model of allometric scaling again: the same questions remain. Funct. Ecol. 19, 739-743.
Kratina, P., Vos, M., Bateman, A., and Anholt, B., 2009. Functional responses modified by predator density. Oecologia 159, 425-433.
Kristensen, N.P., 2008. Permanence does not predict the commonly measured food web structural attributes. Am. Nat. 171, 202-213.
Kuris, A.M., Hechinger, R.F., Shaw, J.C., Whitney, K.L., Aguirre-Macedo, L., Boch, C.A., Dobson, A.P., Dunham, E.J., Fredensborg, B.L., Huspeni, T.C., Lorda, J., Mababa, L., Mancini, F.T., Mora, A.B., Pickering, M., Talhouk, N.L., Torchin, M.E., and Lafferty, K.D., 2008. Ecosystem energetic implications of parasite and free-living biomass in three estuaries. Nature 454, 515-518.
Lafferty, K.D., Dobson, A.P., and Kuris, A.M., 2006a. Parasites dominate food web links. Proc. Natl. Acad. Sci. U. S. A. 103, 11211-11216.
Lafferty, K.D., Hechinger, R.F., Shaw, J.C., Whitney, K.L., and Kuris, A.M., Food webs and parasites in a salt marsh ecosystem, in: Collinge, S. K. and Ray, C., Eds.), Disease ecology: community structure and pathogen dynamics, Oxford University Press, Oxford; New York 2006b, pp. 119-134.
Lafferty, K.D., Allesina, S., Arim, M., Briggs, C.J., De Leo, G., Dobson, A.P., Dunne, J.A., Johnson, P.T.J., Kuris, A.M., Marcogliese, D.J., Martinez, N.D., Memmott, J., Marquet, P.A., McLaughlin, J.P., Mordecai, E.A., Pascual, M., Poulin, R., and Thieltges, D.W., 2008. Parasites in food webs: the ultimate missing links. Ecol. Lett. 11, 533-546.
Law, R., and Morton, R.D., 1996. Permanence and the assembly of ecological communities. Ecology 77, 762-775.
Leaper, R., and Raffaelli, D., 1999. Defining the abundance body-size constraint space: data from a real food web. Ecol. Lett. 2, 191-199.
Leaper, R., and Huxham, M., 2002. Size constraints in a real food web: predator, parasite and prey body-size relationships. Oikos 99, 443-456.
Leaper, R., Raffaelli, D., Emes, C., and Manly, B., 2001. Constraints on body-size distributions: an experimental test of the habitat architecture hypothesis. J. Anim. Ecol. 70, 248-259.
Levine, S., 1980. Several measures of trophic structure applicable to complex food webs. J. Theor. Biol. 83, 195-207.
Levins, R., 1974. The qualitative analysis of partially specified systems. Ann. N. Y. Acad. Sci. 231, 123-138.
Levins, R., Evolution in communities near equilibrium, in: Cody, M. L. and Diamond, J. M., Eds.), Ecology and evolution of communities, Belknap Press of Harvard University Press, Cambridge, Massachusetts 1975, pp. 16-50.
Lewis, H.M., Law, R., and McKane, A.J., 2008. Abundance-body size relationships: the roles of metabolism and population dynamics. J. Anim. Ecol. 77, 1056-1062.
Lindeman, R.L., 1942. The trophic-dynamic aspect of ecology. Ecology 23, 399-417.
Loeuille, N., and Loreau, M., 2005. Evolutionary emergence of size-structured food webs. Proc. Natl. Acad. Sci. U. S. A. 102, 5761-5766.
Loeuille, N., and Loreau, M., 2006. Evolution of body size in food webs: does the energetic equivalence rule hold? Ecol. Lett. 9, 171-178.
Logofet, D.O., 1993. Matrices and graphs: stability problems in mathematical ecology. CRC Press, Boca Raton.
MacArthur, R., 1955. Fluctuations of animal populations and a measure of community stability. Ecology 36, 533-536.
MacArthur, R.H., and Wilson, E.O., 1967. The theory of island biogeography. Princeton University Press, Princeton, N.J.
Marcogliese, D.J., 2003. Food webs and biodiversity: are parasites the missing link. J. Parasitol. 89, 106-113.

Marcogliese, D.J., and Cone, D.K., 1997. Food webs: A plea for parasites. Trends Ecol. Evol. 12, 320-325.
Marquet, P.A., Navarrete, S.A., and Castilla, J.C., 1995. Body size, population density, and the energetic equivalence rule. The Journal of Animal Ecology 64, 325-332.
Marquet, P.A., Quinones, R.A., Abades, S., Labra, F., Tognelli, M., Arim, M., and Rivadeneira, M., 2005. Scaling and power-laws in ecological systems. J. Exp. Biol. 208, 1749-1769.
Martinez, N.D., 1991. Artifacts or attributes?: effects of resolution on the Little Rock Lake food web. Ecol. Monogr. 61, 367-392.
Martinez, N.D., 1992. Constant connectance in community food webs. Am. Nat. 139, 1208-1218.
Martinez, N.D., Hawkins, B.A., Dawah, H.A., and Feifarek, B.P., 1999. Effects of sampling effort on characterization of food-web structure. Ecology 80, 1044-1055.
Marzluff, J.M., and Dial, K.P., 1991. Life-history correlates of taxonomic diversity. Ecology 72, 428-439.
May, R.M., 1973. Stability in randomly fluctuating versus deterministic environments. Am. Nat. 107, 621-650.
May, R.M., 1974. Stability and Complexity in Model Ecosystems. Princeton University Press, Princeton, NJ.
May, R.M., 2006. Network structure and the biology of populations. Trends Ecol. Evol. 21, 394-399.
McCann, K., Hastings, A., and Huxel, G.R., 1998. Weak trophic interactions and the balance of nature. Nature 395, 794-798.
McCann, K.S., 2000. The diversity-stability debate. Nature 405, 228-233.
McCoy, M.W., and Gillooly, J.F., 2008. Predicting natural mortality rates of plants and animals. Ecol. Lett. 11, 710-6.
Memmott, J., Martinez, N.D., and Cohen, J.E., 2000. Predators, parasitoids and pathogens: species richness, trophic generality and body sizes in a natural food web. J. Anim. Ecol. 69, 1-15.
Milo, R., Shen-Orr, S., Itzkovitz, S., Kashtan, N., Chklovskii, D., and Alon, U., 2002. Network motifs: Simple building blocks of complex networks. Science 298, 824-827.
Neubert, M.G., Klanjscek, T., and Caswell, H., 2004. Reactivity and transient dynamics of predator-prey and food web models. Ecol. Model. 179, 29-38.
Neutel, A.-M., Heesterbeek, J.A.P., van de Koppel, J., Hoenderboom, G., Vos, A., Kaldeway, C., Berendse, F., and de Ruiter, P.C., 2007. Reconciling complexity with stability in naturally assembling food webs. Nature 449, 599-602.
Neutel, A.M., Heesterbeek, J.A.P., and de Ruiter, P.C., 2002. Stability in real food webs: Weak links in long loops. Science 296, 1120-1123.
Newman, M.E.J., 2003. The structure and function of complex networks. Siam Review 45, 167-256.
Niklas, K.J., and Enquist, B.J., 2001. Invariant scaling relationships for interspecific plant biomass production rates and body size. Proc. Natl. Acad. Sci. U. S. A. 98, 2922-2927.
O'Connor, M.P., Kemp, S.J., Agosta, S.J., Hansen, F., Sieg, A.E., Wallace, B.P., McNair, J.N., and Dunham, A.E., 2007. Reconsidering the mechanistic basis of the metabolic theory of ecology. Oikos 116, 1058-1072.
Oaten, A., and Murdoch, W.W., 1975. Functional response and stability in predator-prey systems. Am. Nat. 109, 289-298.
Odum, E.P., 1953. Fundamentals of ecology. Saunders, Philadelphia.
Otto, S.B., Rall, B.C., and Brose, U., 2007. Allometric degree distributions facilitate food-web stability. Nature 450, 1226-1229.
Pace, M.L., Cole, J.J., Carpenter, S.R., and Kitchell, J.F., 1999. Trophic cascades revealed in diverse ecosystems. Trends Ecol. Evol. 14, 483-488.
Pascual, M., and Dunne, J.A., 2005. Ecological networks: linking structure to dynamics in food webs. Oxford University Press, New York.
Pascual, M., and Dunne, J.A., 2006. Ecological networks: linking structure to dynamics in food webs. Oxford University Press, New York.
Pascual, M., Dunne, J.A., and Levin, S.A., Challenges for the future: Integrating ecological structure and dynamics, in: Pascual, M. and Dunne, J. A., Eds.), Ecological Networks: Linking Structure to Dynamics in Food Webs, Oxford University Press, New York 2006, pp. 351-370.
Pawar, S., 2009. Community assembly, stability and signatures of dynamical constraints on food web structure. J. Theor. Biol. in press, DOI: 10.1016/j.jtbi.2009.04.006.

Persson, L., Leonardsson, K., de Roos, A.M., Gyllenberg, M., and Christensen, B., 1998. Ontogenetic scaling of foraging rates and the dynamics of a size-structured consumer-resource model. Theor. Popul. Biol. 54, 270-293.
Petchey, O.L., Beckerman, A.P., Riede, J.O., and Warren, P.H., 2008. Size, foraging, and food web structure. Proc. Natl. Acad. Sci. U. S. A. 105, 4191-4196.
Peters, R.H., 1983. The ecological implications of body size. Cambridge University Press, Cambridge.
Piechnik, D.A., Lawler, S.P., and Martinez, N.D., 2008. Food-web assembly during a classic biogeographic study: species' "trophic breadth" corresponds to colonization order. Oikos.
Pimm, S.L., 1982. Food webs. Chapman and Hall, London.
Pimm, S.L., and Lawton, J.H., 1977. Number of trophic levels in ecological communities. Nature 268, 329-331.
Polis, G.A., 1991. Complex trophic interactions in deserts: an empirical critique of food-web theory. Am. Nat. 138, 123-155.
Polis, G.A., Sears, A.L.W., Huxel, G.R., Strong, D.R., and Maron, J., 2000. When is a trophic cascade a trophic cascade? Trends Ecol. Evol. 15, 473-475.
Post, W.M., and Pimm, S.L., 1983. Community assembly and food web stability. Math. Biosci. 64, 169-182.
Proulx, S.R., Promislow, D.E.L., and Phillips, P.C., 2005. Network thinking in ecology and evolution. Trends Ecol. Evol. 20, 345-353.
Raffel, T.R., Martin, L.B., and Rohr, J.R., 2008. Parasites as predators: unifying natural enemy ecology. Trends Ecol. Evol. 23, 610-618.
Ramos-Jiliberto, R., 2005. Resource - consumer models and the biomass conversion principle. Environmental Modelling & Software 20, 85-91.
Reagan, D.P., and Waide, R.B., 1996. The food web of a tropical rain forest. University of Chicago Press, Chicago.
Robinson, J.F., and Dickerson, J.E., 1987. Does invasion sequence affect community structure? Ecology 68, 587-595.
Rosenzweig, M.L., and MacArthur, R.H., 1963. Graphical representation and stability conditions of predator-prey interactions. Am. Nat. 97, 209-223.
Rossberg, A.G., Ishii, R., Amemiya, T., and Itoh, K., 2008. The top-down mechanism for body-mass–abundance scaling. Ecology 89, 567-580.
Roughgarden, J., 1996. Theory of population genetics and evolutionary ecology: an introduction. Prentice Hall, Upper Saddle River, NJ.
Ruiter, P.C.d., Neutel, A.-M., and Moore, J.C., 1995. Energetics, patterns of interaction strengths, and stability in real ecosystems. Science 269, 1257-1260.
Savage, V.M., Gillooly, J.F., Brown, J.H., West, G.B., and Charnov, E.L., 2004. Effects of body size and temperature on population growth. Am. Nat. 163, E429-E441.
Schmitt, R.J., and Holbrook, S.J., 2007. The scale and cause of spatial heterogeneity in strength of temporal density dependence. Ecology 88, 1241-1249.
Schoener, T.W., 1989. Food webs from the small to the large. Ecology 70, 1559-1589.
Schwenk, A.J., 1986. Tight bounds on the spectral radius of asymmetric nonegative matrices. Linear Algebra Appl. 75, 257-265.
Scudo, F.M., and Ziegler, J.R., 1978. The Golden age of theoretical ecology, 1923-1940: a collection of works by V. Volterra, V. A. Kostitzin, A. J. Lotka, and A. N. Kolmogoroff. Springer-Verlag, Berlin.
Sheldon, R.W., Sutcliffe, W.H., and Paranjape, M.A., 1977. Structure of pelagic food chain and relationship between plankton and fish production. J. Fish. Res. Board Can. 34, 2344-2353.
Siemann, E., Tilman, D., and Haarstad, J., 1999. Abundance, diversity and body size: patterns from a grassland arthropod community. J. Anim. Ecol. 68, 824-835.
Spencer, H., 1864. The principles of biology. William and Norgate, London etc.
Springer, M.D., 1979. The algebra of random variables. Wiley, New York.
Stead, T.K., Schmid-Araya, J.M., Schmid, P.E., and Hildrew, A.G., 2005. The distribution of body size in a stream community: one system, many patterns. J. Anim. Ecol. 74, 475-487.
Stephens, D.W., and Krebs, J.R., 1986. Foraging theory. Princeton University Press, Princeton, N.J.
Stouffer, D.B., Camacho, J., Guimera, R., Ng, C.A., and Amaral, L.A.N., 2005. Quantitative patterns in the structure of model and empirical food webs. Ecology 86, 1301-1311.

Strobeck, C., 1973. *N* species competition. Ecology 54, 650-654.
Thompson, R.M., and Townsend, C.R., 2003. Impacts on stream food webs of native and exotic forest: an intercontinental comparison. Ecology 84, 145-161.
Thompson, R.M., Mouritsen, K.N., and Poulin, R., 2005. Importance of parasites and their life cycle characteristics in determining the structure of a large marine food web. J. Anim. Ecol. 74, 77-85.
Townsend, C.R., Thompson, R.M., McIntosh, A.R., Kilroy, C., Edwards, E., and Scarsbrook, M.R., 1998. Disturbance, resource availability and food-web architecture in streams. Ecol. Lett. 1, 200-209.
Uchida, S., Drossel, B., and Brose, U., 2007. The structure of food webs with adaptive behaviour. Ecol. Model. 206, 263-276.
Vasseur, D.A., and McCann, K.S., 2005. A mechanistic approach for modeling temperature-dependent consumer-resource dynamics. Am. Nat. 166, 184-198.
Virgo, N., Law, R., and Emmerson, M., 2006. Sequentially assembled food webs and extremum principles in ecosystem ecology. J. Anim. Ecol. 75, 377-386.
Wahlstrom, E., Persson, L., Diehl, S., and Bystrom, P., 2000. Size-dependent foraging efficiency, cannibalism and zooplankton community structure. Oecologia 123, 138-148.
Warren, P.H., 1989. Spatial and temporal variation in the structure of a freshwater food web. Oikos 55, 299-311.
Webb, C., 2003. A complete classification of Darwinian extinction in ecological interactions. Am. Nat. 161, 181-205.
Weitz, J.S., and Levin, S.A., 2006. Size and scaling of predator-prey dynamics. Ecol. Lett. 9, 548-557.
West, G.B., Brown, J.H., and Enquist, B.J., 1997. A general model for the origin of allometric scaling laws in biology. Science 276, 122-126.
Williams, R.J., and Martinez, N.D., 2000. Simple rules yield complex food webs. Nature 404, 180-183.
Williams, R.J., and Martinez, N.D., 2004. Limits to trophic levels and omnivory in complex food webs: Theory and data. Am. Nat. 163, 458-468.
Woodward, G., Speirs, D.C., and Hildrew, A.G., 2005a. Quantification and resolution of a complex, size-structured food web. Adv. Ecol. Res. 36, 85-135.
Woodward, G., Ebenman, B., Ernmerson, M., Montoya, J.M., Olesen, J.M., Valido, A., and Warren, P.H., 2005b. Body size in ecological networks. Trends Ecol. Evol. 20, 402-409.
Wootton, J.T., and Emmerson, M., 2005. Measurement of interaction strength in nature. Annual Review of Ecology Evolution and Systematics 36, 419-444.
Yodzis, P., 1981. The stability of real ecosystems. Nature 289, 674-676.
Yodzis, P., 1988. The indeterminacy of ecological interactions as perceived through perturbation experiments. Ecology 69, 508-515.
Yodzis, P., 2000. Diffuse effects in food webs. Ecology 81, 261-266.
Yodzis, P., and Innes, S., 1992. Body size and consumer resource dynamics. Am. Nat. 139, 1151-1175.
Yodzis, P., and Winemiller, K.O., 1999. In search of operational trophospecies in a tropical aquatic food web. Oikos 87, 327-340.

Vita

Samraat Shashikant Raghunath Pawar, was born on 1 September 1975, in New Delhi, India to Shashikant Raghunath Pawar and Sheela Pawar cousins of the first order. He was born (rather inbred) under an elbow bush, which is considered an extremely lucky sign among his tribespeople. As he grew up, he converted to Buddhism, Sikhisim, Islam, and then Jainism. Later he became a Hindoo, which inexorably led him towards a life in science. He eventually renounced his newfound religion, and obtained a Bachelor's degree in Biology from the University of Poonah in 1996. In 1999 he obtained his Masters degree in ecology from Saurashra University, and went eastwards. Having returned, in 2002 he set out again but this time westwards towards the land o' milk n' honey, to pursue a PhD at the University of Texas at Austin. And what a pursuin' it was! There he found a ravishing Colombian girl who promptly ravished him, resulting in a marriage and a lovely daughter blessed with hybrid vigor. Amen.

Permanent address: Apt. A2-408, Florida Estate Co-op Housing society, Keshavnagar, Mundhwa, Pune 411036. Maharashtra, India.
Email: mhasoba@gmail.com

This dissertation was typed by the author.